University of Nottingham
UK | CHINA | MALAYSIA

Environmental and Cost analysis of Carbon Fibre Composites Recycling

By

FANRAN MENG

BENG (HONS)

Thesis submitted to the University of Nottingham

for the degree of Doctor of Philosophy

July 2017

This page is intentionally blank

This thesis is dedicated to

My parents

My wife

This page is intentionally blank

Acknowledgements

I would like to firstly acknowledge my supervisors, Dr Jon McKechnie and Prof. Steve Pickering for their patience, invaluable guidance, helpful criticism and encouragement throughout my PhD course. I would also like to thank the Faculty of Engineering who financially made this project possible by kindly providing me the Dean of Engineering Scholarship for International Excellence.

I would also like to acknowledge the technical data provided on the fluidised bed pilot plant, funding for which was provided by the Boeing Company.

I would like to thank all the people from the Composites Group and Bioprocess, Environmental and Chemical Technologies Group at the Faculty of Engineering, who helped me in the course of my project. In particular, I would like to thank the members of the project team, Dr TA Turner, Dr KH Wong, CN Morris, J Liu, JP Heil and Dr G Jiang for the helpful discussions that we had.

Finally, to my parents, for their tireless support and encouragement in the last few years and deepest gratitude to my beloved wife, DEMEI NIU, for all her sacrifices, understanding and support. Without their support, the thesis would not have materialised.

This page is intentionally blank

Abstract

While carbon fibre reinforced plastic (CFRP) can reduce transportation energy use and greenhouse gas emissions by reducing vehicle weight, the production of virgin carbon fibre (CF) itself is energy intensive. CFRP recycling and the reutilisation of the recovered CF have the potential to compensate for the high impact of virgin CF production due to low cost and to open up new composites markets – e.g., in the automotive sector. The aim of the research is to examine the life cycle environmental and financial implications of a fluidised bed process to recycle CFRP wastes and to identify potential markets for CFRP reuse in automotive applications.

Firstly, process models of the fluidised bed carbon fibre recycling technologies are developed based on thermodynamic principles and established modelling techniques to quantify the heat and electricity requirements and predict the energy efficiency of a hypothetical commercial-scale plant. The energy model shows that the energy requirement of recycled CF production is generally less than 10% relative to virgin CF and results are robust across likely operating conditions. Further optimisation of the fluidised bed recycling process is needed to balance to the feed rate per unit bed area to minimise process energy use and potential implications for recycled CF properties. Opportunities exist for recovering stack heat loss which could further improve the energy efficiency of the fluidised bed process.

Secondly, process models for recycled CF processing (i.e., wet-papermaking/ fibre alignment) and subsequent CFRP manufacture (i.e., compression moulding/ injection moulding) technologies are developed to quantify the energy and material requirements of a hypothetical

operating facility. Models are based on optimised parameters based on the best performance from previous experiments, where available, while target values are used for the fibre alignment technologies currently under development.

Thirdly, the life cycle environmental implications of recovering carbon fibre and producing composite materials as substitutes for conventional materials (e.g., steel, aluminium, virgin CFRP) are assessed and proposed as lightweight materials in automotive applications, based on process models of the fluidised bed recycling process and remanufacturing processes or available life cycle assessment databases. Life cycle impact assessments demonstrate the environmental benefits of recycled CFRP compared with end-of-life treatment options (landfilling, incineration). Recycled CF components can achieve the lowest life cycle environmental impacts of all materials considered, although the actual impact is highly dependent on the design criteria of the specific components. Low production impacts associated with recycled carbon fibre components are observed relative to lightweight competitor materials (e.g., aluminium, virgin CFRP). Recycled CF components also have low in-use fuel consumption due to mass reduction and associated reduction in mass-induced fuel consumption. The results demonstrate the potential environmental viability of recycled CF materials.

Finally, financial analysis of carbon fibre recycling, processing, and use in recycled CFRP materials is undertaken to assess potential market opportunities in the automotive sector. Cost impacts of using recycled CF as a substitute for conventional materials are also assessed in the full life cycle, making use of data from energy and cost models, manufacturers and existing cost databases. Recovery of CF from CFRP wastes can be achieved at $5/kg and less across a wide range of process parameters. CFRP materials manufactured from recycled CF can offer

cost savings and weight reductions relative to steel and competitor lightweight materials in some cases, but are dependent on the specific application and associated design constraints– e.g., the material design index - as this drives the weight reduction/in-use fuel consumption and material requirements. Fibre alignment could potentially improve financial performance by inducing larger vehicle in-use fuel cost savings associated with weight reductions. Further investigations to monetise environmental impacts show larger cost benefits for recycled CFRP materials in replacement of conventional steel and lightweight competitor materials.

This page is intentionally blank

Contents

This page is intentionally blank

LIST OF TABLES

This page is intentionally blank

LIST OF FIGURES

NOMENCLATURE

CF	carbon fibre
vCF	virgin carbon fibre
rCF	recovered carbon fibre
CFRP	carbon fibre reinforced plastic
vCFRP	virgin carbon fibre reinforced plastic
rCFRP	recycled carbon fibre reinforced plastic
EOL	end-of-life
FB	fluidised bed
LCA	life cycle assessment

This page is intentionally blank

SYMBOLS

A	part's projected area, m^2
A_0	ram area, m^2
c_p	heat capacity, J/kg °C
D	part depth, mm
D_b	diameter of the barrel diameter, mm
D_s	screw diameter, mm
H	channel depth, mm
H_F	heat of fusion for 100% crystalline polymer, kJ/kg
h_{max}	part thickness, mm
$L_{bed\text{-}cyclone}$	The pipe length between fluidised bed reactor and cyclone, m

$L_{cyclone\text{-}oxidiser}$	The pipe length between cyclone and oxidiser, m
$L_{oxidiser\text{-}bed}$	The pipe length between oxidiser and fluidised bed reactor, m
L_s	maximum clamp stroke, mm
m_i	mass of the material, kg
N	screw rotational speed, rpm
p	compression moulding pressure, MPa
p_a	ambient pressure, MPa
P_i	injection moulding power, W
p_i	recommended injection pressure, Pa
Q_{avg}	average flow rate, m^3/s
R_{th}	Thermal resistance of pipework, K/W·m or K/W·m^2

t	pitch, mm
T_a	ambient temperature input to the component, °C
T_c	compression curing temperature, °C
t_c	cooling time, s
t_d	dry cycle time, s
t_i	injection time, s
T_i	polymer injection temperature, °C
T_{mol}	recommended mould temperature, °C
t_p	plasticizing time, s
t_r	moulding resetting time, s
T_s	torque of the screw, N·m
T_x	recommended ejection temperature, °C

v	pressing speed, m/s
v_f	volume fraction
V_s	required shot size, m^3
W	channel width, mm
w_{FLT}	flight width, mm
α	thermal diffusivity coefficient, mm^2/s
η_F	conveying efficiency for PP
λ	degree of crystallization for PP
ρ_0	bulk density of the polymer, kg/m^3
θ	helix angle, °
ω	angular rotational velocity, rad/s

CHAPTER 1 INTRODUCTION

1.1 Drivers for recycling

Growing demand for carbon fibre reinforced polymers (CFRP) for lightweighting in aerospace applications and, to lesser extent, automotive applications contributes to fuel efficiency objectives in the transportation sector. For instance, the Boeing 787 Dreamliner and Airbus A350 use up to 50% weight of CFRP materials. In the past 10 years, the annual global demand for carbon fibre (CF) has increased from approximately 16,000 to 72,000 tonnes and is forecast to rise to 140,000 tonnes by 2020 (Kraus and Kühnel, 2014). The generation of CFRP-based wastes is correspondingly increasing, arising from manufacturing (up to 40% of the CFRP can be wastes arising during manufacture (Witik et al., 2013)) and end-of-life products/ components. Therefore, quantities of CFRP waste are expected to increase quickly into the future, including 6,000-8,000 commercial aircrafts expected to come to their end-of-life by the year of 2030 (McConnell, 2010, Carberry, 2008).

CF recovery from wastes is a priority due to the high-energy intensity and high financial cost of virgin CF (vCF) production. Boeing aims to recycle at least 90% of retired airplane materials (Boeing, 2014), which will increasingly require CF recovery in the future. Also, by 2020-2025, Airbus targets for 95% of CFRP manufacturing process wastes to go through a recycling channel, with 5% of the waste products to be recycled back into the aerospace sector (Airbus, 2014). Commercial collaborations in recycling have been widely accepted, e.g., the BMW Group (Munich, Germany) and the Boeing Co. (Chicago, Ill., USA) on December 2012 signed a collaboration agreement to participate in joint research for CF recycling, as well as share manufacturing knowledge and explore automation opportunities (BMW group, 2016b). Also,

existing EU regulations aim to reduce the quantities of all wastes sent to landfill (European Council, 1999), while automotive sector-specific policy requires the recycling of at least 85% of end-of-life (EoL) materials from 2015 (European Council, 2000). In contrast to industry and policy goals, the vast majority of CFRP waste at present is not recovered: in the UK, for example, up to 98% of composite waste is disposed of in landfill or incinerated (Shuaib et al., 2015). Recovery of non-composite materials from end-of-life aircraft has proven to be beneficial in terms of cost and energy intensity relative to virgin material production (Carberry, 2008). According to Boeing, while 95% of the electricity consumption may be reduced compared to virgin CF (vCF) production, it is estimated that CF can be recovered with 30% reduction of the cost ($18/kg to $26/kg vs $33/kg to $66/kg) (Wood, 2010).

1.2 Current recycling status

For thermoset composites, the polymer cannot be re-moulded due to the fully cross-linked molecular structure and the recycling processes available are based on either mechanical recycling processes, in which the waste is reduced in size to produce fibrous or powdered materials, or thermal processes in which the polymer is removed to yield a clean CF recyclate (Pickering, 2006). Pyrolysis is a widely used thermal method, being established in commercial operations, e.g., ELG Carbon Fibre Ltd., UK and Carbon Conversion Ltd., US . Chemical recycling process uses a solvent to chemically break down the resin and remove it from the reinforcement. Various possibilities have been observed depending on the solvents, temperature, pressure and catalysts. Chemical recycling process requires lower operation temperature (about 400°C) than other thermal processes such as pyrolysis (Oliveux et al., 2015). A related thermal process is the fluidised bed (FB) process, being the subject of this study, which has been developed for the recycling of glass fibres and carbon fibres at the University

of Nottingham for over 15 years (Pickering, 2006). Although it shows a strength reduction of between 25% and 50% for carbon fibre (Yip et al., 2002, Pickering, 2006, Jiang et al., 2009), this continuous process has been shown to be particularly robust in dealing with varied polymer types containing mixtures of different materials and other contaminants. No residual char remains on the fibre surface as organic material is oxidised and any metallic material, such as aluminium honeycomb, rivets etc. remain in the fluidised bed and can be removed by regrading the sand bed. However, there are few studies systematically quantifying environmental and financial impacts of recycling processes.

It is significant to turn CFRP wastes into advanced manufacturing materials and close the recycling loop for industries to improve the environment and cost impacts. Various routes are available to enable the use of rCF including compression moulding and injection moulding, but few commercial rCF components are currently available. Two demonstrators of rCF- an aircraft seatback (36% aligned rCF volume fraction with PPS matrix) and automobile seat base (42% aligned rCF volume fraction with PP resin) have been manufactured on the UK projects HIRECAR and AFRECAR (University of Nottingham, 2005, University of Nottingham, 2009). However, there is limited consideration of this in research so far, in particular estimating environmental and financial performance of composite product manufactured from rCF and its potential markets.

1.3 Life cycle assessment and life cycle costing

Life Cycle Assessment (LCA) is a structured, comprehensive and internationally standardised method, which qualifies the potential environmental impacts (e.g., natural resource use and pollutant emission) of a product or material over its whole life cycle from the extracting and

processing of raw materials, manufacture of the product, transportation and distribution, use and reuse or end-of-life recycling and final disposal (i.e., cradle-to-grave) (O'Neill, 2003, Henrikke Bumann, 2004). The technique can relate the results to the function of a product; therefore, it can be used to describe a single environmental aspect or make comparisons between alternatives. Life cycle cost analysis is widely used to assess a trade-off of existing and emerging technologies for material production and additional cost for some improvement. Cost analysis includes the capital and operational costs (utilities, labour, maintenance, overheads and taxes) associated with all activities (Dhillon, 2009). Capital and operational costs are generally discounted and totalled to net present value to determine the most cost-effective option among different alternatives.

LCA and cost analysis have been combined to compare environmental and cost impacts on the basis of a functional unit (e.g., one kg CFRP/ one CFRP part produced) to support materials design with the best trade-off between environment and cost (Witik et al., 2011). However, the quality of the analysis is quite dependent on the availability of inventory and cost data covering raw material, manufacturing and recycling process, especially for CFRP industries. In particular, current LCA and cost analysis studies (Witik et al., 2013) in CFRP are using hypothetical recycling data giving more uncertainties of the potential role of CFRP in between weight reductions and environmental and cost savings due to unavailability of recycling inventory and cost data. In order to provide an overall understanding of the CFRP recycling and the subsequent reuse of rCF in contributing to reduce energy consumption, greenhouse gas (GHG) emissions, and cost impacts in lightweighting applications, combination of comprehensive LCA and cost analysis models of recycling process is required to be developed.

1.4 Aims and objectives

The aim of the research is to examine the life cycle sustainability implications of the fluidised bed recycling process for CFRP and to develop a framework to assess and identify routes for rCFRP and reuse for lightweight applications in terms of environmental and cost impacts. Eventually, the framework is intended for researchers and policy-makers in composites and environmental fields to answer the following questions:

- To what extent can fluidised bed recycling process impact the environment?
- How will fluidised bed rCF compete with vCF in the markets?
- To what extent will fluidised bed rCF be reintroduced into automotive applications in terms of environment and cost impacts?
- How will the consequent LCA and cost analysis be changed due to rCF materials' substitution of conventional automotive materials in automotive applications?

The thesis has three objectives:

(i). Develop process models of the fluidised bed recycling process, rCF processing (i.e., papermaking and fibre alignment processes) and manufacture of rCFRP products (i.e., compression moulding or injection moulding) based on thermodynamic principles, mass and materials flows and the experimental operation. The process model will help to understand how the performance of fluidised bed recycling process can be affected by the different process parameters (e.g., feeding rate, plant capacity, air in-leakage rate) and for future optimisation. The model will be demonstrated and validated with the current operation of a pilot plant.

(ii). Develop comprehensive life cycle assessment models of the fluidised bed CFRP recycling process and subsequent reuse of rCF in lightweighting applications. Life cycle inventory data (material and energy inputs; direct emissions) are derived from the process models developed, LCA databases and literature and input to the LCA models. Case studies will be carried out to investigate the environmental feasibility of using rCF products to replace conventional engineering materials typical of transport applications, e.g., steel and compared with other substitution lightweighting materials including magnesium, aluminium and virgin CFRP (vCFRP).

(iii). Develop life cycle cost models of the fluidised bed recycling and subsequent reuse of rCF in lightweighting applications. Capital and operational costs associated with fluidised bed recycling process, rCF processing and rCFRP manufacture will be estimated. The financial viability of inputting rCF in replacing conventional lightweight materials can be thus assessed by case studies selected as in LCA analysis that account for both rCFRP production and its use in transport applications. All costs will be discounted and totalled to net present value to determine the trade-off of environmental and cost impacts by using rCF compared to conventional lightweight materials.

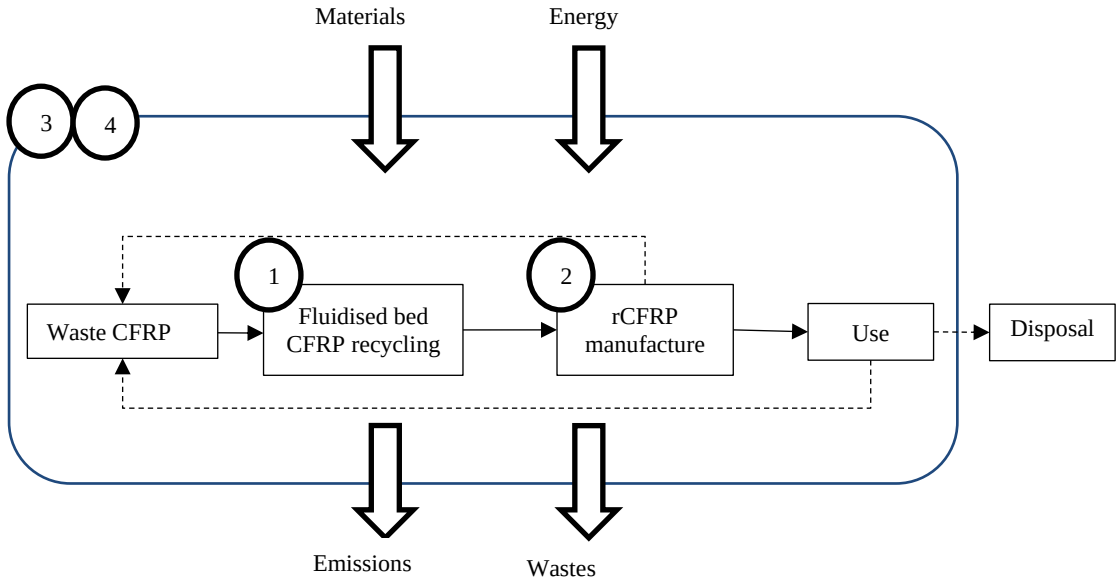

Figure 1.1. The overall framework (system boundary: 1, process analysis; 2, process analysis; 3, life cycle assessment; 4, life cycle cost analysis

1.5 Contributions of this thesis

This study will contribute to current research as follows:

- Provide a mathematical process model and datasets for energy demand in fluidised bed recycling of CFRP. This model is flexible (e.g., can adapt to different operating conditions, capacities). On a thermodynamic basis, it is more than just based on empirical relationships between parameters and energy use.
- Provide a detailed life cycle inventory data of fluidised bed recycling technology of CFRP waste in the first.
- Consider the optimisation of the fluidised bed recycling process operations based on process models

- Assess the life cycle environmental performance of rCF products in potential automotive applications.
- Provide a life cycle cost model of fluidised bed rCF based on a preliminary analysis and can be scaled in size to plant capacity. Perform cost analysis of rCF products in the full life cycle in assessing the cost benefits of rCF use in lightweighting applications.
- Provide a framework for the assessment of the environmental and cost impacts of fluidised bed CFRP recycling and remanufacture, including potential uses for rCFRP materials in automotive applications.
- Assess the sensitivity of design variations, processing parameters (e.g., feeding rate in recycling stage) on the environmental and financial impacts of rCF products.

1.6 Journal papers

- Meng, F., et al., Energy and environmental assessment and reuse of fluidised bed recycled carbon fibres. *Composites Part A: Applied Science and Manufacturing* 2017; Impact factor: 4.075
- Meng, F., et al., Environmental aspects of use of recycled carbon fibre composites in automotive applications (Under review). *Environmental Science and Technology*; Impact factor: 6.198
- Meng, F., et al., Financial analysis of closed loop of fluidised bed recycling carbon fibre in automotive application (In submission, to submit by 09/2017). Target journal: *Environmental Science and Technology*; Impact factor: 6.198
- Meng, F., et al., Life cycle assessment of waste management of carbon fibre composite materials (In submission, to submit by 09/2017). Target journal: *Journal of Cleaner Production*; Impact factor: 5.715
- Sun, X., Meng, F., et al., The carbon fibre application in vehicle lightweight design from the life cycle perspective (under review). *Journal of Cleaner Production*; Impact factor: 5.715

1.7 Conference papers

- Meng F, Pickering SJ, McKechnie J. Inventory analysis of fluidised bed recycling of carbon fibre reinforced polymers. In SAMPE Europe Conference in Amiens, France, September. 2015

- Meng F, Li X, Pickering SJ, McKechnie J. Energy and life cycle environmental impacts of fluidised bed recycled carbon fibre. In The 3rd International Academic Conference of Postgraduates, NUAA, Nanjing, China. 2015. **Outstanding paper award**
- Pickering, S. Turner, TA, Meng, F, et al., Developments in the fluidised bed process for fibre recovery from thermoset composites. In CAMX 2015, Dallas, TEXAS USA. 2015.
- Meng F, Pickering SJ, McKechnie J. Comparative inventory analysis of virgin and fluidised bed recycled carbon fibre. In LINK 15 Student-Led Interdisciplinary Research Conference, UoN. 2015.
- Meng F, Pickering SJ, McKechnie J. Life cycle analysis of composite materials using fluidised bed recovered carbon fibre, In LINK 16 Student-led Interdisciplinary Research Conference, UoN. 2016.
- Meng F, McKechnie J, Pickering SJ. Environmental aspects of recycled carbon fibre composite products. In SAMPE Europe Conference in Liege, Belgium, 2016.
- Meng F, Pickering SJ, McKechnie J. Life cycle assessment of fluidised bed recovered carbon fibre composite material. In 22nd SETAC Europe LCA Case Study Symposium in Monpellier, France, 2016.
- Meng F, McKechnie J, Pickering SJ. Environmental and financial analysis of fluidised bed recycling carbon fibre and its reuse in automotive applications, In 9th biennial conference of the International Society for Industrial Ecology (ISIE) and 25th annual conference of the International Symposium on Sustainable Systems and Technology (ISSST). Chicago, Illinois, USA, June 25-29, 2017.
- Meng F, McKechnie J, Pickering SJ. Towards a circular economy for end-of-life carbon fibre composite materials via fluidised bed process, In 21st International Conference on Composites Materials (ICCM-21). Xi'an, China, 20-25 August 2017.

1.8 Outline of thesis

A total 7 chapters are included in this thesis.

Chapter 1 starts the introduction to the overall theme of the thesis including description of aim and objectives.

Chapter 2 covers literature review of end-of-life treatments of CFRP wastes, life cycle assessment of recycling processes and rCFRP manufacture techniques using rCF, and lightweighting study in automotive application.

Chapter 3 includes process modelling of the fluidised bed process to investigate the thermal performance and estimate energy demand of the recycling plant and the optimisation.

Chapter 4 includes process modelling of composite manufacturing from rCF including rCF processing (wet-papermaking and fibre alignment) and composite manufacturing (compression moulding and injection moulding). This will develop the datasets of energy demand for the whole manufacturing stages for rCF.

Chapter 5 describes life cycle assessment of composite manufacturing from rCF using inventory data developed from process models. Use phase and materials substitution analysis of rCFRP in replacement of conventional materials in lightweighting applications is discussed. Case study of rCFRP automotive displacement of conventional materials is also included.

Chapter 6 describes the financial analysis of fluidised bed rCF composite. Case study of rCFRP automotive displacement of conventional materials is also included.

Chapter 7 discusses the overall conclusions and limitations of the research. It also presents methods by which the framework might be exploited more comprehensively in the future.

CHAPTER 2 LITERATURE REVIEW

2.1 Introduction

Current levels of carbon fibre usage are in excess of 100,000 tonnes per annum with growth forecast to be 10- 20% per annum (JEC Group, 2011). UK revenues of composites are estimated at $2.3 billion in 2015 and are expected to grow to $10.2 billion by 2030 (UK, 2016). The advantages of CFRP materials, such as design flexibility and integrity, mass reduction, chemical resistance and improvement in mechanical properties, are the leading factors bringing their applications to a very wide range of industries such as aircraft, aerospace, automotive, marine, wind energy and electronic equipment (Bader, 2000, Duflou et al., 2009, Witik et al., 2012). The global composites demand in three key markets- aerospace, consumer goods and industrial fields including automotive, are shown in **Figure 2.1** for the year between 2013 and 2020 (projected) (Sloan, 2013). It also illustrates the prediction of both production scrap and end-of-life wastes during this period. Production scrap rate is estimated to be 10% in industrial and consumer fields and 25% in aerospace industries. Typical lifespans of CFRP in industrial, sport and aerospace range from 5 years for sporting applications up to 30 years in aerospace applications (Witik et al., 2013). In the early stage, CFRP waste is mainly from manufacturing scrap and therefore, current recycling projects are focusing on processing of these relatively 'clean' manufacturing scrap. As seen in the future estimates, there will be an increasing amount of CFRP waste generated mainly from end-of-life scraps in the next decades, requiring an environmentally and financially beneficial recycling route with a high tolerance for waste contamination to dispose of, and recover value from, CFRP wastes.

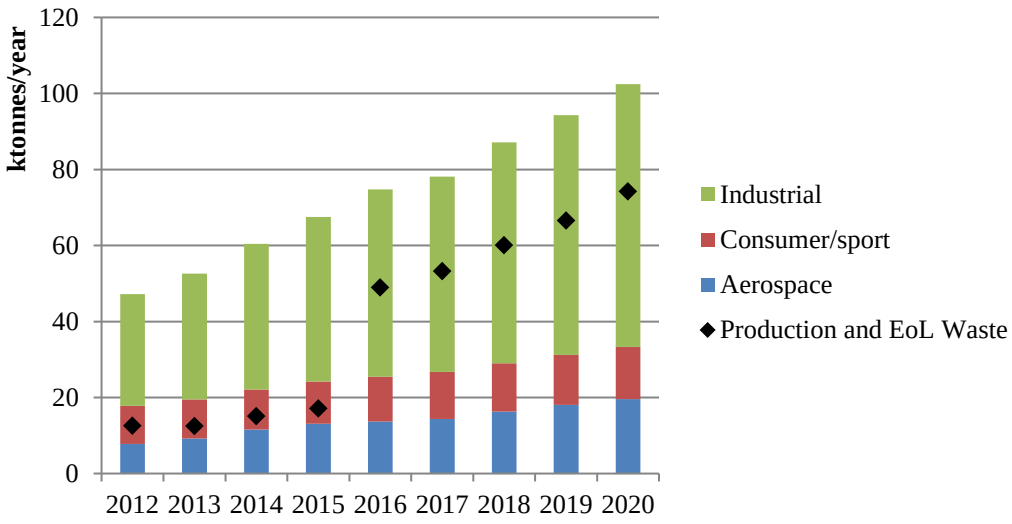

Figure 2.1. Global markets for CF (Sloan, 2013) and predictions of wastes in manufacture and end of life: 2013-2020.

The chapter begins with a review of the current applications of CFRP materials in aviation, automotive, sport and wind power industries for lightweighting applications. Afterwards, the current status of thermosetting composites recycling is reviewed. The chapter then focuses on a review of the life cycle assessment and financial analysis of CFRP from raw materials, manufacture, use phase to recycling in terms of its environmental and financial impacts in automotive applications. The manufacturing techniques and properties of rCFRP products are also discussed for their use in lightweighting industries.

2.2 CFRP applications

2.2.1 Aviation

The aviation industry was amongst the first to realise the benefits of CFRP materials due to the high cost of aviation fuel and the introduction of legislation setting limits on the GHG

emissions in use phase. A growth rate of 5% per year since 2001 in aviation industry has been reported (Witik et al., 2012) and the demand in the aviation sector will grow from 7,694 tonnes in 2011 to 18,462 tonnes by 2020 (Roberts, 2011). CFRP material has been widely used as it provides a range of advantages, e.g., high specific elastic modulus and strength, fatigue and damage tolerance, improved manufacture flexibility through part integration, which reduces product tooling and assembly times. Typically, weight reduction of 20% can be achieved when replacing aluminium part with a carefully designed CFRP part (Abbott, 2000). The new wide-body planes, Airbus A350 and Boeing 787 Dreamliner, have seen the expanded use of CFRP materials. While typical contribution to mass reductions is in the range of 20-30% weight in the early stage, utilising composites in Boeing 787 is for up to 50 wt% of their construction (Boeing, 2017). The mass savings are able to increase the payload and the fuel efficiency.

However, despite various benefits of using CFRP, the high costs still limit its uptake, including raw material (CF), high costs of CFRP processing, costly manufacture equipment as well as the requirements to control the quality. Moreover, with the increased use of CFRP materials, the correspondingly increasing wastes are demanding to be dealt with carefully. Barriers to CFRP use, in particular the high cost, suggest rCFRP to be a potential solution with the current development of recycling technology. However, it is still required to understand the environmental and financial viability of re-introducing rCFRP into aviation applications.

2.2.2 Automotive

Currently, there is a globally increasing demand for low-cost and high-performance lightweight materials to replace metals for the design requirement of environmentally friendly automobiles with lowest fuel consumption (Jacob et al., 2002, Rudd, 2000). In fact, about 75% of fuel consumption (Friedrich and Almajid, 2013) is estimated to be directly connected with the

vehicle weight. Thus, in order to realise the objectives to design clean cars with lowest fuel consumption, car manufacturers are making efforts to develop the manufacturing techniques to reduce car mass by the use of lightweight materials such as CFRP for structural and non-structural parts.

Driven by the excellent specific modulus and specific strength, CFRP has the potential to increase fuel efficiency and reduce emissions from fuel combustion while meeting component design constraints. Reducing a vehicle's weight by 100 kg leads to lower the CO_2 emission by 7.6 g/km (Office of Energy Efficiency and Renewable Energy, 2010). The use of CFRP materials as a substitution for steel as structural parts could achieve a 40-65% reduction in mass (Das, 2001).

The global demand for CFRP in the automotive industries is valued at $2.4 billion in 2015 and is expected to increase to $6.3 billion by 2021 with an average rate of increase of 17.5% per annum (Mazumdar, 2016). However, the EU ELV Directive regulates 85% end-of-life vehicle wastes must be recovered, creating a need for viable CFRP recycling routes. Efforts have been performed in some commercial companies, such as BMW which is working in collaboration with the Boeing company for the removal of existing technological barriers and to recycle CF in order to develop cars with higher CFRP content, e.g., BMW i3 and i8 (BMW GROUP, 2016a). In the future, with the development of CFRP recycling technologies, there could be large quantities of either vCFRP or rCFRP materials utilised in automotive applications.

However, at present, a major breakthrough for CFRP in structural parts in high volume automotive applications has not been made (Brooks, 2000, Mallick, 1998, Mazumdar, 2016). There are many reasons for this, such as high material costs, inefficient production rates,

compatibility with automotive resins and to a lesser extent, concerns about recyclability. Compared to conventional steel and aluminium, the high material cost of CF has constrained the net benefits of lightweighting and is a barrier that needs to be overcome. It is estimated that the global demand of CF would be 1.23 million tonnes if at $11/kg compared to an expected only 0.32 million tonnes at $18-$33/kg currently (Mazumdar, 2016)

2.2.3 Wind energy

Wind power generation which has become a rapidly growing market recently and the worldwide wind energy market even showed a new record in 2003 at an increased growth rate of 15% (Brondsted et al., 2005). The global demand of CF for wind energy market is expected to increase from 10,440 tonnes to 54,270 tonnes by 2020 (Roberts, 2011). This demand is already surpassing that for the traditional aerospace industries which have a demand estimate from 7,694 tonnes in 2011 to 18,462 tonnes by 2020.

Although rotor blades can be produced with glass fibre reinforced plastics, CFRP becomes increasingly necessary to support larger blades. A wind power generator with a large-scale CFRP turbine can save 418 g CO_2 emission per kWh compared to electricity mix (423 g/kWh). Therefore one 3 MW wind power generator enables to deliver a total CO_2 reduction of 720,000 tonnes in 20 years (The Japan Carbon Fiber Manufacturers Association, 2016).

2.2.4 Opportunities for rCF

Carberry (2008) estimated cost for rCF is $18-26/kg compared to $33-66/kg for vCF in 2008. Therefore, recycling at lower cost is a potential solution to recover substantial value from CFRP wastes: rCF could reduce environmental impacts relative to vCF production, while the potentially lower cost of rCF could enable new markets for lightweight materials. However,

there is very limited understanding of the overall financial viability of producing automotive components from rCF. Several recycling and rCFRP production processes are reaching a mature stage, with implementations at commercial scales in operation. Recycled CFRP have shown competitive mechanical performance with vCF materials, and rCFRP structural/non-structural demonstrator components in aerospace and automotive applications have been manufactured (Pimenta and Pinho, 2011). However, CFRP recycling and rCFRP production processes are still making trade-offs between maintaining fibre quality similar to vCF and keeping environment friendly and cost effective.

2.3 End-of-life treatment of CFRP wastes

As CFRP is increasingly used in aerospace and finds emerging applications in the automotive sector, systems need to be developed to deal with wastes arising from associated manufacturing processes and the end of life stage. In the USA and Europe, 6,000-8,000 commercial aircraft are expected to come to their end of life by the year of 2030 generating an estimated 3,000 tonnes of CFRP scrap per annum (McConnell, 2010, Carberry, 2008). As cited by McConnell (McConnell, 2010) 62% of CFRP manufacturing wastes were from woven prepreg with the remaining from fabric selvedge waste (15%), UD prepreg waste (11%), clean fibre waste (8%) and composite manufacturing part waste (4%), as shown in **Figure 2.2**.

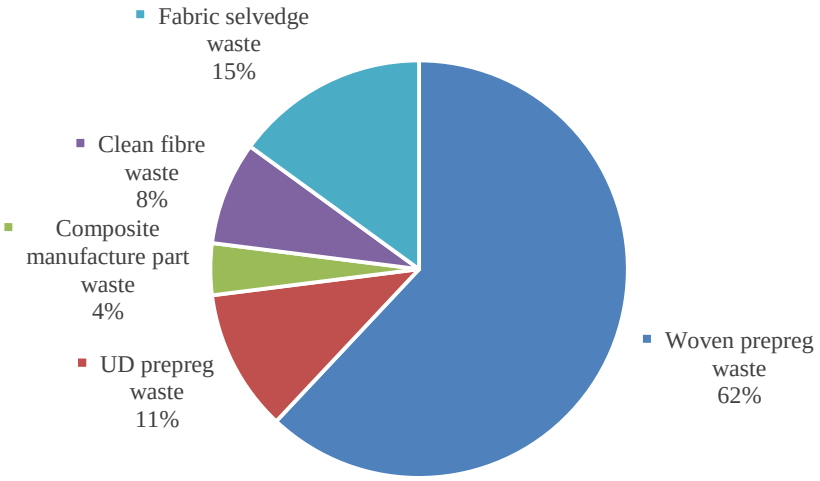

Figure 2.2. Estimates of diverse breakout of manufacturing wastes in Europe (McConnell, 2010).

End-of-life treatment technologies of CFRP waste range from conventional landfill/ incineration to mechanical recycling and thermal recycling (pyrolysis, fluidised bed and solvolysis) for fibre recovery as shown in **Figure 2.3**. For thermoset composites, the polymer cannot be re-moulded and the recycling processes available are based on either mechanical recycling processes, in which the waste is reduced in size to produce fibrous or powdered materials, or thermal processes in which the polymer is removed to yield a clean carbon fibre recyclate and/or chemical products.

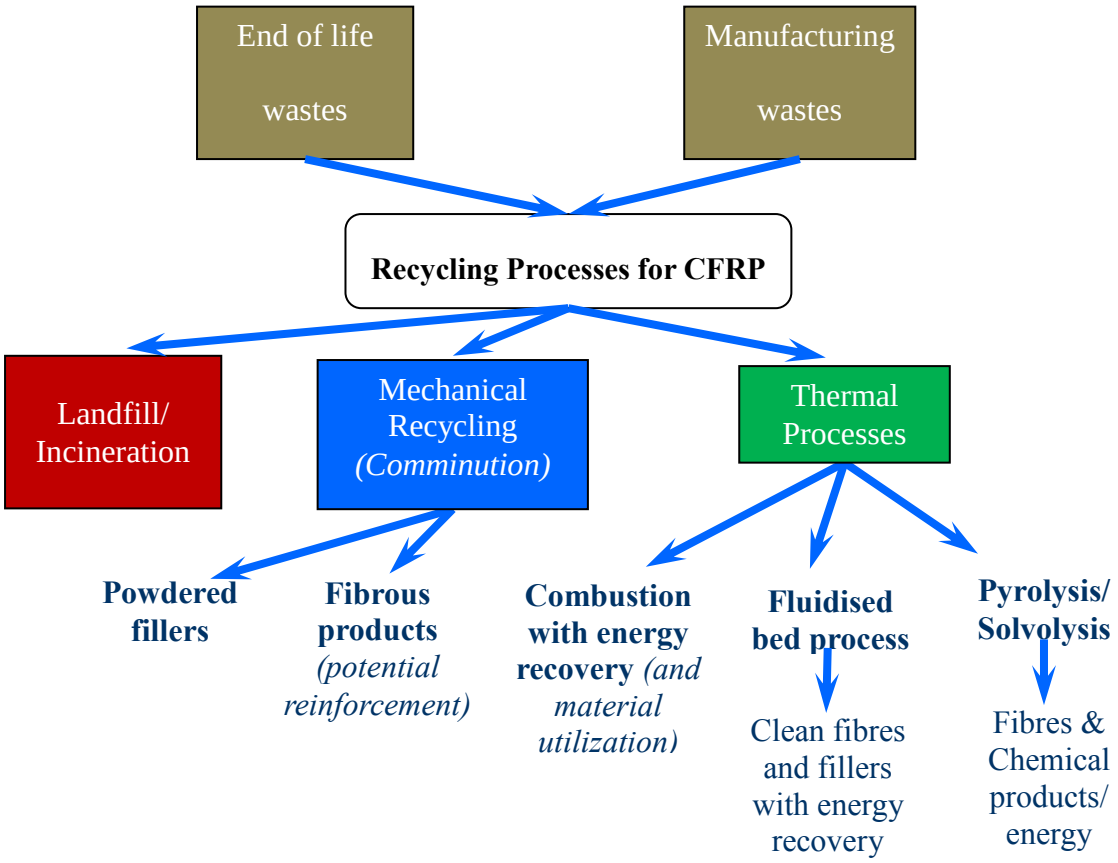

Figure 2.3. Recycling processes for thermoset composites.

2.3.1 Landfilling

Disposing waste CFRP to landfill involves treating in a sanitary landfill site which isolates the waste from environment. Before waste CFRP is buried in landfill, shredding pre-treatment is needed to reduce the size of CFRP waste into a more easily transported form. As the conventional end-of-life waste treatment, landfilling is currently at a relatively low cost of £19/tonnes excluding landfill tax and £102/tonnes including landfill tax in the UK in 2016, however, it is the least preferred option (WRAP, 2017).

2.3.2 Incineration

Incineration of CFRP provides an alternative method to treat the CFRP waste while recovering the embodied energy. Similar with all organic materials, the polymeric matrix has a calorific value and can release energy via combustion. The calorific value of urea formaldehyde is 15.7 MJ/kg while those of the other thermosetting resins are about 30 MJ/kg depending on the specific CFRP composition (Hedlund, 2005, Pickering, 2006).

Incineration for energy recovery has a gate fee of £51/tonne (WRAP, 2017), which represents the net operational cost (capital, labour, maintenance) and revenues gained from the sale of electricity and heat. However, it can increase the GHG emissions during combustion as the carbon content of CFRP is released to the environment as CO_2; 3.1-3.3 kg CO_2 eq./kg CFRP without accounting for the credits of displacement from energy outputs and compared to 0.002-0.005 kg CO_2 eq./kg CFRP for landfilling (Wernet et al., 2016, Li et al., 2016).

2.3.3 Mechanical recycling

Among various recycling methods, one of the most mature technologies is mechanical recycling. It is currently used on an industrial scale to recycle waste composites, especially glass fibre reinforced plastic (Palmer et al., 2010). After initial size reduction, the material is ground in a hammer mill and graded into different lengths. Using mechanical recycling, CFRP wastes can be reduced to two fractions: resin powder and a fibrous fraction, products are commonly used as fillers in lower value materials, such as bulk moulding compound or sheet moulding compound. However, the resulting materials have poor mechanical properties compared to vCFRP materials (Pimenta and Pinho, 2011) and so are not suitable for lightweighting or high modulus/ strength applications.

2.3.4 Pyrolysis

Figure 2.4 shows the schematic diagram of a pyrolysis process. It is a thermal decomposition of polymers without oxygen at high temperatures between 300 °C and 800 °C, enabling the recovery of long fibres with high modulus. An elevated temperature of 1000 °C can be applied but it will result in a significant degradation of mechanical properties of the fibre products. Due to the significant impact of temperature and residence time on the final quality of the rCF, the two factors must be controlled strictly in the pyrolysis reactor. As waste is heated in low oxygen conditions, pyrolytic char remains on fibres. The commercial processes, such as ELG's process has an extra stage to introduce oxygen to oxide char. Care is needed to ensure all char is removed without oxidising rCF (Pickering, 2006).

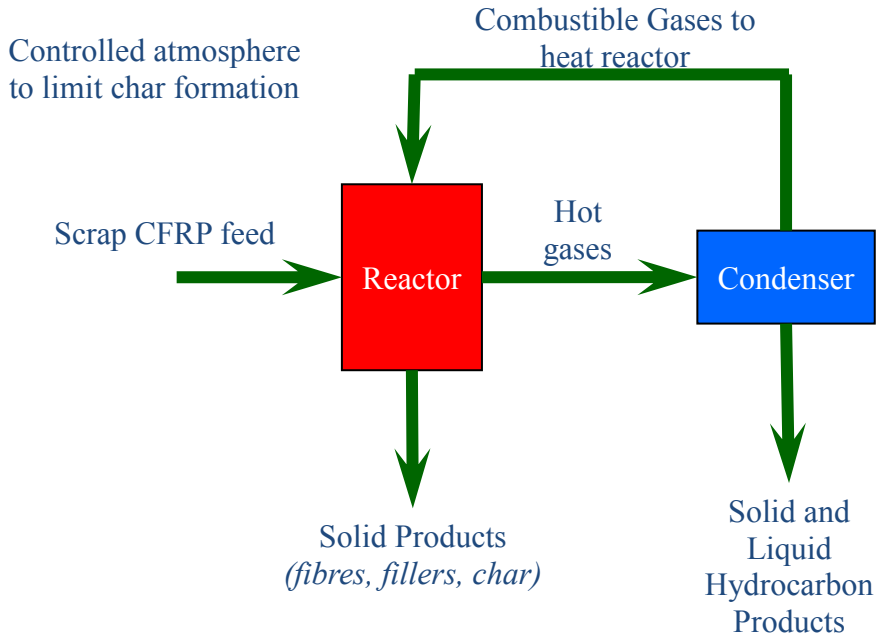

Figure 2.4. Pyrolysis process recycling reactor.

As a thermal method, a shredding preparation of CFRP wastes before feed into the pyrolysis recycling plant is required. Pyrolysis process uses external heat to allow for recovering fibres with minimum properties reduction which could be reused into the composite manufacture industries as rCF could maintain 90% or more of the original mechanical performances. Also, polymeric matrix can potentially be recycled as chemical feedstocks and reused in more than one form (Cunliffe et al., 2003, Job, 2010). Pyrolysis has now reached early stages of commercialisation, e.g., ELG Carbon Fibre Ltd. has 2,000 t/yr recycling capacity with an estimated energy intensity of 30 MJ/kg (Shuaib and Mativenga, 2015).

2.3.5 Solvolysis

Solvolysis utilises a solvent fluid (such as water, acid, or an alcohol) to break down polymer resin and separate them from CF, as shown in **Figure 2.5**. The recycling process is able to recover high quality CF with only about 1.1% tensile strength loss and recover polymeric matrix as an organic compound with a solvent method in nitric acid solution as reported in Liu (2004). The rCF is normally semi-long or long with low contamination. However, the decomposition temperature and nitric acid concentration have an impact on the mechanical properties.

Depending on the temperature and pressure process, the chemical process can be categorised into super-, sub- or near-critical solvolysis. Schneller et al. (2016) investigated the fibre-matrix separation via solvolysis using sub- and super-critical fluids (pure water and a water/ ethanol-mixture). After solvolysis separation, the majority of resin content could be removed at high temperature and at long processing time. Due to this, there may be no requirement for an additional oxidising surface treatment which is used to remove the char resulted from oxidation

of resin. Solvolysis recycling technique is feasible but processing temperature, time, solvents and equipment may have negative effects on the environment. Also processes at high pressure have a high capital cost.

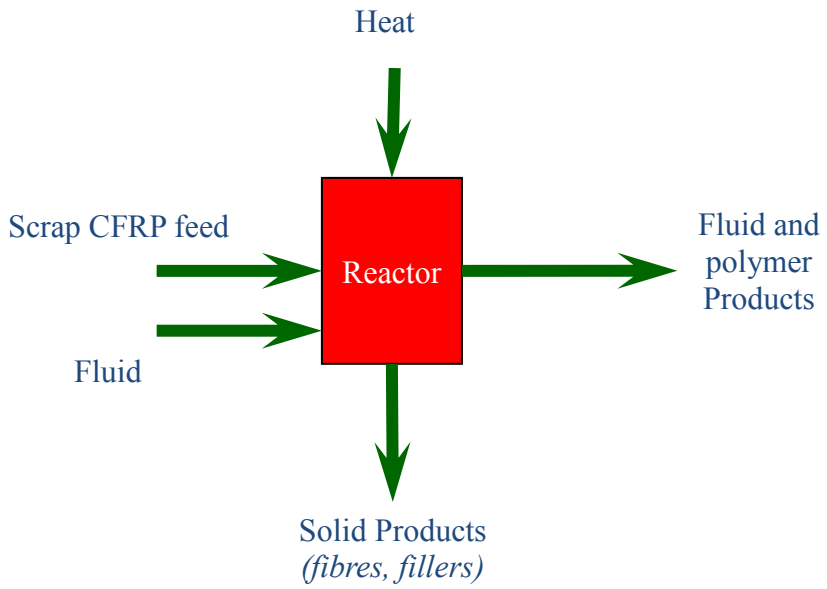

Figure 2.5. Solvolysis process recycling reactor.

2.3.6 Fluidised bed

2.3.6.1 General characteristics

Fluidised bed process involves the thermal decomposition of the polymer matrix followed by the release and collection of dispersed CF filaments. A schematic diagram of the fluidised bed recycling process is shown in **Figure 2.6**. The fluidised bed is a convenient way of heating the scrap material rapidly in an air stream and provides the attrition necessary to release the fibres once the matrix has been removed. The fluidising air is able to elutriate the released fibres for a typical time of 20 minutes, but degraded material remains in the bed. The fibres can then be

removed from the gas stream by a cyclone or other gas-solid separation device. The operating temperature of the fluidised bed is chosen to be sufficient to cause the polymer to decompose, leaving clean fibres, but not too high to degrade the fibre properties substantially. The polymer matrix decomposes in the sand bed into low molecular weight hydrocarbon products that are carried out of the fluidised bed in the gas stream. These out-gases can be fed to power a combined heat and power unit. In the state-of-the-art test rig at Nottingham, an afterburner is used to complete the oxidation process for energy recovery to heat the hot air feed to the process.

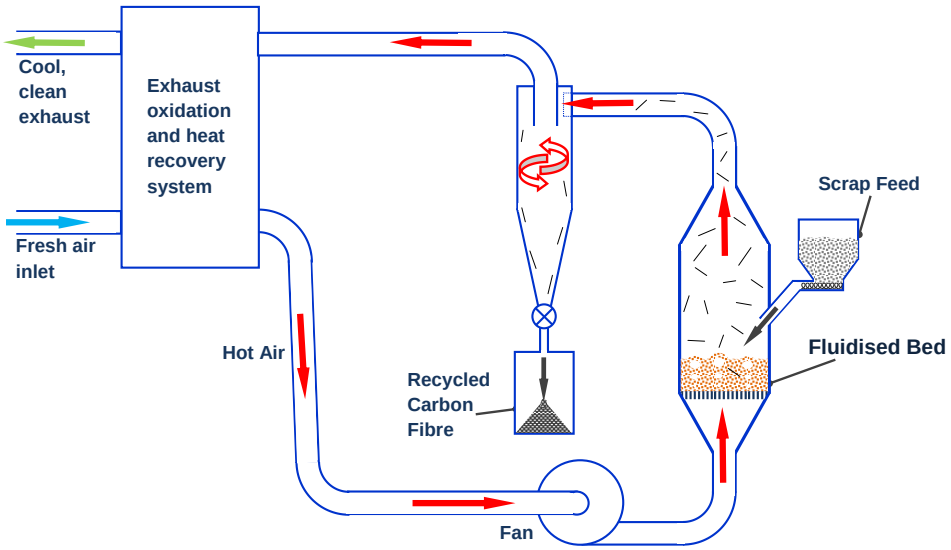

Figure 2.6. Main components and flow directions of the fluidised bed CFRP recycling process.

This process has been developed for the recycling of glass fibres and carbon fibres at the University of Nottingham over 20 years (Bell et al., 2002, Jiang et al., 2008, Pickering et al., 2015), which has demonstrated potential as a cost-effective recycling technique and is the focus of this thesis. The advantages of the fluidised bed are high heat transfer rates and great

temperature control, allowing a relatively short cycle time, high energy efficiency and high product reliability.

The CFRP waste being recycled must be reduced in size so that it can be fed into the FB process. The length of the filaments has to be controlled to avoid agglomeration in the FB and generally it is no longer than 30 mm. The current process utilises a two-stage size reduction – large structures would first need to be reduced in size to metre-sized pieces that could then be fed into a twin shaft shredder to reduce the size of the pieces to around 25-100 mm scale. Thereafter, the waste is fed to a hammer mill with a screen size of 5-25 mm appropriate for the FB process.

In-process scraps (e.g., out-of-life prepreg, ply cutter offcuts, end of bobbins etc.) and end-of-life composite wastes (e.g., sporting goods, aircraft) and often involve other materials bonded such as aluminium honeycomb core with metal inserts. Process compatibility with contaminated, end-of-life CFRP waste is a key advantage of FB over other recycling techniques. Contaminants remain at the bottom of the fluidised sand bed and can be removed by regrading sand particles.

The rCF are in a fluffy, discontinuous, 3D random and highly entangled structure with a typically low bulk density of 50 kg/m^3 (see **Figure 2.7**). The fibre length of rCF is dependent on the fibre length of CFRP wastes. The fibre length measurement is achieved by burning off the resin to separate fibres from the waste followed by image analysis. Fibre degradation has been found to be a function of input fibre length.

Figure 2.7. Recycled carbon fibre showing fluffy, discontinuous, 3D random and highly entangled structure.

The rCF shows a clean fibre surface under scanning electron micrograph as shown in **Figure 2.8**. The mechanical properties of different rCF are measured by single fibre tensile tests according to BS ISO 11566 as shown in **Table 2.1**. The tensile modulus of rCF is almost unchanged with the vCF; however, tensile strength has shown a loss of 18% - 50% (Pickering et al., 2015). This may be because of the mechanical damage due to abrasion with sand particles in the process and also the effect of the oxidising atmosphere and high temperature.

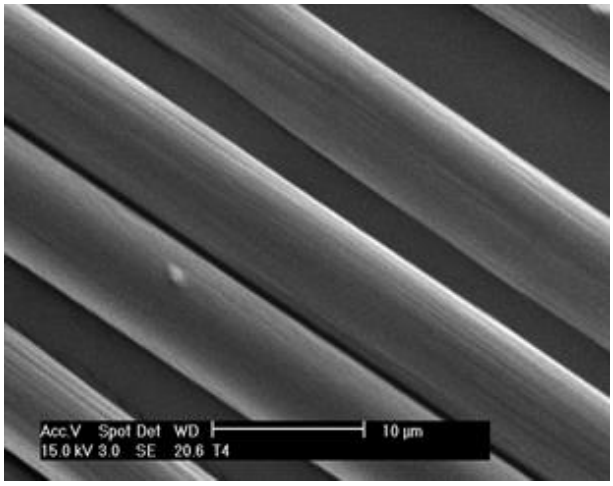

Figure 2.8. CF recovered from fluidised bed process, showing a clean surface free from polymer residue.

Table 2.1. Measured tensile properties of carbon fibre recovered in the fluidised bed process (Pickering, 2010, Wong et al., 2009a)

Fibre type	Tensile modulus (GPa)	Tensile strength (GPa)	Tensile strength reduction in rCF (%)
Toray T300s virgin	227	4.24	2
Recycled at 550°C	218	4.16	
Toray T600s virgin	208	4.84	34
Recycled at 550°C	218	3.18	
Toray T700 virgin	219	6.24	54
Recycled at 550°C	205	2.87	
Hexcel AS4 virgin	231	4.48	38
Recycled at 550°C	242	2.78	
Grafil MR60H virgin	227	5.32	51
Recycled at 550°C	235	2.63	
Grafil 34-700 virgin	242	4.09	25
Recycled at 450 °C	243	3.05	

2.3.6.2 Future development

A pilot fluidised bed plant has been developed at the University of Nottingham (see **Figure 2.9**), in order for the transition from lab to fully commercial scale. However, there are still key technical and economic challenges about recycling to be addressed, e.g., development of a cost effective, high throughput process.

Figure 2.9. Pilot plant of FB recycling process at University of Nottingham.

Previous work has shown the significant impact of process temperature on the processing time and fibre properties (Yip et al., 2002, Jiamjiroch, 2012). In addition, Jiamjiroch (Jiamjiroch, 2012) found the fibre agglomerates within the fluidised bed process which has demonstrated to be determined by the fibre aspect ratio and concentration occurs at higher feeding rates of CFRP waste (Jiang et al., 2005). The formation was believed to occur providing a state of percolation (i.e., the fibres contact each other). For a fluidised bed with a diameter of 0.33 m

and a sand bed of 7 kg, when the unidirectional CFRP prepreg waste with a thickness of 0.2 mm fed in, the maximum rCF throughput that could be achieved before agglomeration takes place was 1.6 g/minute. It was concluded that the shorter the fibres in the CFRP waste and the higher the fluidising velocity, the higher the feeding rate can be achieved.

Current research is investigating how high feed rates can be achieved and considering the possibility of continuous regrading of sand to reduce agglomeration. Moreover, more care has to be made between increasing the throughput and maintaining high properties of rCF associated with its market competitiveness during recycling process. Therefore, within focus of this thesis, the feed rate together with other FB parameters such as plant capacity, feed rate and air in-leakage will be investigated to assess their impacts on environmental and cost impacts of and markets for rCF.

2.4 Life cycle assessment and financial analysis of CFRP

LCA (O'Neill, 2003, Henrikke Bumann, 2004) and financial analysis (Fabrycky and Blanchard, 1991, Dhillon, 2009) is a structured, comprehensive and internationally standardised method, qualifying the potential environmental impacts (e.g., natural resource use and pollutant emission) and cost impacts of a product or material over its whole life cycle from the extracting and processing of raw materials, manufacture of the product, transportation and distribution, use and reuse or end-of-life recycling and final disposal (i.e., cradle-to-grave). The techniques can relate the results to the function of a product; therefore, it can be used to describe environmental and financial aspects or make comparisons between alternatives. They have been shown to be a particularly worthwhile technique for comparing different materials in terms of cost and environmental impacts to support materials selection and enabling the best

trade-offs between cost and environment (Witik et al., 2012, Witik et al., 2011, Schwab Castella et al., 2009, Ilg et al., 2016). The applications of LCA and financial analysis method are growing in the composite field in which they have been adopted to investigate the environmental and cost impacts of substituting conventional material types with CFRP in transport applications. As specified in **Figure 2.10**, the study has covered all life cycle stages from raw material (i.e., CF manufacture) and CFRP manufacture to the end-of-life treatments (e.g., fluidised bed recycling process in this research).

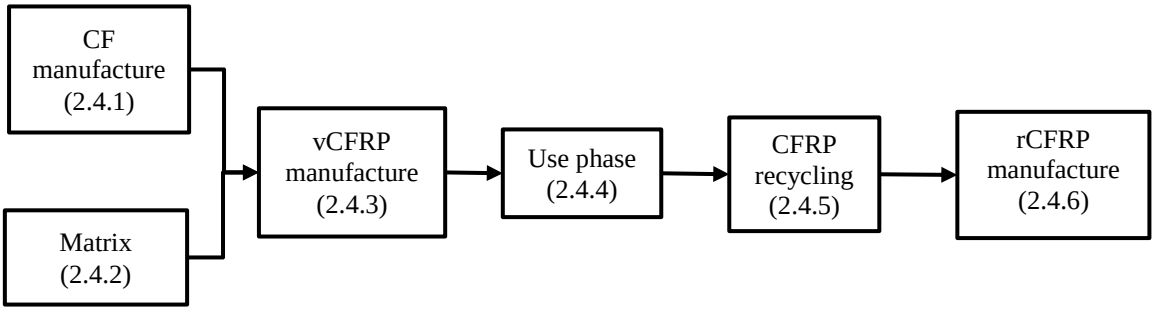

Figure 2.10. Diagram of life cycle stages of CFRP materials

2.4.1 Carbon fibre manufacture

One of the main raw material - CF can be classified into polyacrylonitrile (PAN)-based, pitch-based and rayon-based. Among them, PAN-based CF is in the largest production and best used in volume (about 90%) (Zoltek, 2017, The Japan Carbon Fiber Manufacturers Association, 2016). Alternative precursors (e.g., biomass-derived lignin (Das, 2011) are under investigation but are not yet commercially produced.

PAN-based CF manufactured by production processes as illustrated in the **Figure 2.11**, has a higher tensile strength than pitch-based CF. Its manufacture consists of five phases: PAN

polymerization, oxidation, carbonization, surface treatment and sizing. The raw material acrylonitrile (AN) is produced in the process of ammoxidation of propylene, known as Sohio process. The production of PAN precursor fibre is traditionally by polymerisation of AN using a solvent, e.g., sodium thiocyanate, nitric acid, dimethylacetamide or dimethylformamide, followed either by wet or air-gap spinning process including the stretch and wash of the fibres. After spinning, a sizing process is applied to complete the precursor fibre production.

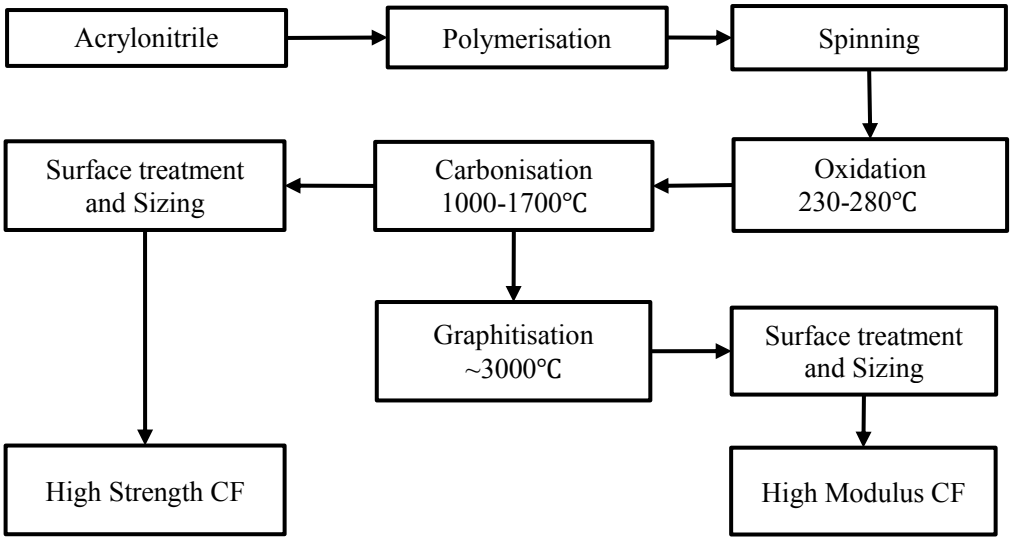

Figure 2.11. Manufacture process of PAN type CF

The PAN fibre is then converted into CF in a sequence of steps. First, in most commercial processes, tension is applied to the fibres at the oxidation stage during which fibres are exposed to air at temperatures between 230 and 280 °C (Delhaes, 2003) (also called stabilisation stage).

Once stabilised, the PAN fibre is carbonised at temperatures between 1000 and 1700 °C in an inert atmosphere, which may contribute largely to the total energy consumption. During this

step most of the non-carbon elements (hydrogen, nitrogen and oxygen atoms) are removed from the fibre in the form of CH_4, H_2, HCN, NH_3, CO, CO_2 and various other gases. The evolution of these compounds causes about 40% to 45% weight reduction of the fibre (Delhaes, 2003). As a consequence, the fibre diameter is decreased with the removal of non-carbon elements. This step is important in energy perspective as the furnace is heated by electricity together with the material loss.

After oxidation, increasing the final heat treatment (called graphitisation) temperature increases tensile strength (ranging from 0.5GPa to 4.0GPa) and modulus. As a consequence, manufacturers can produce different grades of PAN-based CF by changing the heat treatment temperature in this stage. Graphitisation is the transformation of disordered carbon structure by heat treatment in addition to thermal decomposition at an elevated temperature. During graphitisation, carbonised fibres are placed in argon condition at a temperature up to 3000 °C to produce typically high modulus fibres (modulus of 325 GPa or higher).

2.4.1.1 Life cycle inventory of carbon fibre manufacture

In order to perform LCA of CFRP materials, life inventory data of CF production is essential. The typical inventory data of CF production is assumed to link energy and emission data to CF manufacturing process parameters, CF properties, disaggregated inputs and outputs for each sub-process. However, the data of CF manufacture is kept in high confidentiality, publicly available data on CF manufacture is very limited and, in many cases, is lacking in key details that should be incorporated into LCA studies.

Table 2.2. Energy requirement of CF production from different sources

Direct energy consumed (MJ/kg CF)	Reference	Origin
22.7	(Lee et al., 1991)	Calculated
478	(Nagai et al., 2000, Nagai et al., 2001)	Original data from a producer
171	(Bell et al., 2002)	Original data
478, 286	(Suzuki and Takahashi, 2005), JCMA, 2006 (The Japan Carbon Fiber Manufacturers Association, 2006)	JCMA, METI (Ministry of Economy, Trade and Industry)-Industrial data
400	(Hedlund, 2005)	Personal Communication
198-595	(Carberry, 2008)	Original data from a producer
353	(Duflou et al., 2009)	Original data
183-286	(Song et al., 2009)	Previous publication(Suzuki and Takahashi, 2005)
9.62	(Griffing and Overcash, 2010)	Calculated
405.24	(Das, 2011)	Original data from a producer
478,286	(Zhang et al., 2011)	JCMA
198-594	(Asmatulu, 2013)	Previous publication (Carberry, 2008)
353	(Witik et al., 2013, Michaud, 2014)	Previous publication (Duflou et al., 2009)
9.62	(Schmidt and Watson, 2014)	Previous publication (Griffing and Overcash, 2010)
353	(Prinçaud et al., 2014)	Previous publication (Duflou et al., 2009)

Currently, only a small number of LCA analyses for CF and CFRP have been carried out and reported and **Table 2.2** shows that there are significant inconsistencies between reported results in prior studies. Energy intensity of CF production lies in a big range of 198-595 MJ/kg as reported by William Carberry of Boeing Company in 2008 (Carberry, 2008) based on

industrial production while some of data (9.62 and 22.7 MJ/kg) is full out of this range (Lee et al., 1991, Griffing and Overcash, 2010). CFs require a considerable amount of energy to produce, however, neither of these studies link energy requirements to production parameters and fibre properties such as variations in CF mechanical properties (high strength vs high modulus).

Energy mix of the resources are inconsistent in the currently available studies in CF production. Duflou et al. (2009) assumed 162 MJ of electricity and 191 MJ of heat from natural gas and 33.87 kg of steam for 1 kg CF production. This dataset has been used in several subsequent studies (Prinçaud et al., 2014, Witik et al., 2013, Witik et al., 2012) related to CFRP production and assessment of CFRP recycling processes. According to personal communication (Michaud, 2014), impact assessment results using this data corresponded well with the results from a confidential dataset obtained from an industrial contact. Another study (Das, 2011) was performed to investigate the CF production process where the disaggregated energy inputs for PAN precursor and final CF production were presented based on data from industrial production in the United States. In this dataset, natural gas is the dominant energy input: natural gas and electricity consumption per kg of PAN precursor production were estimated to be 232.62 MJ and 2.78 MJ, respectively, and natural gas and electricity consumption per kg of final CF conversion were estimated to be 97.62 MJ and 72.22 MJ, respectively. Asmatulu (2013) presented an approximate 400 MJ of total electrical energy to produce 1 kg of CF, of which 200 MJ/kg was from electricity and the remaining from oil. Nevertheless, there was no explanation for either the acquisition of this value or description of CF manufacture parameters. A specific life cycle inventory model based on available industry information, standard methods of engineering process design, and technical reviews, was theoretically carried out by

Overcash (2010). Total energy mix to produce 1 kg CF was estimated at 6.99 MJ electricity, 3.10 MJ steam and other resources. This analysis, however, is based on simplified assumptions of process efficiency and is supported by insights of actual production processes. As such, energy input data reported in Overcash (2010) is unlikely to be as reliable as that available from other sources. A comparison between the Duflou and Das values is presented in **Table 2.3**.

Table 2.3. Parameters for CF manufacture in Duflou and Das

Parameters	Energy use	Energy mix	Yield	Non-energy Inputs
Duflou	162MJ electricity and 191MJ natural gas,33.87kg steam	Electricity, steam, natural gas	53%	AN, nitrogen, DGEBA
Das	75MJ electricity, 330.24MJ natural gas	Electricity, natural gas	45.6%	AN, vinyl acetate, solvent

Apart from the energy mix data presented above, additional studies have reported total energy consumption for vCF manufacture. The Japan Carbon Fibre Manufacturers Association (JCMA) has published industrial production data for PAN based CF, which is reviewed every five years (Zhang et al., 2011). Initial direct energy consumption data published in 1999 indicated total energy requirement of 478 MJ/kg (42 MJ for raw material and 436 MJ for CF conversion). This data was updated in 2004 as 286 MJ/kg (39 MJ for raw material and 247 MJ for CF conversion) and has not been revised since then. Reported energy consumption decreased significantly between 1999 and 2004 reports. According to Takahashi (2005), this

was because the small CF production scale generated some inefficient manufacturing process, producing various types and qualities of CF. Bell et al. (2002) presented the energy consumption of 171 MJ/kg CF (natural gas and crude oil) in a life cycle analysis of CF (high modulus CF from PAN precursor without graphitisation) and CFRP materials. Song et al. (2009) summarised the energy intensity to be 183-286 MJ/kg based on figures from Suzuki and Takahashi (2005) but the source of the lower value of 183 MJ/kg was not specified in the study. However, these sources did not present either disaggregated energy types or energy data related to processing parameters and fibre properties. Despite these limitations, a number of subsequent studies still employed JCMA data, e.g., (Nagai et al., 2000, Nagai et al., 2001) utilised the initial 1999 data. Takahashi (2005) used the 2004 energy intensity data to calculate the energy consumption of CFRP for automotive applications.

Mass balances of CF production are typically built based on mass yields of PAN production and CF conversion. CF is manufactured by means of PAN pre-fabrication, stabilising (up to 330 °C), carbonisation (1000-1700 °C), surface treatment and sizing. PAN precursor fibre is prepared by a solvent-based polymerisation process from the acrylonitrile (carbon content is 68%) and vinyl acetate as co-monomer. Total yield at this step is about 90%- 95%. During carbonisation, the fibres lose about 40% by weight due to volatilisation of HCN, NH_3, H_2, CO_2, and CO and the final high strength fibre contains 92- 95% carbon (Griffing and Overcash, 2010). Overall efficiency of CF production process is 45.6%- 62% (Das, 2011, Griffing and Overcash, 2010, Duflou et al., 2009). However, mass inputs and mass yields were not described in most studies other than stated above to the best knowledge of the author.

Emissions generated to produce CF are key to measure environmental and health impacts in a LCA study, however, only limited understandings are described in literatures. Carbon losses

can be seen during the carbonisation stage to help remove nitrogen, hydrogen and oxygen during the production processes and the emitted gases thus consist of NH_3, N_2, H_2O, H_2, CO, CO_2, HCN, CH_4, C_2H_4 and C_2H_6. Off-gases from the oxidation process are combusted into H_2O, low-NO_x, and CO_2. HCN and NH_3 can be removed at an efficiency of 95%. However, the quantities of the emissions were only stated in one study (Griffing and Overcash, 2010) based on stoichiometric balances. Therefore, from the perspective of non-energy inputs and outputs of CF manufacture, this literature can be potentially incorporated into a LCA study.

Therefore, it is seen that the main limitations of the CF inventory data up to date are the lack of details of CF manufacture process parameters and disaggregated quantified data (energy inputs and emissions) among CF production stages related to the CF properties. Therefore, a better systematic study based on the industrial data is still demanded to investigate standard manufacture source of CF production to assess the environmental impact.

2.4.1.2 Financial cost of carbon fibre manufacture

In 2015, UK revenues of composites are estimated at $2.3 billion and are expected to grow to $10.2 billion by 2030 (UK, 2016). Virgin CF manufactured from PAN precursor costs $33-88/kg (approximately £20-40/kg based on the exchange rate in 2015) (Carberry, 2008). The cost varies depending on the fibre properties, e.g., high and ultra-high modulus CF for aerospace industry is $1980/kg compared $55/kg for standard modulus CF for the civil infrastructure industry in 2010 (Prince Engineering, 2016). Innovations are being pursued to reduce vCF production cost by developing a less-expensive alternative to PAN precursor and optimising the processing steps (Sloan, 2013). The high cost of vCF is mainly due to the PAN precursor and manufacturing costs which each represent up to approximately 50% of vCF costs

(Warren, 2011). As the manufacturing costs ($9.88/lb or $21.79/kg) account for 53% of the total vCF cost, the vCF price can be estimated at $41.10/kg. Significant cost reduction may be achieved by increased scale-up of plant and line size. Under high volume (see **Figure 2.12** b)), the cost of vCF manufacture can be reduced to $7.85/lb ($17.31/kg), giving a total selling price of vCF at $32.65/kg (Warren, 2011).

Current research aims to reduce the cost of CF production by considering alternative renewable feedstocks (e.g., lignin, textile-grade PAN) and production methods (plasma oxidation, microwave assisted plasma carbonisation). The Oak Ridge National Laboratory (ORNL) (Oak Ridge National Laboratory, 2016) estimates cost of CF production could be reduced by as much as 50% with these approaches, while energy used in its production could be reduced by more than 60%. A key goal of the recently announced Institute for Advanced Composites Manufacturing Innovation (IACMI) is to reduce the embodied energy of CFRP by 50% in five years to ensure and accelerate the use-phase benefits of CFRP (DOE Office of Energy Efficiency and Renewable Energy, 2014). Quadrennial Technology Review 2015 shows that CFRP energy intensity savings would be up to 83%, based on a 40 wt% epoxy – 60 wt% carbon fiber composite part fabricated via resin transfer molding (DOE, 2015).

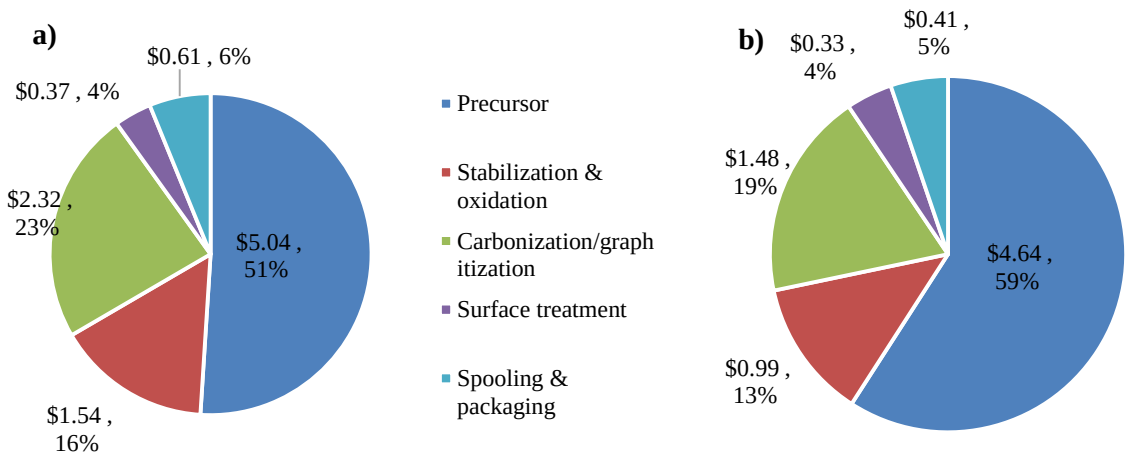

Figure 2.12. a) Baseline b) Scale-up cost breakdown of vCF manufacturing.

2.4.2 Matrix materials

Common matrix materials used for composites manufacture include thermoset and thermoplastic polymers. Matrix materials are associated with different extraction and production energy intensities as shown in **Table 2.4**. These thermosetting and thermoplastic polymers are produced from energy intensive chemical processing, of which the energy intensities vary in a wide range depending on technology, methods, and infrastructure. Epoxy resin as thermosetting resin is commonly used in aircraft and automotive applications. Its energy intensity is relatively larger while providing superior specific stiffness, specific strength and durability. Although thermoplastic resin has the disadvantage of costs, the selection of matrix depends on the performance of composites required. Sometimes, in the composites design, mechanical performance requirement comes first rather than the energy consumption especially in aviation industries.

Table 2.4. Energy consumption of matrix materials

Matrix	Energy intensity(MJ/kg)	References
Epoxy resin	76-137	(Song et al., 2009, Suzuki and Takahashi, 2005, Patel, 2003, Gabi, 2014, Wernet et al., 2016)
Unsaturated polyester	62.8-78	(Song et al., 2009, Suzuki and Takahashi, 2005, Gabi, 2014, Wernet et al., 2016)
Phenol	32.9	(Suzuki and Takahashi, 2005, Gabi, 2014, Wernet et al., 2016)
Flexible polyurethane	67.3	(Suzuki and Takahashi, 2005, Gabi, 2014, Wernet et al., 2016)
High-density polyethylene	20.3	(Suzuki and Takahashi, 2005, Gabi, 2014, Wernet et al., 2016)
Low-density polyethylene	65-92	(Song et al., 2009, Gabi, 2014, Wernet et al., 2016)
Polypropylene	24.4-112	(Song et al., 2009, Suzuki and Takahashi, 2005, Duflou et al., 2012, Gabi, 2014, Wernet et al., 2016)
PVC	53-80	(Song et al., 2009, Gabi, 2014, Wernet et al., 2016)
Polystyrene	71-118	(Song et al., 2009, Gabi, 2014, Wernet et al., 2016)

2.4.3 CFRP manufacture

The manufacturing of CFRP product is the second stage of the life cycle. Typical energy intensities for some common CFRP manufacturing processes are shown in **Table 2.5**. Energy consumed during the CFRP manufacturing is normally used to provide heat and pressure for curing of the matrix. However, energy consumption data on manufacture processes is limited and, in many cases, is lacking in key details that should be incorporated into LCA studies. Data is particularly rare relating to variations in processing temperatures, pressures and mechanical properties of CFRP materials to corresponding energy requirements and specific part geometries and materials.

Table 2.5. Energy intensities of manufacturing processes*

Manufacturing Methods	Energy intensity (MJ/kg)
Spray up	14.90
Filament winding	2.70
Hand lay up	19.2
Pultrusion	3.10
Resin transfer moulding	12.80
Injection moulding (hydraulic)	19.00
Vacuum assisted resin infusion	10.20
Sheet moulding compound	3.50
Cold press	11.80
Preform matched die	10.10
Prepreg production	40.00
Autoclave moulding	21.9-135
Compression moulding	9.06

*Ref: (Witik et al., 2012, Scelsi et al., 2011, Das, 2011, Song et al., 2009, Suzuki and Takahashi, 2005, Duflou et al., 2012)

According to the technical cost models (Dhillon, 2009), the cost of manufacturing is affected by several factors, such as capital equipment, maintenance, utilities, floor space and building, tooling, labour, materials and transportation. All process parameters and production variables are required to be identified throughout the manufacturing process.

2.4.4 Use phase

Use phase is the third stage of the life cycle before leading the CFRP products to end of life. Most studies indicate that use phase consumes 60%- 70% of the total life cycle energy of the

automobiles (Wheatley et al., 2013). Therefore, we can understand the effect of replacement of conventional steel with lightweight aluminium and CFRP in automobiles for lightweighting in terms of environmental impact. Fuel reduction values which can be used to quantify fuel savings via substitution have been reported to be in the range 0.15-0.48 L/ (100km·100kg) (Eberle, 1998, Ridge, 1998, Helms and Lambrecht, 2007, Koffler and Rohde-Brandenburger, 2010, Witik et al., 2011) in automotive applications. Therefore, the quantity of the energy saving from lightweighting is significant to assess the net benefits of substitution as production of lightweight materials are generally more energy intensive than conventional materials.

Previous studies have applied LCA methods to investigate vCF for lightweight vehicle applications but insights from these studies are not consistent. Some studies have found lightweight CFRP components to reduce life cycle energy use and GHG emissions (Suzuki and Takahashi, 2005, Witik et al., 2011, Kelly et al., 2015). Witik et al. (2011) assessed the environmental and cost impacts of replacement using CFRP for a steel vehicle bulkhead component and found weight savings using vCFRP to replace mild steel gives limited environmental and financial benefits in the total life cycle mainly due to high-energy intensity of vCF production.

The JCMA undertook quantitative LCA of contribution of CF for CO_2 discharge reduction in aircrafts, automobiles and wind power generation in the total life cycle (The Japan Carbon Fiber Manufacturers Association, 2016). In aviation, adopting CFRP in 50% of body-wings material results in 20% weight reduction of the total body in comparison with that of conventional type aircraft. Thus the weight reduction can lead to total CO_2 discharge curtailment of 27,000 tonnes/ aircraft/ 10 years as analysed in medium-sized passenger aircraft (Boeing 767). In automotive application, adopting CFRP in 17% of body parts, in total, attains

30% curtailment of total car weight. As a consequence, overall total CO_2 emission reduction is 5 tonnes/ automobile/ 10 years compared to conventional automobiles made of metallic materials.

Contradictory studies, however, have found that weight savings and associated improved fuel economy during the vehicle life are greatly reduced by the high environmental impact of manufacturing components from CFRP, resulting in minimal net benefit (Witik et al., 2011) or even an increase in GHG emissions over the full life cycle (Suzuki et al., 2002). Suzuki et al. (2002) found that the life cycle environmental impacts of lightweight automobiles increased due to the high energy consumption (460 MJ/kg) and CO_2 emission (30 kg/kg) associated with the CFRP production compared to steel (33 MJ/kg and 2.6 kg CO_2/kg). The inconsistency results primarily from data limitations for CF production and assumptions regarding CF production process energy sources (as discussed in Section 2.4.1) and distances a vehicle travels in its life. As shown in **Figure 2.13**, the benefits of lifetime CO_2 reduction of CF materials in replacement of steel depend on the assumptions of travelling distance of a vehicle: the longer travelling distance, the more benefits. However, all studies clearly indicate that CF production is energy intensive and associated with significant GHG emissions relative to conventional materials.

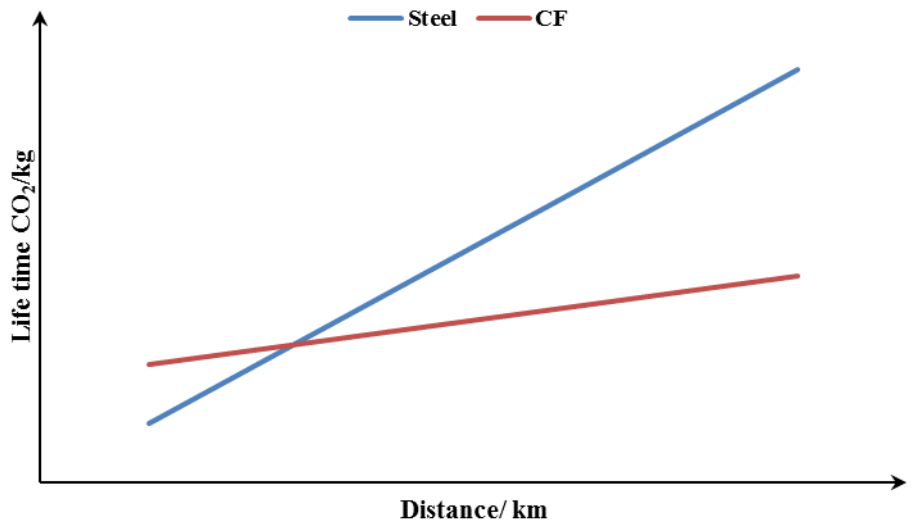

Figure 2.13. Life time CO_2 emissions with respect to travelling distance of a vehicle using steel and CF materials respectively.

Even though, these studies have not considered the end of life of CFRP components and therefore do not completely assess environmental impacts.

2.4.5 CFRP recycling

Recycling has been investigated as an end-of-life method to deal with CFRP wastes as it has the potential to recover the value from the waste materials rather than being disposed of in landfill or incineration. The current recycling methods vary from conventional mechanical recycling to thermal recycling (e.g., pyrolysis and fluidised bed process) and chemical recycling, which have been discussed in Section 2.3. For a comprehensive LCA and financial study, it is therefore significant to include recycling stage in the full life cycle to assess environmental and financial impacts.

Very few studies have been undertaken to assess environmental impacts or financial aspects of CFRP recycling processes. Li et al. (2016) evaluated mechanical recycling of CFRP wastes and compared the environmental and financial performance of reutilising rCF to displace virgin glass fibre and vCF with conventional disposal routes (landfill, incineration). Mechanical recycling was found to be able to reduce GHG emissions, primary energy demand, and landfill waste generation compared to landfilling. This is mainly because mechanical recycling requires the lowest energy intensity which was estimated to be 0.27-2.03 MJ/kg at a recycling capacity of 10-150 kg/h for CFRP compared to 0.17-1.93 MJ/kg for GFRP at the same recycling rate (Howarth et al., 2014, Shuaib and Mativenga, 2016). However, mechanical recycling was found to be not economically competitive when displacing virgin glass fibre due to the high cost of recycling and low revenue.

Although pyrolysis process has been in its early commercial stage, very little data is publically available related to energy efficiency or life cycle impacts of actual processes. An initial estimation of energy requirement is 3MJ/kg for GFRP and 30 MJ/kg for CFRP (Shuaib and Mativenga, 2016). Witik et al. (2013) assessed the environmental impacts of a CFRP pyrolysis recycling technology against landfilling and incineration; however, the study relied entirely on hypothetical data for pyrolysis energy inputs resulting in significant uncertainties. Neither study considered the financial performance of the pyrolysis process.

Hitachi Chemical (2004) calculated the life cycle energy consumption of rCF recycled by depolymerisation of cured epoxy resin under ordinary pressure (Shibata and Nakagawa, 2014). They recycled the tennis rackets made of CFRP having 50 wt% of CF using a processing liquid consisting of alcohol solvent and alkali metal salt as a catalyst under ordinary pressure. The recycling rate varied at 1,000, 2,000 and 17,000 rackets/ month. The energy requirement for

dissolution, cleaning and drying processes was also calculated and summed to get the total energy consumption of rCF. It was 91, 78 and 63 MJ/kg for 1,000, 2,000 and 17,000 rackets /month, respectively. The distillation energy of 38 MJ/kg made up about 60% of the total energy use for 17,000 rackets/month, indicating a further investigation for regenerating cleaning fluids required to reduce energy consumption of rCF.

Keith et al. (2016) made a direct measurement of energy consumption for experimental-scale solvolysis recycling process which is a single process step excluding solvent recovery. The constant power for heating stage was estimated at about 450 W for 85 minutes and fluctuated between 50 and 400 W after reaching 320 °C for 2 hours. Considering the process capacity of 300 g rCF, the specific energy intensity was calculated to be 19.2 MJ/kg rCF. They also predicted that for an optimised process where a lower temperature required and higher reactor loading utilised, the energy demand would be significantly reduced. Solvolysis process allows recovery of valuable organic chemicals and avoid GHG emissions as in thermal recycling process. However, energy is still consumed for the recovery of the solvent and organic chemicals, leading additional environmental impacts.

Although fluidised bed CFRP recycling technique has attracted a great interest among composites community, to date, no study has been reported for an evaluation of the environmental and financial impacts. Compared to other recycling processes, fluidised bed has a key advantage of process compatibility with contaminated and mixed CFRP wastes. Therefore, a LCA study of fluidised bed recycling will have significant implications for researchers in the composites and environment fields, and policy-makers, particularly those investigating the recycling of carbon fibre composites and the environmental and cost impacts.

Overall, prior analyses indicate reduced energy consumption for rCF compared to vCF. However, relevant inventory data for CFRP recycling is not well documented in the literature to date. Energy data for CFRP recycling is based on either hypothesis or literature for lab-scale operation. This results in uncertainties/ limitations of the environmental and financial results as a comprehensive assessment of recycling processes can only be implemented when high quality data is available (Shuaib and Mativenga, 2016). The knowledge gap is also existing in the subsequent manufacturing processes of rCFRP in considering the rCFRP applications as will be discussed in the following sections.

2.5 Manufacturing of rCFRP

It is significant to turn CFRP wastes into advanced manufacturing materials but challenges exist in rCF use. As the rCF is typically in a discontinuous, filamentised form with low bulk density, it is difficult to handle and process directly compared to vCF which is available in the form of continuous tow. A lack of suitable rCF manufacturing methods has limited the penetration of rCF into vCF markets so far.

A range of techniques have been explored for preparing composite materials from rCF, involving rCF specific conversion processes (wet papermaking process (Wong et al., 2009a, Wong et al., 2014) and fibre alignment (Yu et al., 2014a, Wong et al., 2014, Liu et al., 2015)), and adaptations of composite manufacture techniques (sheet moulding compound (Palmer et al., 2010), compression moulding of non-woven mats and aligned mats (Wong et al., 2009a, Pimenta and Pinho, 2011), injection moulding (Wong et al., 2012)) as shown in **Figure 2.14**. As the processes of CFRP recycling, rCF conversion processes, and rCFRP manufacture are energy intensive, there is a need to assess the environmental and financial impacts of the

production routes based on the various processing parameters. As shown in **Figure 2.14**, different manufacturing processes produce different rCFRP products with various fibre volume fractions and as such different mechanical performance. As discussed in Section 2.4.3, energy and cost data on manufacture processes is limited and, in many cases, is lacking in key details that should be incorporated into LCA and financial analysis studies. Therefore, in order to perform LCA and financial analysis, reviews of the manufacturing routes especially the processing parameters, matrix types, fibre volume fractions and mechanical properties are essential for establishment of LCA data.

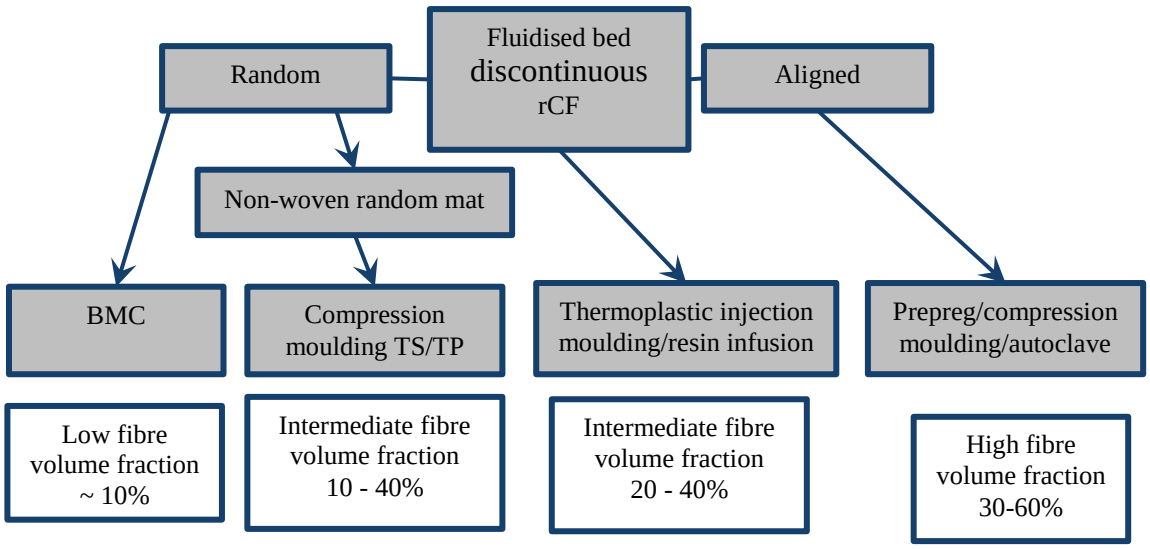

Figure 2.14. Applications for fluidised bed rCF as a reinforcement.

2.5.1 Recycled CF conversion processes

2.5.1.1 Milling

Milled rCF, with fibre lengths in sub-mm scale, can be utilised as a reinforcement or filler in a range of polymers. On a batch basis, milled fibres can be incorporated directly to be used as

filler for thermoplastics mainly for non-structural applications (Pickering et al., 2013). However, because of low mechanical properties as a reinforcement, milled fibres are unlikely for structural applications (Pickering et al., 2016). It is either not financially viable as is very low value.

2.5.1.2 Nonwoven fabric

The wet-papermaking process is used to convert chopped discontinuous rCF into nonwoven CF mats (**Figure 2.15)** which can be manufactured into CFRP with fibre volume fractions (vf) of 20%-40% (Wong et al., 2014, Wong et al., 2009a, Pickering, 2012). The rCF is in a random and predominantly 2D structure existing in the CF fabric. The process starts from the dispersion of rCF using viscosity modifier such as glycerine and water and dispersion agents where the fibre volume fraction of the dispersion fluid is typically less than 1%. The fibre dispersion passes through a slurry to disperse onto a moving mesh experiencing a vacuum suction to drain the liquid for the formation of nonwoven fabric. The final stage is thermal drying to minimise the moisture content of fibre mat for subsequent CFRP manufacture.

Figure 2.15. Random mat manufactured from rCF using modified papermaking process from TFP.

Different techniques are also developed to produce nonwoven fabric, including the dry method introduced in Japan using a carding machine (Wei et al., 2014). The rCF was fed into a carding machine directly without any preparation process. The fibres were carded and the produced thin CF sheets were stacked layer by layer to manufacture CF mats. This method can produce semi-finished nonwoven mat continuously with the cooperative operation of needles and conveyer belt. It makes rCF aligned distributed towards the moving direction.

A method utilising a paper pressing machine in a wet process was also developed to produce nonwoven CF mats comingled with PA fibre (Wei et al., 2016). The process also had mixing stage before the liquid medium (i.e., water) was drained from the container to produce a piece of CF sheet. The size of container thus determined the dimensions of fibre sheet. The fibre volume fraction of the nonwoven mat before subsequent manufacture was experimentally measured to be 20%.

Nonwoven manufacturing processes have been in pilot scale research and can readily be scaled up for commercial application. However, before the scaling up, environmental and financial viability are required to be assessed in the rCF conversion process into intermediate mats for subsequent CFRP manufacture. No such analysis has been conducted previously.

2.5.1.3 Fibre alignment

Fibre alignment is a technique to improve the mechanical properties of CFRP produced using discontinuous rCF. The mechanical performance of CFRP improve along preferential fibre direction after fibre alignment. It is under investigation to achieve higher fibre volume fractions and allow greater control of fibre orientation and resulting higher performance CFRP materials (Liu et al., 2015, Jiang et al., 2006)

Since 1960s, the fibre alignment technique has been in development, e.g., extrusion process (James, 1968), filtration process (Bagg et al., 1971) and centrifugal process (Bagg et al., 1977). The extrusion process could achieve a maximum fibre volume of 50% but ammonium alginate which is solution solvent was non-recyclable, making the process financially infeasible (Wong et al., 2009b). The filtration fibre alignment process is the most widely reported technique which consists of three steps - fibre dispersion, alignment and separation. It can achieve alignment of over 90% in the range ±15° of the preferred direction as with centrifugal process. However, this process is not suitable for production of thicker mats as the permeability decreases across the thickness of mats (Wong et al., 2009b). A hydrodynamic centrifugal alignment rig has been in development at the University of Nottingham based on (Edwards and Evans, 1980) and (Bagg et al., 1977) for aligning and comingling rCF from fluidised bed process with the resin to form a fibre mat (Wong et al., 2009b, Liu et al., 2015) (see **Figure 2.16**). This method can achieve alignment of 90% of fibres within ±10° (Wong et al., 2009b).

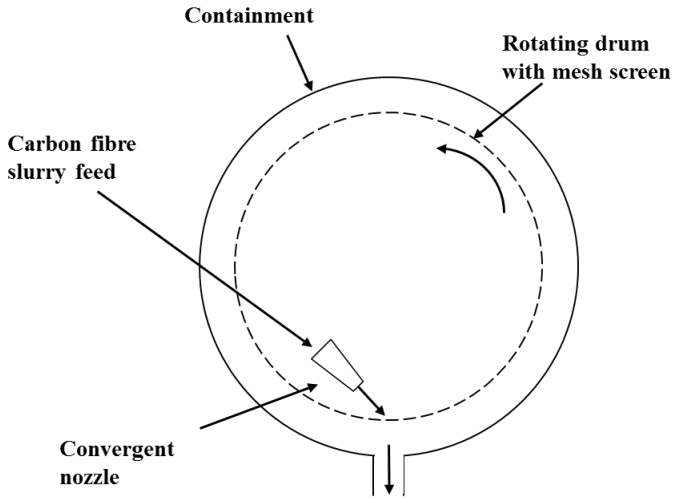

Figure 2.16. A diagram of the fibre alignment process rig.

Parameters such as fibre length and fibre dispersion concentration have a significant impact on alignment quality. It was found that higher fibre volume fraction (44% vf) was achieved at lower moulding pressure (10 bar) without reducing the fibre length (Liu et al., 2015). However, the alignment quality of longer fibre (>5mm) was more sensitive to the increasing of fibre concentration. Nozzle geometry also had an impact on the alignment quality: using nozzle with larger exit open area could reduce fibre volume fraction compared to a nozzle with small exit open area but could bring a higher processing rate and less nozzle blockage.

A High Performance Discontinuous Fibres alignment method has been developed at University of Bristol (Yu et al., 2014b, Yu et al., 2015). The method is based on the momentum change of the fibre suspension in water to align short rCF. It achieved good alignment of 67% in the range of ±3°. The mechanical performance of CFRP using aligned fibre showed improvement compared to that using traditional fibre alignment techniques (Longana et al., 2015). More importantly, as the dispersing medium is water rather than glycerine, it is environmental friendly and cost effective.

Gaps exist in current understanding of fibre alignment techniques while there are significant opportunities to produce high performance rCFRP materials with high fibre volume fraction obtained through fibre alignment. However, trade-offs between the performance benefits and alignment cost and environmental impacts are required to be addressed.

2.5.2 Compression moulding

Compression moulding process is a widely used composite manufacturing technique that is cost efficient for high-volume manufacture and efficient in material usage with minimal

wastage. It has been widely used for moulding of both 2D or 3D nonwoven mats and aligned mats in recycling sector.

The nonwoven mat fabrics discussed previously can be compression moulded with matrix resin (Wong et al., 2009a, Wong et al., 2007, Wong et al., 2014, Wei et al., 2013, Wei et al., 2014) to produce rCFRP products. Mechanical properties of rCFRP manufactured by compression moulding are presented in **Table 2.6**, which are comparable to virgin structural materials.

Previous work at University of Nottingham (Wong et al., 2007, Wong et al., 2009a, Wong et al., 2014, Turner et al., 2010) produced 2D random nonwoven mats using rCF from fluidised bed process and manufactured rCFRP by compression moulding process. It was found that random and discontinuous rCF produced using epoxy resin yielded a fibre volume fraction of 40% at 14 MPa. The mould pressure increased correspondingly with the increase of fibre volume fraction between 10%-40% as shown in **Figure 2.17**. But this consequently broke the fibres during manufacture. Therefore, the maximum strength was found at 30 vf% under moulding pressure of 70 bar. Despite the damage, the specific modulus and specific strength were still comparable to virgin general engineering materials and SEM analysis also showed good fibre-matrix adhesion. Meanwhile, higher pressure requires higher energy consumption, which needs to be assessed for trade-offs between fibre properties and environmental impacts.

Nakagawa et al. (2009) manufactured rCFRP using rCF from depolymerisation of thermoset CFRP under ordinary pressure. Mechanical properties compared favourably to mass production GFRP: tensile modulus of rCFRP is 1.1 times higher and tensile strength is 1.4 times higher than GFRP.

Table 2.6. Mechanical properties of rCFRP produced from different routes

Process	Matrix	Vf, %	E, GPa	σ. MPa	Comment	Source
Mechanical recycling	ABS	24	12	102		(Ogi et al., 2007)
	ABS	24	19	180	Flexural properties Injection moulded	(Takahashi et al., 2007)
	PP	24	6	70	Flexural properties Injection moulded	(Takahashi et al., 2007)
BMC moulding/ SMC moulding	Epoxy resin	10	20	71	Together with calcium carbonate, moulded at 2 MPa.	(Turner et al., 2010)
Compression moulding of nonwoven mats	Epoxy resin	30	37	314		(Wong et al., 2009a)
	Epoxy resin					
	PA fibre	51	25	260	Flexural properties	(Wei et al., 2013)
	UP	16	5.5	90		(Nakagawa et al., 2009)
Compression moulding of aligned mats	Epoxy resin	44	80	422		(Turner et al., 2010)
	Epoxy resin	60	82	1248	Flexural properties	(Liu et al., 2015)
	PP	29	12.6	220		(Jeon, 2015)
Injection moulding	PP	18	16	126	With 5 wt% of G3003 MAPP coupling agent.	(Wong et al., 2012)
	Polycarbonate	16	14	124		(Connor, 2008)

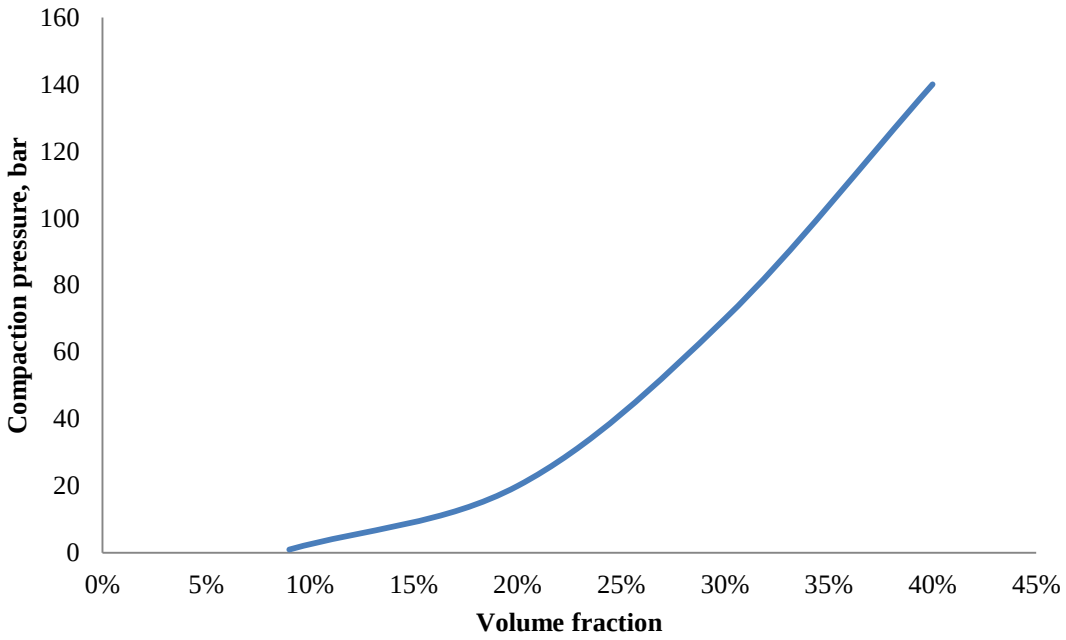

Figure 2.17. Compression moulding pressure against fibre volume fraction for short random nonwoven mats (Wong et al., 2009a).

Compression moulding is also the simplest method to manufacture rCFRP with high fibre volume fraction from aligned mat. CFRP manufactured from 3 mm rCF showed good flexural properties with a fibre volume fraction of 62% and void content of less than 1% (Liu et al., 2015). Although a composite fibre volume fraction of 60% from aligned rCF has been achieved, processing pressures of up to 100 bar were required. This is a question of financial and environmental viability against cost effectiveness due to the high energy and cost requirements and further work is currently being undertaken to gain a better understanding of the process of fibre alignment with the aim of being able to achieve better alignment at lower moulding pressures (Pickering et al., 2016).

Some additional processes might be employed before compression moulding. Wei et al. (2013) produced rCF/PA6 fibre mat using dry carding method and before compression moulding, they utilised a heat and cooling forming process to form substrates following a defined temperature and pressure profile, which might consume additional energy. But to save the compression moulding time, the preform was pre-melted outside and then quickly moved to the mould for forming within 1 minute. A fibre volume fraction of 51% was finally achieved giving the plate a flexural modulus of 25 GPa and flexural strength of 260 MPa.

2.5.3 Injection moulding

Using injection moulding, rCF is normally mixed with typical thermoplastic resin and fillers to be compounded into pellets before injection moulding at the melting temperature of resin and under pressure between 10-100 MPa (Pimenta and Pinho, 2011). There are mainly four parts in an injection moulding facility (i) injection unit, (ii) clamping unit, (iii) driving unit, and (iv) cooling unit. In the injection unit, raw polymer together with additives is fed into the hopper and heated to the molten temperature, and then injected under pressure into the mould. The clamping unit provides the force to open, close and clamp the mould and adequate pressure for injection operation. Normally, it requires a high pressure, typically in the range of 100 to 200 MPa. After injection, the polymer in the mould is cooled down to form a solid state. Cooling is typically achieved by circulating water through chambers within the moulding plate. Ejection step follows the cooling stage to finish the part forming. The drive unit in a hydraulic injection moulding machines consists of a pump and electric motor while it includes only high-speed electric motors in an all-electric machine. Finally, the equipment control unit of the machine controls parameters like barrel temperatures, clamping forces and flow rates (Johannaber, 2008).

Typically, moulding pellets containing 20-40 wt% of short fibres are fed via the hopper into the heated barrel where the temperature is critically controlled. Although the viscous mixture is homogenised by shear deformation, shear has to be controlled to the minimum to avoid overheating and pre-curing for moulded CFRP product. Afterwards, the molten polymer is injected into the mould cavity under recommended pressure. In general, moulding temperatures for CFRP are higher than that for normal thermoplastic process. The typical fibre volume of the CFRP is normally no more than 40%.

Wong et al. (Wong et al., 2012) used injection moulding process to manufacture rCFRP from fluidised bed rCF and polypropylene. The rCF was firstly processed into nonwoven mats using papermaking process and cut into small pellets. After that, the rCF mats were compounded with the pre-compounded polypropylene/ coupling agents into final injected moulding pellets. The interfacial bonding and mechanical performance was improved by adding coupling agent, especially 5 wt% of maleic anhydride grafted polypropylene (see **Table 2.6**). Future technique of extrusion of CF at moderate volume fraction may enable the application of injection moulding method to process rCFRP of high fibre volume fractions.

Connor (Connor, 2008) compounded rCF with thermoplastic polycarbonate resin and injection moulded the compounded pellets to manufacture rCFRP. The rCFRP demonstrated a tensile modulus of 14 GPa, which had 25% reduction compared to vCFRP. The tensile strength, flexural strength and impact resistance were respectively 88%, 98% and 136% of those of vCFRP.

2.5.4 Moulding compounds

Bulk moulding compound (BMC) with rCFs directly incorporated into filled matrices (typically 10% vf), sheet moulding compound (SMC) with fibre volume fraction of 23% (Turner et al., 2010) and advanced SMC with some in-mould flow with high fibre volume fraction (typically 45-50% vf) have been manufactured at University of Nottingham (Pickering et al., 2013). The mechanical properties of the rCFRPs from BMCs was better than that of commercial glass BMCs. However, it is not clear whether the environmental and financial impacts can compete with vGF and vCF products.

2.5.5 Resin infusion

Resin infusion (Jeon, 2015) has been introduced to manufacture rCFRP where reinforcement is laid into the mould with bagging materials but with no resin under vacuum pressure. After bagging process, liquid resin is applied onto the compressed reinforcement materials for infusion under vacuum pressure. After infusion, the curing process is occurred inside the mould under the same vacuum pressure condition. The rCFRP parts have excellent strength and surface quality as reported.

2.5.6 Autoclave

Autoclave moulding is widely used to manufacture high performance CFRP products mainly for aerospace and super cars applications. It is mainly used to manufacture CFRP from unidirectional continuous fibres with typically high fibre volume fractions up to 70%. Therefore, autoclave moulding has also been used to manufacture rCFRP from aligned rCF to achieve a high fibre volume fraction by moulding at pressures of less than 10 bar. The process

started from a standard vacuum bag of rCF and resin to remove trapped air as normally before compression moulding. The compacted materials were then moulded at 120 °C, 7 bar pressure, for 1 hour. Finally, it was cooled down to around 60 °C under pressure before demoulding (Pickering et al., 2016).

2.6 Summary

Due to superior specific strength and stiffness compared to other general engineering materials, the demand for CFRP materials has been increasingly used in transportation sectors. With use of CFRP, weight savings in the lightweight applications lead reductions in energy use and cost and as such reductions of environmental and financial impacts. A number of LCA and financial analysis studies of CFRP use in lightweighting have been undertaken, however, the data of CF manufacture is kept in high confidentiality, publicly available data on CF manufacture is very limited and, in many cases, is lacking in key details that should be incorporated into LCA studies. Moreover, these studies have not considered the end-of-life of CFRP components or relied on hypothetical data and therefore do not completely assess life cycle environmental impacts. The lack of data regarding CFRP recycling process inputs and impacts is a barrier to developing informative LCA and cost models.

Meanwhile, more CFRP wastes will be generated corresponding to the increase of CFRP use and the problem of recycling has been realised as in the review. A range of recycling technologies are at varying stages of development; the fluidised bed process is particularly promising for processing end-of-life products with higher risk of contamination and has been demonstrated at pilot scale. Prior studies have estimated energy requirements of various CFRP recycling technologies, finding substantially lower energy requirements relative to vCF

manufacture while the potentially lower cost of rCF could enable new markets for lightweight materials. However, little systematic work was focused on energy demand and environment burdens of CFRP recycling. No data related to recycling capacity or other processing details were specified in most literature, nor the modelling methodology for the energy intensity. Moreover, there is very limited understanding of the overall financial viability of producing automotive components from rCF. These knowledge gaps are demanded to be addressed for optimisation of recycling practice to produce high quality rCF for lightweighting applications in a cost-effective and environmentally friendly manner.

The handling of rCF and its processing to CFRP are difficult due to its discontinuous, filamentised form and low bulk density; these challenges risk limiting the penetration of rCF into vCF markets. Recycled CF conversion processes (wet-papermaking and fibre alignment) and final rCFRP manufacturing processes have been developed at lab scale and the resulting rCFRP products show competitive mechanical properties compared to vCFRP products. While potential environmental and cost benefits are claimed in technical studies of CFRP recycling processes and fibre reuse opportunities, these benefits have yet to be demonstrated. Their environmental and cost impacts are unknown and no comprehensive LCA and financial study has been conducted previously.

To comprehensively assess the environmental and financial performance of CF recycling, however, evaluations should extend beyond the recycling process and account for the reutilisation of rCF in place of current materials. Due to its excellent retention of mechanical properties after recycling, rCF has potential market in automotive applications. However, the trade-offs of rCF between mechanical performance and cost and environment impacts in substituting conventional automotive materials should be addressed. Process models of

recycling and subsequent manufacturing technologies are thus essential to support the development of LCA model and improve understanding of the overall environmental and financial performance of recovering and reusing CF from waste materials.

CHAPTER 3 ENERGY MODELLING OF FLUIDISED BED PROCESS

3.1 Introduction

Understanding the energy efficiency of the carbon fibre recycling process is critical: energy inputs will be a major factor for environmental impacts of the recycling process, as well as an important operating cost for evaluating financial viability. To date, there are no publicly-available studies assessing the energy requirements of recycling CFRP waste by thermal processes (fluidised bed, pyrolysis) or chemical processes. In the chapter, process models of the fluidised bed recycling process are developed to quantify heat and electricity requirements and predict the energy efficiency of a commercially operating facility. A range of plant capacities are considered in the thesis in order to better understand the implications of plant capacity on energy performance and as such financial and environmental performance. A range up to 6,000 t/yr is considered to evaluate impact of capacity and model outputs are validated with with pilot plant data with a representative plant capacity of 50 t rCF/yr. The model results are then input to subsequent life cycle environmental impact and financial analysis where information on energy inputs of the process are necessary.

The main components of the fluidised bed recycling plant are shown in **Figure 3.1**. CFRP wastes are shredded to smaller sizes before entering the fluidised bed reactor. The silica sand bed is used to volatilise the shredded scrap material and thus to decompose the epoxy resin and release the fibres. The fluidising air is able to elutriate the released fibres, while non-organic contaminants (e.g., metal) remain in the bed. The operating temperature of the fluidised bed is chosen to be sufficient to cause the polymer to decompose, leaving clean fibres, but not too

high to degrade the fibre properties substantially. At the operating temperatures of 450°C to 550°C, resin decomposition products are oxidised to recover energy content. The fibres are then removed from the gas stream by a cyclone or other gas-solid separation device and collected. In the current pilot plant, the gas stream after fibre separation is directed to an oxidiser (combustion chamber) to fully oxidise the polymer decomposition products. Heat is recovered from the oxidiser outlet stream to raise the temperature of fresh air input.

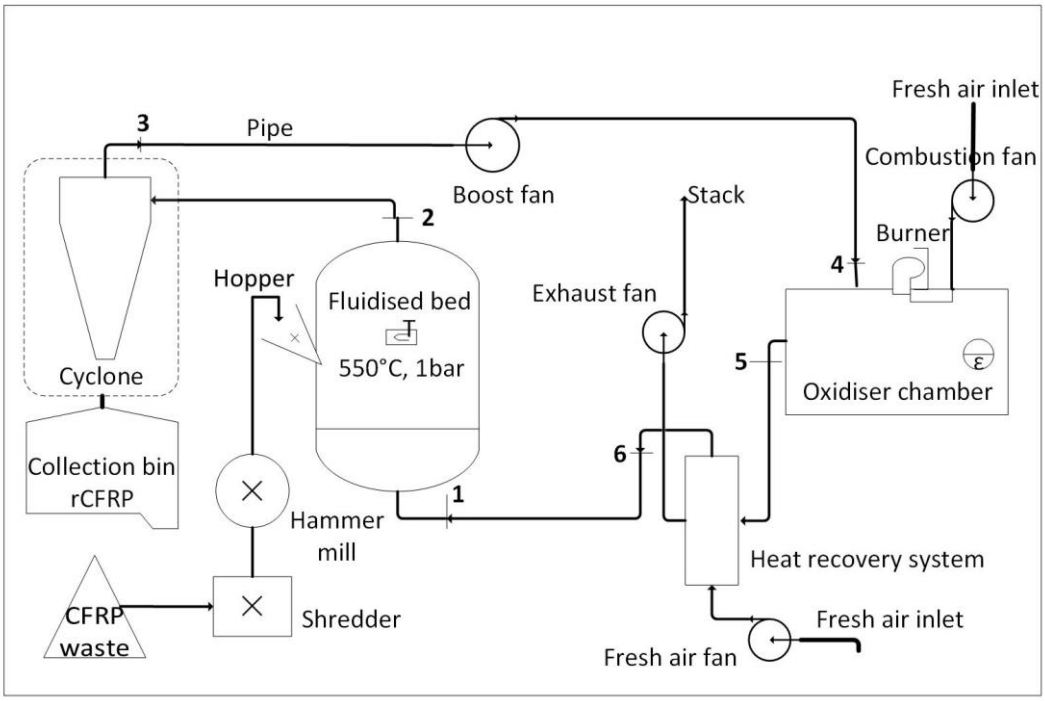

Figure 3.1. Main components and flow directions of the fluidised bed CF recycling process

Mass and energy balances are developed to estimate the energy requirements (electricity and natural gas) of the recycling activities including CFRP shredding, matrix oxidation in fluidised bed, fibre recovery by cyclone, high-temperature oxidation of gas stream and heat recovery. The overall mass and energy balances of the fluidised bed process are assessed by analysing net mass and energy balances of each component within the fluidised bed plant. Parameters for

the fluidised bed model are based on experience from operation of the pilot plant but are selected to best represent expected conditions of a commercial operating facility. Key operating parameters (e.g., plant capacity, feed rate etc.) have an impact on the energy efficiency of the recycling process and thus are evaluated in the model. Energy inputs to the system include natural gas energy input in the oxidiser, electricity input from fans across the plant and additional energy input from resin decomposition. Inefficiencies arise in the process from heat loss to the surroundings and in-leakage of air due to the operation of the system below atmospheric pressure. The fluidised bed plant configuration is optimised to minimise pipework length but allow for practical operation and maintenance. Insulation of equipment and pipework can reduce heat loss and, by extension, the energy requirements of the fluidised bed recycling process. To ensure the evaluation of a realistic process, a financially optimal insulation type and thickness that balances insulation cost (capital cost, CAPEX) and energy savings (operational cost, OPEX) are determined. Fan electrical power is another significant energy input to the fluidised bed system in order to draw air into the system, draw the fluidising gas stream with a set mass flow rate, and to keep the system pressure at a required level. Power requirements for fans are calculated based on mass flow rate in the system (including air in-leakage) and the pressure drop across equipment and piping in the system, which are estimated using standard procedures for conventional equipment utilised in the fluidised bed process.

3.2 Recycling Plant layout

Fluidised bed plant configuration is optimised to minimise pipework length but allow for practical operation and maintenance as shown in **Figure 3.2**. Lengths of pipework are varied as a function of plant capacity as pipe length adapts to maintain adequate spacing when equipment becomes larger. The layouts of components are based on the minimum operating

length between each part while providing adequate spacing around equipment. Considering the maintenance of the facilities and feed materials, two times width of an adult is added to the minimum distance between components.

a)

b)

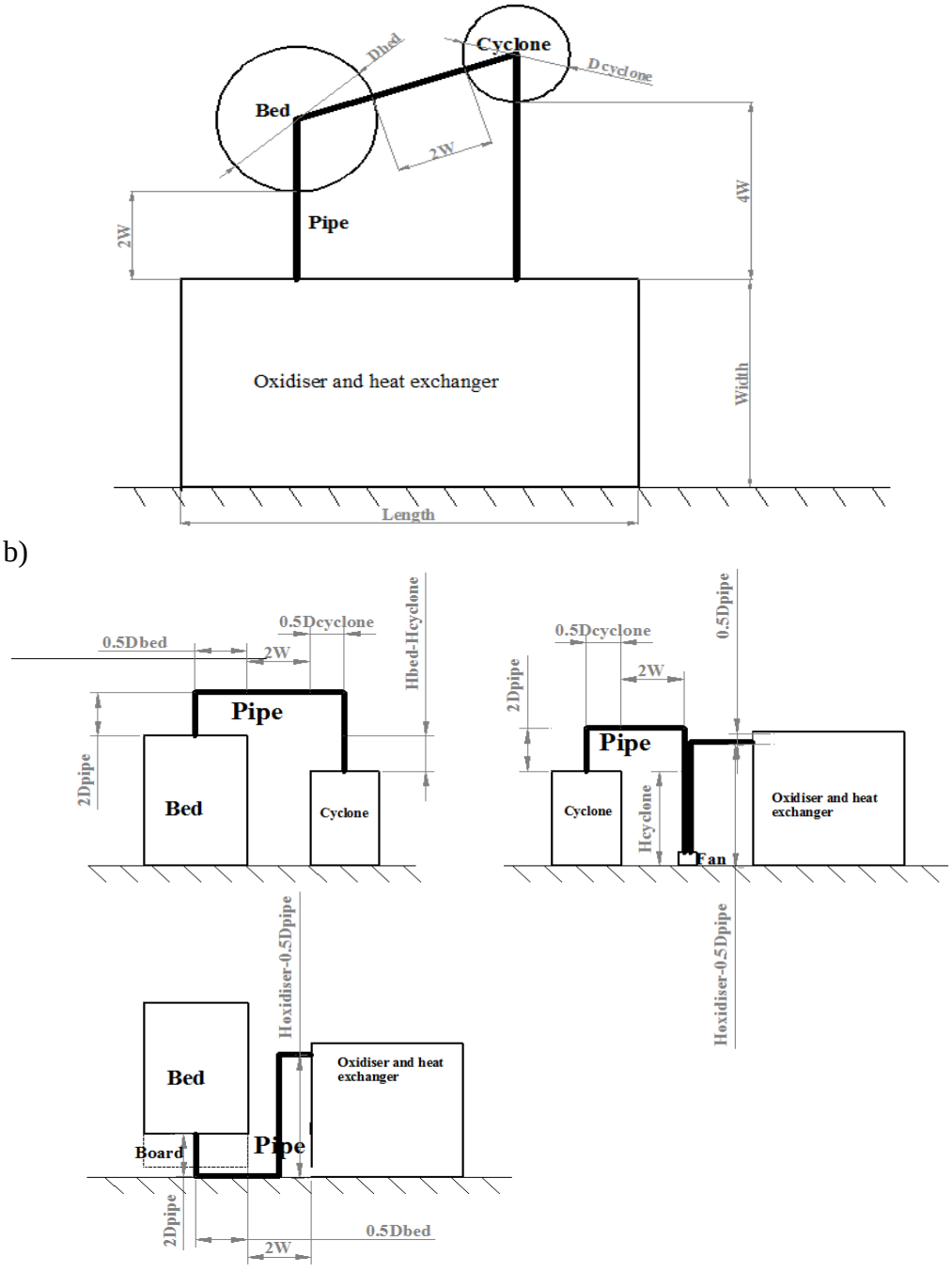

Figure 3.2. a) Plan view of the plant b) Side view of pipework design between each part.

For instance, from the fluidised bed reactor to the cyclone, the pipe exits at the centre of bed to the top centre of cyclone (see **Figure 3.2** b)). The horizontal length is $0.5D_{bed}+ 0.5D_{cyclone}+2W$ while the vertical length is $4D_{pipe}+h_{bed}-h_{cyclone}$, where D_{bed} is the diameter of bed reactor (m), $D_{cyclone}$ is the diameter of cyclone (m), D_{pipe} is the diameter of pipe (m), h_{bed} is the height of bed reactor (m), $h_{cyclone}$ is the height of cyclone (m) and W=0.50m is the average width of an adult. The lengths of pipe can be expressed:

$$L_{bed-cyclone} = 0.5D_{bed} + 0.5D_{cyclone} + 6D_{pipe} + h_{bed} - h_{cyclone} + 2W \quad 3.1$$

$$L_{cyclone-oxidiser} = 0.5D_{cyclone} + h_{cyclone} + h_{oxidiser} + 7.5D_{pipe} + 4W \quad 3.2$$

$$L_{oxidiser-bed} = 0.5D_{bed} + h_{oxidiser} + 1.5D_{pipe} + 2W \quad 3.3$$

3.3 CFRP waste shredding

CFRP wastes are normally found in different sizes and their dimensions are mostly not suitable to be fed directly into the FB reactor; therefore, prior size reduction is required. The selection of a comminution process is dependent on the specific material. The shredding process utilises a two-stage size reduction – large structures would first need to be reduced in size to metre-sized pieces that could then be fed into a twin shaft shredder to reduce the size of the pieces to around 25-100 mm scale. Thereafter, the waste is fed to a hammer mill which is widely used in industry with a screen size of 5-25mm. This enables all CFRP waste materials, including EOL scrap or CFRP manufacturing waste containing contaminants such as backing paper on prepreg, to be processed similarly after shredding (Turner et al., 2011). The following images show the form of the composite after secondary and tertiary size reduction processes.

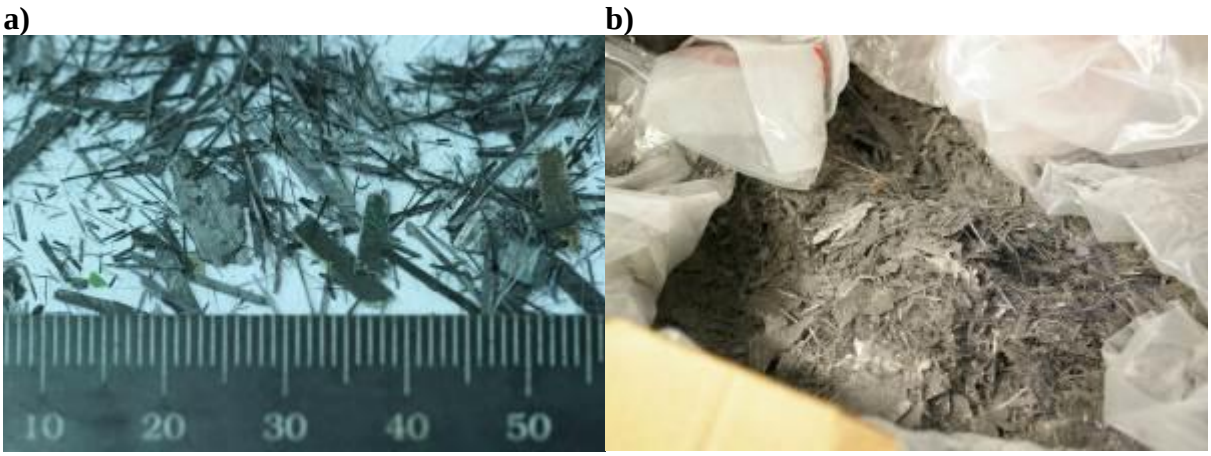

Figure 3.3. a): Shredded carbon/epoxy prepreg laminate (secondary size reduction), b): Composite ready for feeding to the fluidised bed.

The fibre length of 6 mm was identified in previous experimental work to give a good balance of fibre properties and feed rate, but further work is needed to optimise for particular rCFRP applications (Jiang et al., 2005). Current research is investigating how high feed rates of high quality fibre can be achieved considering possibility of continuous regrading of sand to reduce agglomeration.

The electrical energy requirement for the shredding process is modelled using the energy demand model (Howarth et al., 2014, Kim, 2014) where it has been evaluated as a function of the capacity of the shredder that is being utilised in the study. Specifically, the process energy is found to be 2.03 MJ/kg at 10 kg/hr (Howarth et al., 2014) and is expected to be reduced to 0.52, 0.33 and 0.27 MJ/kg if the process rate was increased to 50, 100 and 150 kg/hr, respectively. It demonstrates that when the recycling rate is in a certain range given the shredding machine capacity available, the energy consumption maintains at a similar level. Shredding energy consumption of 0.27 MJ/kg is assumed, based on expected FB capacities.

3.4 Mass and energy balance model of the fluidised bed recycling plant

Mass and energy models of the fluidised bed recycling process are developed based on an optimised plant layout (to minimise pipe length) and assessment of the mass and energy balances of the total process. The models are then utilised to evaluate the impact of key operating parameters (CF feed rate per unit of fluidised bed area (kg/hr-m^2); annual plant capacity (t/yr)) on energy consumption and associated environmental impacts. Key assumptions are established for the energy model development which include:

1) For a given FB plant with an annual capacity (t/yr), the operating hours are assumed to be 7500 hrs/yr.
2) The model is developed based on 1 kg CF recovered from FB process. Waste CFRP is assumed to be from aircraft scrap or EOL prepregs, typically composed of Toray T600SC CF (53% vf; 62% wt) and MTM28-2 epoxy resin. The epoxy resin is assumed to be made of Diglycidyl ester of bisphenol A (DGEBA) in 87 % wt and Isophorone Diamine (IPD) in 13 % wt.
3) The ambient temperature with the system is assumed to be 25 °C. The representative fluidised bed temperature of 550 °C and oxidiser temperature of 750 °C are assumed.
4) For all model variations, equipment and piping are sized assuming a representative fluidising velocity of 1 m/s, pipework air velocity of 20 m/s and optimised pipe length to accommodate equipment size for practical operation and maintenance.
5) There are three heat transfer types in the fluidised bed, i.e., conduction, convection and radiation. Radiative heat loss from pipework has demonstrated less impact on the total heat loss compared to conduction and convection heat loss. This is because the insulation is covered with aluminium cladding that has a low emissivity. In order to

simplify the model, radiation heat loss is assumed to be zero as the bed temperature is below 1000 °C (Jiamjiroch, 2012).

6) As the temperatures in the FB system vary in the range of 500-750 °C, the change of heat capacity (c_p) is very small (Rogers and Mayhew, 1995). In order to simplify the model, we consider c_p to be the same value of 1000 J/(kg·K).

The overall mass and energy balances of the fluidised bed process are assessed by analysing net mass and energy balances of each component within the fluidised bed plant as in **Figure 3.1**, including fluidised bed reactor, cyclone, oxidiser, heat exchanger, stack and pipework between each item of equipment. The outlet temperature and mass flow rate are calculated by accounting for i) heat transfer to and from the component (e.g., heat loss to surroundings; heat input from epoxy oxidation) and ii) in-leakage of air due to system operation at below atmospheric pressure. Mass and energy balance flow of a generic component is shown in **Figure 3.4**. Due to the nonlinear simulations, an iterative method is used to meet the two temperature constraints (i.e., fluidised bed reactor temperature of 550 °C and oxidiser temperature of 750 °C) in the closed fluid flow loop based on the spreadsheet based program. The bed temperature is maintained at 550 °C by adjusting the effectiveness of the heat exchanger that transfers energy from the oxidiser outlet (750 °C) to fresh air prior to input to the fluidised bed reactor. The energy and mass balances for each component are determined by:

$$\Delta E = H_{in} - H_{out} \tag{3.4}$$

$$\dot{m}_{out} = \dot{m}_{in} + \dot{m}_{leakage} \tag{3.5}$$

Where ΔE is the change of the energy of the system (i.e., heat loss $\dot{Q}_{loss}$ from the component or input of thermal energy $\dot{Q}_{in}$), H_{in} is the enthalpy input to the system, H_{out} is the enthalpy out of the system, $\dot{m}_{in}$ is the mass flow rate input to the part or the system (kg/s), $\dot{m}_{leakage}$ is the air leakage rate at the joint point between each part with the system (kg/s) and $\dot{m}_{out}$ is the mass flow rate out of the specific part or the system (kg/s).

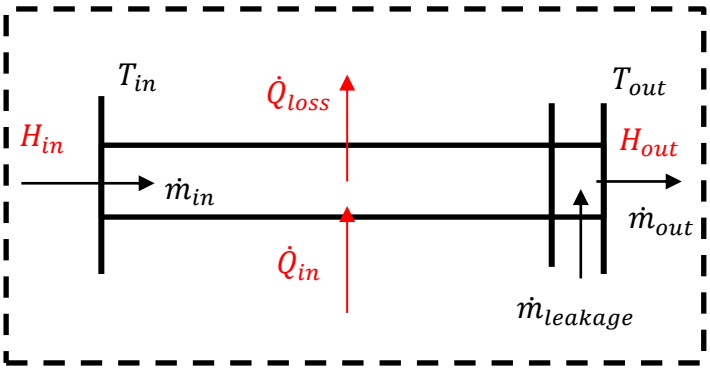

Figure 3.4. Mass and energy balance for a component in the fluidised bed recycling plant

Inefficiencies arise in the process from heat loss to the surroundings and in-leakage of air due to the operation of the system below atmospheric pressure. Energy inputs to the system are quantified by estimating process energy requirements and heat losses for each section within the FB system.

Pipework and equipment insulation is determined by economic optimisation of insulation costs and potential energy savings (see Section 3.6). Fan power requirements are calculated to achieve airflow through the system and to maintain fluidised bed operating pressure at 500 Pa below atmospheric pressure to ensure that there is no leakage of gases from the system into the air (Jiamjiroch, 2012). The energy model is verified by comparing with experimental results from the pilot plant (see Section 3.8). Heat losses from components are assessed based on heat

transfer theory. Heat flows from equipment to the surroundings ($\dot{Q}_{loss}$) are calculated based on (Incropera et al., 2013):

$$\dot{Q}_{loss} = \frac{(T_h - T_{amb})}{R_{th}} \quad 3.6$$

Where T_h is the fluid temperature (K), T_{amb} is the ambient temperature around the FB system (298.15 K) and R_{th} is thermal resistance (K/W) of the component (see details in Section 3.3.5)

With all energy inputs, heat losses and energy outputs, a closed energy flow of FB system can be built. The two model temperature constraints are fluidised bed reactor temperature of 550 °C and oxidiser temperature of 750 °C. Heat losses reduce temperatures between each part and more energy is required to meet the temperature constraints in the model development.

3.4.1 Insulation optimisation

Insulating equipment and pipework can reduce heat loss and, by extension, the energy requirements of the fluidised bed recycling process. To ensure an evaluation of a realistic process, a financially optimal insulation type and thickness is determined that balances insulation cost (i.e., capital cost (CAPEX)) and energy savings (i.e., operational cost (OPEX)).

Throughout the plant, it is assumed that all equipment exteriors will consist of three materials: stainless steel wall, insulation materials, and aluminium cladding. Thermal conductivity values of the materials are obtained from the polynomial plot of varying thermal conductivity against their corresponding surface temperatures respectively. The following insulation properties and natural gas price are employed in the research:

a) 316 Stainless steel walls & ducting, k=21.973 W/(m·K), t = 3 mm, density ρ=7990 kg/m^3

b) Insulation materials (Aspen Aerogels, 2015, The Engineering Toolbox, 2015)

   (a). Ceramic wool (Superwool 607 HT Blanket): ρ = 96 kg/m^3, P=67.81 £/m^3, insulation temperature range is 0-1200 °C.

   (b). Rock wool (RW5 rigid insulation slabs) 2 x 80 mm: ρ = 100 kg/m^2, P=£27.13/m^3, insulation temperature range is 0-760 °C.

   (c). Pyrogel XT-E: ρ=200 kg/m^2, P=148.51 £/m^3, insulation temperature range is 0-650°C.

   (d). Calcium silicate: ρ=280 kg/m^2, P=159.36 £/m^3, insulation temperature range is -18-650 °C.

   (e). Fibreglass: ρ=100 kg/m^2, P=38.54 £/m^3, insulation temperature range is -30-540 °C.

c) Aluminium alloy 3003 H16 exterior protection: thermal conductivity k=190 W/(m·K), t = 1 mm, P=2.41 £/kg, ρ=2740 kg/m^3 (Metal Suppliers Online Inc., 2015)

d) Natural gas in UK is 0.0125 £/MJ with the average value in the year of 2013 (Dempsey et al., 2015).

The analysis considers only the cost of insulation materials and aluminium cladding and the cost of natural gas. All the other costs (e.g., capital equipment; construction; non-gas plant operation costs) are assumed to remain constant and are therefore not considered. This simplified analysis allows us to evaluate the marginal impact of insulation on recycling costs and therefore determine the financially optimal insulation type and thickness. All costs are converted to a present value assuming an insulation life of 10 years and discount rate of 15%.

The formula concerned with determining the present value of electricity and natural gas usage is developed as followed (Dhillon, 2009):

$$PV = PA \cdot \frac{1-(1+i)^{-n}}{i} \qquad 3.7$$

Where *PV* is present value of the total cost, *PA* is present value made at the end of the first year, *i* is annual compound interest rate (15%), *n* is the interest period (10 years).

Figure 3.5 describes the resistance network for the pipework from the hot fluid to steel wall to insulation materials to cladding in the system and finally to the ambient environment. To simplify the development of the model, we assume radiative heat loss is negligible, thus there are only convective and conductive heat transfers within the system. We can then determine the overall thermal resistance for the pipe as the sum of the thermal resistances of each layer within the steel wall, insulation and aluminium cladding. Thermal conductivity is dependent on temperature and therefore should be calculated using the mean temperature ((T_1+T_2)/2) across a solid material.

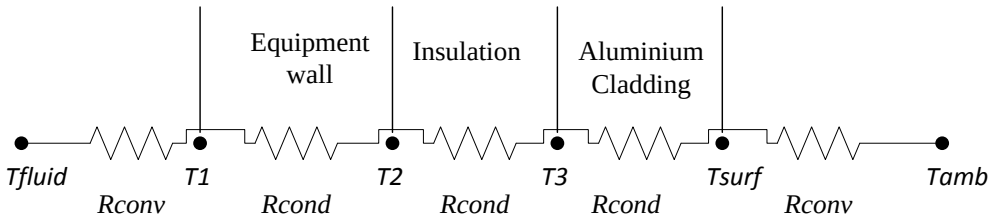

Figure 3.5. Network of nodes and connecting resistances for calculating heat loss form system components.

3.4.2 Thermal model of the fluidised bed reactor

The fluidised bed reactor energy balance includes heat input (energy input + that from matrix oxidation) and heat loss to the surroundings. The heat released by matrix oxidation is calculated based on the matrix energy content (32.22 MJ/kg (Hodgkin et al., 1998)), assuming all heat is released within the reactor.

To calculate heat loss from the fluidised bed reactor, the reactor size must first be determined. For a given feed rate per unit bed area (q_a), the bed cross-sectional area can be calculated based on the waste CFRP feed rate. The feed rate per unit bed area is an important factor in FB process design; a range of 3-12 kg/m^2-hr is considered.

For a fluidised bed reactor, there is a constant bed diameter/height ratio of 1.36:1, which has been justified in the current pilot plant design and is assumed to be relevant for the facility capacities considered in this study. As such, the fluidised bed reactor surface area can be calculated based on the determined bed area. Since the fluidising bed velocity is assumed to be 1 m/s previously, the mass flow rate can be therefore calculated by the equation below;

$$\dot{m}_{bed} = \rho \mathrm{A}_0 v_{bed} \tag{3.8}$$

Where ρ is the air density at 550 °C at 1 bar, which is 0.43 kg / m^3; A_0 is the cross sectional area in the fluidised bed; v_{bed} is the air velocity in the bed which is assumed to be 1.0 m/s.

Considering the bed temperature constraint of 550 °C, the input temperature to fluidised bed reactor can be calculated as below:

$$T_{bed} = \frac{\left(c_p(\dot{m}_{bed} - m_{leakage})R_{th} - L_{oxidiser-bed}\right)((T_{bed-in} + 550)/2 - T_{amb}) + Q_{epoxy}R_{th}}{c_p R_{th} \dot{m}_{bed}} + T_{amb} \tag{3.9}$$

Where $\dot{m}_{bed-in}$ is the air mass flow rate before going into the fluidised bed reactor (kg/s), T_{bed-in} is the temperature before going into the fluidised bed reactor (K) (see **Figure 3.1**), Q_{epoxy} is the energy released from oxidation of epoxy resin (W), $L_{oxidiser-bed}$ is the pipe length from oxidiser to the bed (m) as described in Section 3.3.2.

Based on the experimental performance of FB plant, more than 90% of oxidation of epoxy resin occurred in the fluidised sand bed reactor. The energy release from oxidation of the polymer can be considered as an additional energy input to the fluidised bed reactor, which is calculated based on the matrix energy content (32.22 MJ/kg (Hodgkin et al., 1998)), assuming all heat is released in the fluidised bed reactor. Considering fibre mass fraction of CFRP waste is 62.4%, heat value (kW) of oxidation of epoxy resin for 1 kg CFRP can be calculated as:

$$Q_{epoxy} = \frac{1000\Delta H_c^0 q(1-M)}{3600} \quad 3.10$$

Where ΔH_c^0 is the calorific value of epoxy resin (MJ/kg), q is the feed rate of CFRP waste (kg/hr), M is the fibre mass fraction of CFRP

Due to the energy contribution from oxidation of epoxy resin, the energy balance of the flow going to fluidised bed reactor can be altered:

$$Q_{epoxy} + H_{in} = Q_{loss} - H_{out} \quad 3.11$$

3.4.3 Thermal model of pipework

Pipework diameter is sized to achieve an air velocity of 20 m/s (neglecting in-leakage of air). We can calculate the cross sectional area through the pipe as below;

$$A = \frac{\dot{m}_{air}}{\rho v_{pipe}} \quad 3.12$$

Where $\dot{m}$ is the air mass flow rate with no air leakage in the system, calculated by **eq 3.11** to achieve the set fluidising velocity; ρ is the air density at 550 °C at 1 bar, which is 0.43 kg / m^3; v_{pipe} is the air velocity in the pipe which is assumed to be 20 m/s. Pipework heat loss is then calculated based on the pipe geometry (including insulation) and minimum length as described in Section 3.2.

3.4.4 Thermal model of cyclone

The cyclone is utilised to separate CF from the gas stream using centrifugal force from the spinning gas stream. It is sized assuming a constant ratio between the fluidised bed height and cyclone height to separate a certain ranges of sizes of rCF as in the current pilot plant. Therefore, the height of cyclone can be determined and as such cyclone diameter based on the constant diameter/height ratio of cyclone. Heat loss from the cyclone is modelled from all surfaces.

3.4.5 Thermal model of oxidiser

The mass and energy balance of the oxidiser accounts for energy inputs from the combustion of natural gas, associated combustion air to achieve a fixed air-fuel ratio, and heat loss to surroundings. Natural gas combustion in the oxidiser has been experimentally investigated, indicating an air/fuel ratio of 18.5:1 and natural gas calorific value (ΔH_c^0) of 39.30 MJ/m^3 (Hodgkin et al., 1998). Efficiency of delivering heat from gas combustion is considered to be 100% as combustion occurs within the process air flow; heat losses from the oxidiser are calculated separately. Heat input in the oxidiser is to raise the temperature of the air flow to 750 °C and is dependent on the inlet temperature and heat loss from the oxidiser to its

surroundings. The quantity of gas required to deliver a quantity of heat input (Q_{gas}) can be calculated as:

$$\dot{V}_{gas} = \frac{Q_{gas}}{\Delta H_c^0} \quad 3.13$$

Combustion air input can then be calculated by:

$$\dot{m}_{combustion\ air} = \rho_{air} \dot{V}_{gas}\, \mu \quad 3.14$$

Where ρ_{gas} is the density of natural gas and μ is the air/fuel ratio.

Heat loss is calculated based on the oxidiser dimensions. The oxidiser is sized assuming that its volume is proportional to the air flow rate within the system and that relative dimensions (length, width, height) are constant as in the current pilot plant. The mass flow and dimensions are present in **Table 3.1**, which have been demonstrated to deliver the required performance.

Table 3.1. Properties of oxidiser of pilot plant

	Mass flow (kg/s)	Length (m)	Width (m)	Height (m)	Volume (m^3)
Oxidiser of pilot plant	0.66	4.24	2.16	2.07	18.96

Surface temperature of the oxidiser used for convection heat loss is estimated at 35 °C based on the experimental measurements taken at the pilot plant facility.

3.4.5.1 Heat exchanger

Two heat exchangers in the system are utilised to recover heat from the oxidiser outlet and transfer to the fresh air inlet. A high-temperature heat exchanger included in the oxidiser can minimise gas input and a low-temperature heat exchanger can recover the heat out of oxidiser.

According to the expression of effectiveness (ε) of heat exchanger below of which the maximum effectiveness is 95%, the outlet temperature to the chamber can be obtained:

$$\varepsilon = \frac{T_{chamber-in} - T_{oxidiser-in}}{T_{chamber} - T_{oxidiser-in}} = \frac{T_{heat\ exchanger-out} - T_{amb}}{T_{heat\ exchanger-in} - T_{amb}} \qquad 3.15$$

Where $T_{chamber}$ is the chamber temperature which is set to be 750 °C, $T_{oxidiser\text{-}in}$ is the input temperature to the oxidiser, which is based on the energy balance in the pipe from cyclone to oxidiser, $T_{chamber\text{-}in}$ is the temperature input from the heat exchanger to the combustion chamber, $T_{heat\ exchanger\text{-}in}$ is the input temperature to the heat exchanger, $T_{heat\ exchanger\text{-}out}$ is the outlet temperature of the heat exchanger going to the fluidised bed.

3.4.6 Stack

The heat exchanger outlet is assumed to be vented to the surroundings through the stack at the temperature of gas leaving the system. Assuming no heat losses from the heat exchanger, we can calculate the stack temperature based on the energy balance across the low-temperature heat exchanger as below. Vice versa, using the stack temperature, the heat loss from stack can be calculated as well based on **eq 3.11**.

$$T_{stack} = T_{heat\ exchanger-in} - \frac{\dot{m}_{air} c_p \left(T_{heat\ exchanger-out} - T_{amb}\right)}{\dot{m}_h c_p} \qquad 3.16$$

Heat losses in the exhaust are mitigated by high efficiency heat recovery from the oxidiser outlet prior to exhausting. Opportunities exist for recovering stack heat loss which could further improve the energy efficiency of the fluidised bed process. The steam may be used to provide onsite heating or to generate electricity through use of a steam turbine and would be the means of recovery of the energy released from the oxidation of resin and fuel used in the oxidiser.

3.5 Electrical energy model of the fluidised bed recycling plant

Electricity is consumed to run fans – boost fan, fresh air fan, combustion fan and system fan as shown in **Figure 3.1**. These fans are operated to draw air into the system or draw the fluidising gas stream at a required flow rate. They achieve slight vacuum through system to prevent release of matrix decomposition products prior to complete oxidation in oxidiser. In-leakage of air thus increases electrical requirement as more air is moved through the system.

Fan power consumption is a function of air volume flow and pressure change through the fan (Schild and Mysen, 2009), which can be expressed as

$$P_f = \frac{\dot{V}}{\eta} \sum_j \Delta p_j \qquad 3.17$$

Where P_f is the fan power (kW); $\sum_j \Delta p_j$ is the total pressure increase in the fan (kPa), which covers pressure drops across the fluidised sand bed, distributor, cyclone, pipes and other components of the fluidised bed plant; $\dot{V}$ is the air volume flow delivered by the fan (m^3/s); η is the total fan system efficiency. The fan system efficiency is assumed to be 50% and the motor efficiency to be 90%, so the total efficiency η is 45%.

Power requirements for fans utilised in the fluidised bed process are then calculated based on mass flow rate in the system (including air in-leakage), which has been calculated in the fluidised bed energy model, and pressure drops across equipment and piping in the system. Pressure rise through boost fan is equal to total pressure drops across the fluidised sand bed, distributor, cyclone and pipes in the fluidised bed plant as present below. The other pressure

drops with the fluidised bed system are covered by the fresh air, combustion and system fans (see **Figure 3.1**).

3.5.1 Fluidised sand bed

According to Davidson et al. (1985), the total pressure drop across the fluidised sand bed is equal to the effective weight of the solid sand particles in the bed.

$$\Delta p_b = \left(1 - \varepsilon_f\right)\left(\rho_p - \rho_a\right)gH \qquad 3.18$$

Where ρ_p is particle density, ρ_p=2560 kg/m^3; ρ_B is particle bulk density, ρ_B=1560 kg/m^3; ρ_a is air density at 550 °C, ρ_a=0.466 kg/m^3; ε_f is the voidage at fluidisation assumed to be the same as the voidage at static condition, $\varepsilon_f = \varepsilon = 1 - \rho_B/\rho_p = 0.391$; H is sand height at fluidisation (assuming zero expansion in sand bed in the onset of fluidization, H=0.12 m; g is the standard gravity, g=9.8 m/s^2.

From the above equation, the pressure drop across the sand bed is closely related to parameters of the sand particle and the height of the sand bed which are constant with the size of the plant.

3.5.2 Distributor

The distributor has two functions in the fluidisation process. Firstly, it acts as a support, holding sand particles, and secondly, it disperses the incoming fluidising air evenly with the sand bed.

Air pressure drops when flowing through a distributor and the pressure drop Δp_d has to be sufficiently large to result in a uniformly distributed flow of air into the bed. The distributor pressure drop could be estimated using a fluidisation engineering rule of thumb (Davidson et al., 1985, Wong, 2006) as shown in equation below

$$\Delta p_d = \varepsilon \Delta p_b \quad 3.19$$

Where ε=0.2-0.4, typically 0.3, Δp_b=pressure drop across fluidised bed (Pa).

3.5.3 Cyclone

The cyclone is utilised to separate rCF from the gas stream using centrifugal force from the spinning gas stream. The total pressure drop across the cyclone, which is considered as an important factor determining the cyclone performance, covers pressure drops at the inlet, inside the cyclone and outlet. According to (Gimbun et al., 2005), about 80% pressure drop is within the cyclone body because of the energy use by the viscous stress of the flow while the remaining 20% is from the flow shrinkage at the outlet, expansion at the inlet and the friction on the surface of cyclone. In general, the cyclone pressure loss depends on pressure drop coefficient and velocity as expressed:

$$\Delta P_c = k \frac{\rho_a v^2}{2} \quad 3.20$$

Where *k* is pressure drop coefficient which is a function of cyclone dimensions (Gimbun et al., 2005), ρ_a is air density at the cyclone temperature (kg/m^3), v is air velocity in the cyclone cylinder (m/s) (20 m/s as assumed).

As the dimension of cyclone has been designed for the specific size of rCF, we can scale up the cyclone using the dimension ratio for various plant sizes. This indicates that the pressure drop from cyclone can be considered to be the same as the current pilot plant based on **eq 3.20**. Experiments have been done to measure the pressure drop through the cyclone where a mean pressure drop of 0.75 kPa at the steady state has been selected for the fan power calculation.

3.5.4 Pipework pressure loss

According to the extended Bernoulli equation (Clifford et al., 2009), frictional head loss is more easily measured and determined from changes in total head, expressed in terms of pressure.

$$H_{T1} - H_{T2} = H_f \qquad 3.21$$

Where H_f is friction head loss ($H_f = \frac{(u_2 - u_1) - q}{g}$), which represents the amount of mechanical energy converted into heat (internal energy), g is the standard gravity, g=9.8 m/s^2. It is the difference in internal energy in a flow between inlet and outlet of the control volume (u_2-u_1) after allowing for any heat transfer (q) and so represents the conversion of energy into heat.

For fully developed flow in round pipes of uniform roughness it is found experimentally that piezometric head falls uniformly along the pipe. The Darcy equation for friction loss in pipes is

$$H_f = \frac{4fl}{d}\frac{v^2}{2g} \qquad 3.22$$

Where f is the friction factor in the range 0.002-0.02, l is the length of pipe (m), d is the pipe diameter (m) and v is the mean flow velocity (m/s). The friction factor, f, is dimensionless; its value depends on the pipe roughness and also on the Reynolds number. For turbulent flow (Re > 2000) in fluidised bed system, roughness is important, and it is usually expressed as relative roughness (k/d), where d is the diameter of the pipe and k is the roughness, the size of the bumps in the wall of the pipe. The Moody chart is a widely accepted method to predict the

friction factor *f*. Therefore, we can obtain the friction factor using the known Reynolds number and pipe roughness of stainless steel pipe.

In a pipe flow system, as well as the losses in the long straight pipes there are head losses due to friction in other parts of the system such as entrances, exits, bends and in components such as valves. It is expressed in the equation below (Clifford et al., 2009):

$$H_f = K\left(\frac{v^2}{2g}\right) \qquad 3.23$$

Where *K* is the loss factor (*K*=0.1 for entry loss, *K*=1 for exit loss) and has a value which depends on the geometry and component involved as described below.

a) Pipe entry loss

When a flow enters a pipe from a larger reservoir, the head loss depends critically on the shape of the inlet. When there is an inlet with a sharp corner there is flow separation, the flow reduces in area at the vena contracta and there are frictional losses due to eddies. The value of *K* is approximately 0.5. For a rounded smooth pipe entry, the *K* value is much lower with a typical value of 0.1 (Clifford et al., 2009). In this study, we utilised a smooth entry, therefore, the head loss due to friction in the entrance is calculated below:

$$H_f = 0.1\left(\frac{v^2}{2g}\right) \qquad 3.24$$

v is the mean velocity in the pipe.

b) Pipe exit loss

Where a pipe exits into a larger reservoir, the velocity reduces to zero and all the dynamic head is lost as friction, so the loss factor K=1.0 (Clifford et al., 2009).

$$H_f = \left(\frac{v^2}{2g}\right) \tag{3.25}$$

v is the velocity in the pipe.

In order to calculate the pressure drop through pipes in the steady state, assumptions have been made as followed:

- Ignore any pressure differences due to changes in height in the pipework;
- There is no external heat transfer, so q=0 (there is frictional dissipation, and so the fluid will get hotter, but there is no external heat input);
- The flow is incompressible (ρ is constant).

Therefore, the steady flow pressure drop through pipes is shown below,

$$\Delta p_p = \rho g \sum_i H_{f,i} \tag{3.26}$$

Where $H_{f,i}$, is the friction head loss along pipes, entry and exit of pipes.

3.5.5 Fresh air, combustion and system fans

Apart from boost fan, there are fresh air, combustion and system fans in the fluidised bed system. Fresh air fan is used to deliver fresh air to the fluidised bed through the heat exchanger system, while combustion fan delivers fresh air to the oxidiser to support the combustion of natural gas. In addition, system fan can extract the off-gases out of the oxidiser through to the stack.

All the other pressure losses within the fluidised bed system are calculated using the fan power measured on the pilot plant (i.e., fresh air, combustion and system fan power). The pressure increases delivered by these fans are considered to be unchanged although the plant would be scaled up. Therefore, these fan electrical power can be easily determined by using **eq 3.27** as below.

$$\Delta p_o = \frac{P_o \eta}{\dot{V}} \qquad 3.27$$

Where Δp_0 are pressure losses from other parts as described above, P_0 is the total power of fresh air, combustion and system fans, η is the total fan system efficiency which is assumed to be 45%, $\dot{V}$ is the air flow rate through fans.

3.5.6 Fan heat generation

Due to mechanical losses in the motor, only 90 % of fan electrical power can be input to the fluidised bed system. Therefore, the heat loss from fan can be expressed

$$\sum_j \dot{Q}_{loss,fan,j} = (1 - \eta') \sum_j P_{f,j} \qquad 3.28$$

Where $\dot{Q}_{loss,fan,j}$ are heat losses from boost fan, fresh air, combustion and system fans, η' is the efficiency of fan power input to the system (90%), $P_{f,j}$ are fan power inputs from boost fan, fresh air, combustion and system fans

3.6 Model verification and validation

3.6.1 Model verification

The FB energy model is verified by calculating the overall system energy balance. The total energy input should equal the total heat losses:

$$\sum_i \dot{Q}_{loss,i} = H_{gas} + \eta' \sum_j P_{f,j} + Q_{epoxy} \quad 3.29$$

Where $\dot{Q}_{loss,i}$ are heat losses including heat losses from each component and fan heat losses due to inefficiency, H_{gas} is natural gas power input; $P_{f,j}$ are electrical power inputs from boost fan, fresh air, combustion and system fans, η' is the efficiency of fan power input to the system (90% in the current work), Q_{epoxy} is heat input from oxidation of epoxy resin in the fluidised bed reactor.

Results of calculations show a correct energy balance, demonstrating that the model accurately applies the desired calculation method.

3.6.2 Model validation

The energy model is validated by comparing outputs with experimental results from the pilot plant. At a steady state, energy consumption of the pilot plant is measured to be 90.9 MJ/kg (natural gas) and 6.5 MJ/kg (electricity) at a feeding rate of 10 kg CFRP per hour. Key properties of the current pilot plant are shown in **Table 3.2** and 26% air in-leakage rate has been estimated based on experimental data. Adjusting parameters including the air leakage rate and pipe length in the energy model, energy consumption required for the plant is estimated to be 84.8 MJ/kg (natural gas) and 12.3 MJ/kg (electricity). This agrees to within 1% of the pilot plant data, demonstrating the model is reliable to be used as life cycle inventory data.

Table 3.2. Representative data for current pilot FB plant

	Bed temperature (◦C)	Chamber temperature (◦C)	Feed rate (kg/hr-m^2)	Air leakage rate (%)	Bed diameter (m)	Pipe diameter (m)	Pipe Length(m)			Cyclone diameter (m)
							Bed to cyclone	Cyclone to oxidiser	HE to bed	
Pilot plant	550	750	6.5	26	1.4	0.31	5.11	23.63	11.12	1.39

CHAPTER 4 ENERGY MODELLING OF RECYCLED CARBON FIBRE COMPOSITE MANUFACTURE

4.1 Introduction

The handling of rCF and its processing to CFRP are difficult due to its discontinuous, filamentised form and low bulk density and this risks limiting the penetration of rCF into vCF markets. A range of techniques have been explored for preparing composite materials from rCF, involving rCF-specific processes (wet papermaking process (Wong et al., 2009a, Wong et al., 2014) and fibre alignment (Yu et al., 2014a, Wong et al., 2014, Liu et al., 2015)), and adaptations of composite manufacture techniques (sheet moulding compound (Palmer et al., 2010), compression moulding of non-woven mats and aligned mats (Wong et al., 2009a, Pimenta and Pinho, 2011), injection moulding (Wong et al., 2012)). Understanding the energy efficiency of the manufacturing process is critical as energy requirements are major inputs to evaluate environmental impacts of the manufacturing process of rCFRP as well as important operating cost for evaluating financial viability. As the processes of rCF conversion and rCFRP manufacture are emerging technologies in the CFRP recycling field, to date, there are no publicly-available studies assessing the energy requirements of rCF processing and rCFRP manufacture techniques. In the chapter, we develop process models for rCF conversion processes (wet-papermaking; fibre alignment process) and rCFRP manufacturing processes (compression moulding; injection moulding) to quantify heat and electricity requirements of hypothetical operating facilities. The process model is based on optimized parameters based on the best performance from previous experiments. Model outputs are validated with literature

values where available and are input to subsequent life cycle environmental impact and financial analysis where required (see Chapter 5 and Chapter 6, respectively).

4.2 Wet-papermaking process

The wet papermaking process has been successfully demonstrated to be an effective way to produce non-woven mats from rCF. CF are dispersed in an aqueous solution for 24 hours' stirring to form a well-distributed fibre suspension, laid into a mat in random orientation, and dried (see **Figure 4.1**). The non-woven mat can then be impregnated with polymer to manufacture composites, or alternatively thermoplastic fibres can be co-mingled with CF during the dispersion stage. Co-mingling has the advantage of bringing reinforcement and polymer fibres close together, reducing the melt flow distance in subsequent manufacturing stages, promoting more complete resin impregnation with minimal void formation. In this study, we evaluate the production of CF mats produced with rCF. Energy and material requirements of the papermaking process are estimated based on experimental data and, where possible, energy efficiency data for standard equipment. Process parameters are selected to achieve fibre dispersion and drying with minimised energy input, based on experimental evidence and model outputs. A critical parameter is the total fibre volume content of the dispersed slurry, which is assumed here to be 0.1% to avoid agglomeration of fibres during processing (Turner et al., 2015). Increasing the fibre content while avoiding fibre agglomeration could substantially reduce the energy requirements for papermaking and is the subject of ongoing research. Details regarding the wet-papermaking process model development are as follows.

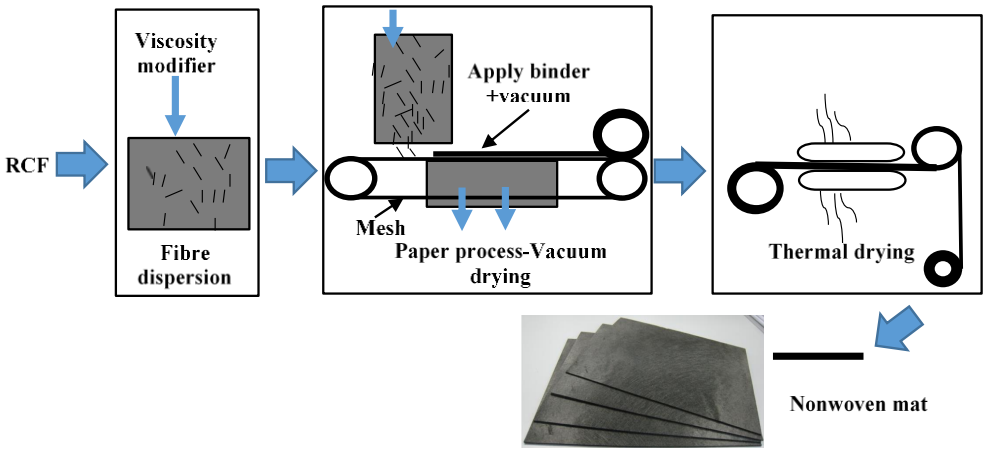

Figure 4.1. Papermaking process for non-woven wet mats.

4.2.1 Fibre dispersing

In this stage, the liquid is assumed to be Newtonian fluid. In a stirred tank with Newton fluid, power consumption has been demonstrated to be influenced by the shear rate and the shear stress (Kumar, 2010, Pérez et al., 2006) as followed:

$$P \propto \mu\gamma^2 V \qquad 4.1$$

Where P is the power input (W), μ is dynamic viscosity of the fluid (Pa·s), γ is the shear rate (s^{-1}) and V is the volume of the fluid in the tank (m^3). It is applicable for laminar, transitional and turbulent flows.

In laminar regimes, γ is linearly related to the rotational speed of the impeller (N) while in turbulent flow γ is a function of $N^{2/3}$. The stirred tank is assumed to be baffled. Shear rate can be estimated using a simple method for all laminar, transitional and turbulent flow. One of the

simple methods is agitator tip speed over the distance between the tip and the tank wall (Kumar, 2010):

$$\gamma = \frac{Nd}{D - d} \qquad 4.2$$

Where *D* is the vessel diameter (mm), *d* is the impeller diameter (mm).

Dispersion energy is estimated assuming commercial-scale process would require the same shear rate as indicated in experimental investigation. In this study, the outer baffled tank has a diameter of 500 mm and a height of 540 mm. The rotating impeller is made of stainless steel (see **Figure 4.2**). It has three 3-mm thick blades with a cross-configuration. The impeller has a diameter of 100 mm and is mounted on an overhead stirrer where the rotation speed can be continually adjusted. The rotational speed is 810 rpm for stirring time of 24 hours and fibre volume fraction is 0.1% according to best performance experimental operation (best fibre dispersion; shortest process time).

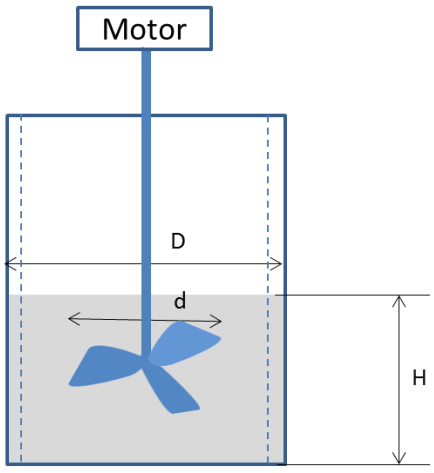

Figure 4.2. A Schematic diagram of the fibre dispersion device.

4.2.2 Drying

Drying is assumed to be achieved by a combination of vacuum drying (with recovery of aqueous dispersion media for subsequent reuse) and thermal drying. The minimum total energy consumption is identified to achieve a final mat moisture content of 1% by these two methods.

4.2.2.1 Vacuum drying

Electricity consumption for vacuum drying is estimated assuming a compressor efficiency of 50% to operate the vacuum at 0.5 bar (50 kPa), taking into account the mass flow rate of air through the vacuum system and energy requirements of the compressor. In the vacuum drying step, the original fibre mat of about 92% moisture content (experimentally measured) is vacuum dried. Vacuum drying can achieve a mat moisture content of as low as 5%, depending on the duration of exposure to vacuum which can be affected by the belt speed and vacuum area. The effects of these processing parameters on the total wet-papermaking process have been analysed and optimized for minimal net energy consumption combination with thermal drying based on experimental operation.

The amount of mechanical energy wasted as a unit mass of air escapes is equivalent to the actual amount of energy it takes to compress it and can be expressed as (Cengel and Boles, 1998)

$$P = \frac{\dot{m}RT_v}{\eta}\frac{\gamma}{\gamma-1}\left(\frac{p_a}{p_v}^{\frac{\gamma-1}{\gamma}} - 1\right) \qquad 4.3$$

Where R is specific constant for dry air (J/kg^{-1}·K^{-1}), $\dot{m}$ is the air mass flow rate (kg/s), η is fan/pump efficiency assumed to be 50%, γ is the specific heat ratio, γ =1.4 for air as the compression is isentropic, T_v is air inlet temperature (K), p_a is atmospheric pressure (Pa), p_a=1 bar=10^5 Pa, p_v is vacuum pressure (Pa).

The specific heat ratio (γ) and the Mach number are the parameters to characterise the static properties and stagnation properties of an ideal gas. In this study, the flow is assumed to be isentropic and the gas has constant specific heats. The critical properties of a fluid are defined as the property under a uniform Mach number and are expressed as (Cengel and Boles, 1998):

$$\frac{p_v}{p_a} = \left(\frac{2}{\delta + 1}\right)^{\frac{\gamma}{\gamma - 1}} \tag{4.4}$$

For air, we have γ =1.4 as discussed above, p_v /p_a =0.5283. This means if p_v <0.5283 p_a then flow through the slots will be supersonic and is independent of p_v. We assume p_v =0.5 bar =0.5×10^5 Pa.

Applying compressible-flow theory, it can be shown that the velocity of air at the slots must be equal to the local speed of sound. Then the mass flow rate of air through cross-sectional area of slots becomes (Cengel and Boles, 1998)

$$\dot{m} = c_d A p_a \sqrt{\frac{\gamma}{RT_v}\left(\frac{2}{\gamma + 1}\right)^{\frac{\gamma+1}{\gamma-1}}} \tag{4.5}$$

Where γ is the specific heat ratio, γ =1.4 for air, c_d is a discharge coefficient that accounts for imperfections in flow through the slots, in a range of 0.60 to 0.97. For the rectangular slots, we use c_d =0.60, A is the cross-sectional area of slots (m^2) as in **Figure 4.3**.

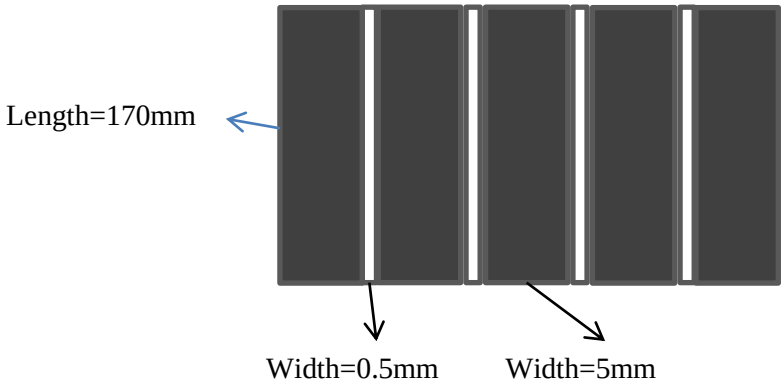

Figure 4.3. Diagram of slots for vacuum sucking.

The belt speed has been optimized to be 60 mm/s going through 4 slots, the time for vacuum sucking of a non-woven mat (100 gsm) with 170×170 mm is 2.83 s. Thus the specific energy consumption for vacuum drying can be calculated using power and time profile.

4.2.2.2 Thermal drying

Similar to a thermal drying process in conventional papermaking industry, the non-woven mat passes over rotating dryer and most of the moisture can be removed by evaporation. Thermal drying is accomplished by passing the non-woven mat over a rotating dryer to achieve the final mat moisture content (the definition of moisture content is given below) of 1%, which has been measured experimentally using an oven drying of the fibre mat product for 24 hours at 110 °C.

$$m_f = m_i \frac{1 - M_i}{1 - M_f} \quad 4.6$$

Where m_f is the final mass after thermal drying, m_i is the initial mass before thermal drying, M_i is the initial moisture content before thermal drying, M_f is the final moisture content after thermal drying.

The thermal energy in this process consists of the heating up, the evaporation load and some amount of heat losses from the dryer body (Kemp, 2012, Ghosh, 2011). It is estimated assuming a dryer temperature of 100°C and accounting for the latent heat of water vaporisation.

$$Q_{actual} = \left(m_w c_{p,w} + m_r c_{p,r}\right)(T_{\mathrm{e}} - T_{\mathrm{amb}}) + mL + Q_{loss} \quad 4.7$$

Where m_w, m_r is the mass of water and rCF mat (kg), $c_{p,w}$,$c_{p,r}$ is specific heat capacity of water and rCF mat ($J/kg^{-1}\cdot K^{-1}$), L is the specific latent heat of vaporization of water with respect to the temperature of drying air (kJ/kg), L=2260 kJ/kg at 100°C, T_e is the evaporation temperature (100 °C) and T_{amb} is the ambient temperature (25 °C), Q_{loss} is the heat supply system loss Q_{loss} = 20%.

Dryer efficiency is expressed as latent heat of evaporation divided by actual heat supplied to the drying system. As heat loss in the thermal process is uncertain under some circumstances, the thermal energy is calculated based on the dryer efficiency. The efficiency of a dryer can be 48.9%-79.4% (Ghosh, 2011, Kemp, 2012) considering the heat losses from the dryer body. A mean thermal efficiency value of 64% is adopted in this study.

4.2.3 Other steps in papermaking process

As shown in **Figure 4.1**, energy is also consumed in the belt conveying, washing and winding process. The fibre suspension is injected onto a moving mesh and then washed to form fibre mat. The blower needed to pressurise the washer consumes electricity and no live steam is required for washing. Waste water generated after washing will be recirculated. The electricity requirement is estimated to be 0.11 MJ/kg fibre mat (Francis et al., 2002) and process yield at this step is assumed to be 95%. The moving mesh is employed to transfer the original form of fibre mat to the following positions. The energy required in belt conveying is mainly in forms of electricity for the motor operation. Electricity use for conveyers is estimated to be 0.07 MJ/kg fibre mat and the process yield is assumed to be 98% (Francis et al., 2002, Suzuki and Takahashi, 2005). Finally, after all previous steps of forming, the fibre mat is wound into a 600 mm roll and energy requirement for winding is estimated to be 0.20 MJ/kg fibre mat (Suzuki and Takahashi, 2005).

4.2.4 Verification

Based on expected process parameters, the total energy requirement is estimated as 14 MJ/kg CF mat with approximately half from fibre dispersion and half from drying. Model parameters for fibre dispersion and drying affect energy requirements of the papermaking process; an assessment of the sensitivity of results due to variations in these parameters and insights are presented in the Chapter 5. As results are based on expected process parameters, it is noted that these could be varied in actual processes which could impact results presented.

4.3 Fibre alignment

A fibre alignment process is under investigation to achieve higher fibre volume fraction and allow greater control of fibre orientation and resulting CFRP properties. As shown in **Figure 2.16**, a fibre alignment process consists of fibre dispersion, alignment, and comingling with resin to form a fibre mat. It can align and comingle the rCF from the fluidised bed process with the resin to form a fibre mat. In general, discontinuous rCF is dispersed in a glycerine aqueous liquid to form a fibre suspension. The suspension is pumped into a pressure pot and then pressurized to form a consistent flow via a convergent nozzle. The nozzle is located above a nylon mesh inside a rotating drum. The mesh screen filters the fibre dispersion to separate the carbon fibres. Vacuum suction is utilised under the mesh to accelerate the dewatering step. The width of the fibre mat can be controlled by the range of the nozzle movement with a linear actuator. One cycle finished when the required veil areal density has been met. After washing, the mat is later subjected to an epoxy based binder application via the paper making process as discussed previously.

Energy is consumed in the steps including fibre dispersing, pressuring, drum rotation, vacuum suction, washing, vacuum drying and thermal drying. This fibre alignment process is still under development, and so energy consumption is estimated based on a target for technology development. For a fibre alignment plant with an annual capacity of 100 tonnes per annum, total power consumption is estimated at 300 kW. Working hours are based on 8 hours per day in the 260 days in a year giving an hourly production rate of 48 kg/hour. Therefore, the target energy consumption of the plant is 22 MJ/kg rCF mat. Due to confidentiality of the process under development, limited details of the fibre alignment process can be given. The implications of this assumption on the results are discussed in Chapter 5.

4.4 Manufacture of composites via compression moulding

The compression moulding process has been widely used as a composite manufacturing technique in rCFRP production. Compression moulding of co-mingled mats to form generic composite components is evaluated as a method to produce rCFRP components. Compression moulding production of rCFRP requires CF mats (random or aligned mats from rCF; prepreg from vCF) and epoxy resin film to be cut to size required to fit into the mould with cutting energy use of 0.37 MJ/kg (Witik et al., 2012). Before applying compression pressure, a standard vacuum bagging procedure is implemented to reduce air entrapment during ply collation and thus to reduce the void content inside the composite (Wong et al., 2009a). Energy consumption for vacuum bagging can be obtained from literature (Witik et al., 2012). Energy requirements of compression moulding consist of thermal energy and mechanical energy are modelled based on the characteristics of standard equipment and required moulding pressure (see **Figure 4.4**). Thermal energy requirement is calculated based on process temperatures, pressure profile and cycle time and heat capacity of materials/equipment using heat transfer theory. To calculate mechanical energy, a hydraulic press has to be selected based on the force/ moulding pressure required. For random rCFRP, the mould is subsequently compressed under pressure of 2 to 14 MPa depending on fibre volume fraction required: higher fibre fraction components requiring higher pressures (Wong et al., 2009a, Quinn and Randall, 1990, Toll and Månson, 1994). For aligned rCFRP, high fibre volume fractions require relatively lower compression pressure (8 MPa) (Liu et al., 2015).

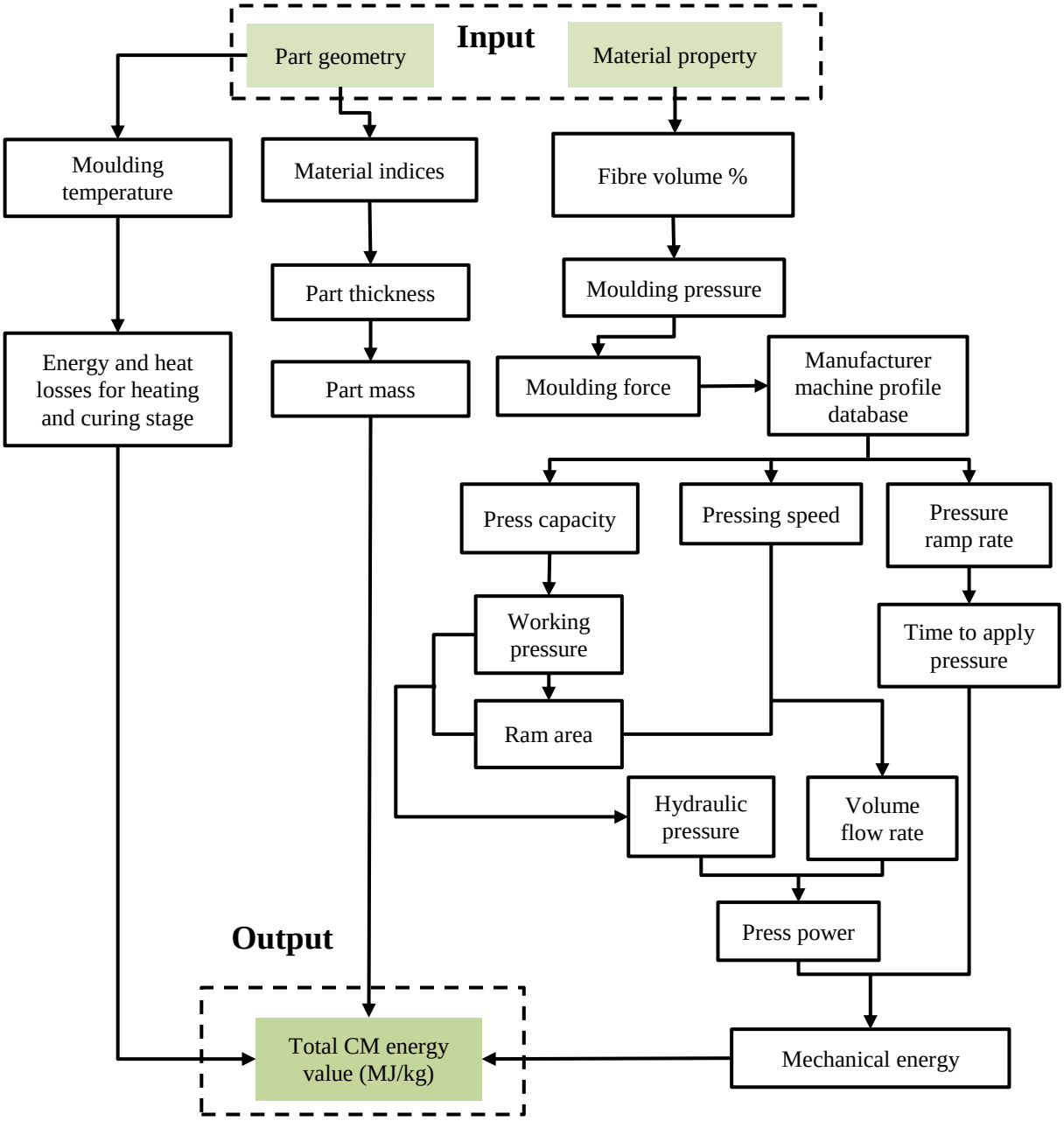

Figure 4.4. Overall approach for estimating compression moulding energy consumption.

The thermal energy required for the moulding process is calculated based on temperature profile and estimated heat losses. In the heating stage, the energy is used to heat the charge and the fibre mats placed in the mould. In the curing stage, the energy supply is equal to heat losses of the mould. To simplify the development of the model, conductive heat loss is assumed to be

negligible. Thus there is only convective and radiative heat loss from the moulding system. Insulation around the mould is assumed to be 40 mm ceramic wool. Energy requirements of the heating stage are calculated by:

$$\sum \mathrm{Q} = \int_{T_a}^{T_c} \left(\sum_i m_i \times c_p \right) dT \qquad 4.8$$

Where c_p and m_i are the heat capacity (J/(kg·K)) and mass of the material (kg), T_a is the ambient temperature input to the component (K) and T_c is the compression curing temperature (°C). The parameters of the compression mould required for the calculation can be found in **Table 4.1**.

Table 4.1. Parameters of the steel tool and mould

Heat capacity of steel, c_p	420	J/(kg·K)
Heat capacity of CFRP mat, c_p	750	J/(kg·K)
Density of steel, ρ	7.8	g/cm^3

Mechanical energy is required to compress the mats at required pressure. Compression is assumed to be provided by hydraulic press and energy requirements are calculated based on the force/ process pressure required for compression and component thickness. Energy consumption is assumed to be in the pressure applying stage. A machine's capacity (F) is a function of the moulding force for the parts. It includes excess capacity and a 25% safety factor beyond the force required. So the moulding force required can be expressed as:

$$F = pA \tag{4.9}$$

Where A is the part's projected area (m^2), p is the compression moulding pressure (MPa).

The moulding force is also related to the hydraulic fluid-pressure. The hydraulic pressure (p_0) can be expressed as moulding pressure as below:

$$p_o = \frac{p \cdot A}{A_0} \tag{4.10}$$

Where A_0 is the ram area (m^2).

The moulding force prediction needs to be adjusted depending on the part thickness as defined by (Strong, 2006):

$$F = A\big(p\ + \rho(t - d)\big) \tag{4.11}$$

Where p is the compression moulding pressure (10-55 MPa), d is the reference thickness (2.5 cm), ρ is the excess depth factor, t is the part thickness (ρ=1.4-2.0 MPa/cm for $t > d$, ρ=0 for $t \leq d$).

Air flow rate through the ram of the press can be expressed as:

$$\dot{V} = A_0\ v$$

Where v is the pressing speed depending on the machine selected (m/s).

Equipment-specific parameters such as the pressing speed, pressure ramp rate and ram area can be used for calculation of mechanical energy. The power (*P*) needed for the compression moulding can be expressed as the flow rate (determined by press speed) times the pressure drop across the hydraulic motor (determined by force) where efficiency of applying pressure is assumed to be 100% (Strong, 2006):

$$P = \Delta p \dot{V} = (pA - p_a A_0)v \qquad 4.12$$

Where *A* is the part's projected area (m^2), *p* is the compression moulding pressure (MPa), A_0 is the ram area (m^2), *v* is the pressing speed depending on the machine selected (m/s), p_a is the ambient pressure (MPa)

The time required to apply the pressure can be calculated based on the pressure ramp rate of the machine profile. Therefore, the energy to build pressure profile for the part can be estimated.

The remaining energy consumed for the finishing step and cooling step. Power consumption and cycle time for the step are assumed to be 10 kW and 2 min (Das, 2011). Water cooling system is utilised in the compression moulding process and the energy consumption is estimated to be 0.90 MJ/kg (2006). Therefore, the total energy consumption of compression moulding is 14.4 MJ/kg for manufacture rCFRP with 20% vf.

4.4.1 Validation

The energy requirement of the compression moulding process has been reported to be 7.2-13.1 MJ/kg (Suzuki and Takahashi, 2005, Das, 2011) for composites. To accommodate for rCF manufacturing process to obtain the mechanical properties assumed in this study, an additional

vacuum bagging procedure (approximately 35% of total energy consumption) was implemented for 30 mins at room temperature before applying the compression pressure to reduce the void content as in previous work (Wong et al., 2009a). Therefore, energy consumption of the compression moulding of rCFRP is slightly higher than normal.

4.5 Manufacture of composites via injection moulding

Injection moulding has been successfully demonstrated to be an efficient way to manufacture high performance rCFRP with fibre volume fraction of 20% -40% in previous work (Turner et al., 2010). As shown in **Figure 4.5**, first, the rCF is compounded with a thermoplastic matrix (polypropylene) to produce composite pellets for input to the injection moulding. To produce rCF-PP pellets, randomly aligned rCF mat (100 g/m^2) is chopped to pellets 4 mm wide and 6 mm long. This may not be the efficient method to manufacture rCF-PP pellets but will be optimized where available in the future study. To ensure bonding between the rCF and PP matrix, PP is first compounded with a coupling agent (MAPP). PP granules and maleic anhydride grafted polypropylene coupling agent (5% by weight) are mixed and extruded at 210 °C with a screw rotational speed of 80 rpm and a residence time of 130 s. The rCF pellets are subsequently compounded with the PP pellet at 18% volume fraction (30% weight fraction) by screw extrusion (210 °C, 50 rpm, and 150 s residence time).

For injection moulding of CF-PP pellets to form the automotive components, recommended parameters are obtained from previous experiments (Wong et al., 2012): injection temperature is 210 °C, ejection temperature is 88 °C, mould temperature is 50 °C, injection pressure is 120-160 MPa and rotational speed is 125 rpm. Although injection moulding is normally used to manufacture relatively small parts and might not be the most appropriate manufacturing

technique for larger parts such as automotive closure panels, it is still a comparable alternative manufacturing route for rCF and worthwhile for investigation of its environmental feasibility.

Compounding energy consumption is calculated accounting for polymer melting, screw driving, and cooling and combined with output of the compounder obtained by the function of solid flow rate and simulation of factors. Injection moulding energy requirements are calculated to account for specific component geometry (mould cavity volume, projected area). Moulding machine parameters, specifically the clamping force, injection pressure/temperature, ejection temperature, and screw drive rotational speed, are used to determine power requirements and combined with cycle time to estimate total energy requirements, based on relationships developed in prior studies (Boothroyd et al., 1994, Madan et al., 2014). Further details on the injection moulding model development and parameters are given as follows.

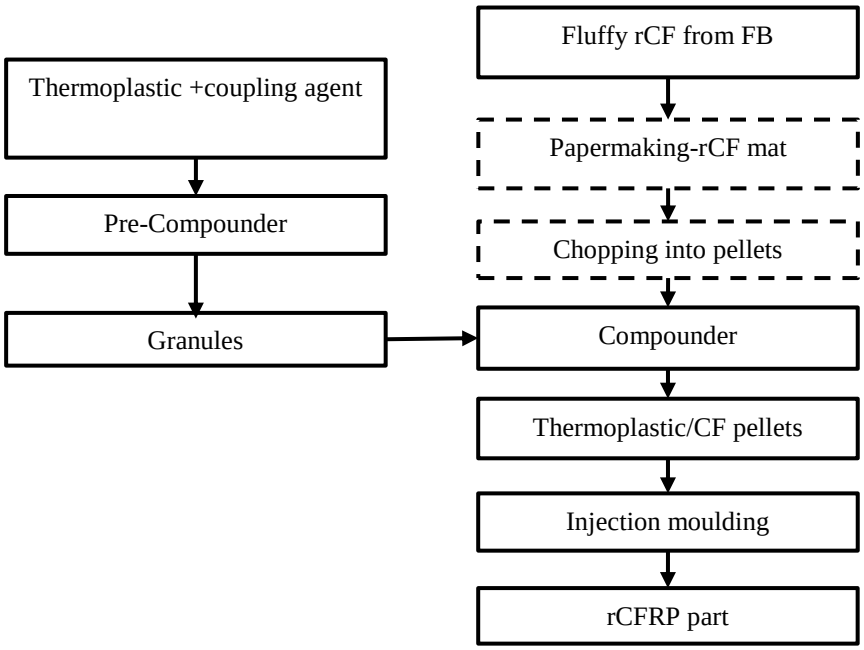

Figure 4.5. Overview of injection moulding processing routes of rCF (dash-lined steps expect to be excluded in future optimisation).

4.5.1 Compounding process

Compounding is considered as one of the fundamental processing stages in the polymer manufacture industry. It is a forming process where polymer is melted, mixed and formed through a die at the end of the channel to solidify the final polymeric materials with a relatively useful size and shape (e.g., pipes, profiles, sheets or films). A typical extrusion system consists of feeding hoppers, a heated barrel to heat, melt and mix the polymer and other fillers, a motor to drive the screw, a die to form the molten polymer into the final size and shape and chiller units for cooling mechanism.

It is typically an energy-intensive process and normally achieves poor energy efficiencies (Abeykoon et al., 2014). Energy requirements for the compounding process are calculated accounting for polymer melting, screw driving, and cooling and combined with the output of the compounder as shown in **eq 4.13** below. With energy consumption and output of compounding process, specific energy requirement can be calculated.

$$E_{total} = E_{melt} + P_{plasticizing} t_p + P_{cool} t_c \qquad 4.13$$

Where E_{melt} is the energy used to melt the resin (MJ), $P_{plasticizing}$ is the energy to drive the screw (kW), t_p is plasticizing time to melt and deliver them for injection (s), P_{cool} is the energy used to cool the mould to return it to a solid state (kW), t_c is cooling time required to cool the polymer to a temperature to solidify within the mould (s).

The output (G) (kg/hr) of the compounder can be obtained as a flow rate function of the conveying efficiency and the feed depth and simulating the effect of these factors on the flow rate using **eq 4.14** (Rao and Schott, 2012)

$$G = 60\rho_0 N\eta_F \pi^2 H D_b (D_b - H)\frac{W}{W + w_{FLT}} sin\theta cos\theta \qquad 4.14$$

Where ρ_0 is bulk density of the polymer (kg/m^3), N is the screw rotational speed (rpm), η_F is conveying efficiency for PP (=25%), H is the channel depth (mm), D_b is the diameter of the barrel diameter (D_b=D_s+2H) (mm), D_s is the screw diameter (mm), W is the channel width (mm), w_{FLT} is the flight width (mm), θ is the helix angle ($\theta = \tan^{-1}\frac{t}{\pi D_b}$) (°), t is the pitch (t=D_s) (mm).

The energy needed to melt the polymer varies according to the crystalline nature of the polymer and as PP is a crystalline polymer, it can be expressed in equation below (Thiriez, 2006):

$$For\ non-crystalline\ polymers:\ E_{melt} = c_p m(T_{mel} - T_a) \qquad 4.15$$

$$For\ crystalline\ polymers:\ E_{melt} = mc_p(T_{mel} - T_a) + \lambda m H_F \qquad 4.16$$

Where c_p is the specific heat capacity of the polymer (J/kg·K), m is the mass of injection shot (kg), T_a is the ambient temperature (K), T_{mel} is the melting temperature of the polymer (K), λ is the degree of crystallization, for PP, λ is assumed to be 60%, H_F is the heat of fusion for 100% crystalline polymer (kJ/kg).

The rotary driving unit of the rotating screw plays an important role in compounding machines. Screw torque and rotational speed convey the polymer and provide the recommended level of shear and homogenisation. The screw speed is required to be constant over the total feeding stroke, therefore, the torque of the drive motor, of whether an hydraulic or electric motor,

should be well-designed. The recommended torque below may be used for a screw diameter of 50 mm (D_{50}) and a screw length of 1000-1400 mm with the L/D ratio of 20-22 (Johannaber, 2008).

For engineering thermoplastics: $T_{50} = 800\ Nm\ to\ 850\ Nm$

As an injection moulding machine is designed to process a large variety of plastics of various viscosities, the drive motors is required to own a wider torque range. By employing the principles of similarity, the torque needed for a specific screw diameter can be expressed using equation below (Johannaber, 2008):

$$T_x = T_{50}\left(\frac{D_x}{D_{50}}\right)^{2.7} \qquad 4.17$$

Where D_{50} is the referenced screw diameter of 50 mm, T_{50} is the corresponding torque value. This equation is related to the principles of transformation, which is also valid for extrusion process.

The dissipated power at a given speed may be calculated using the torque and the rotational speed of the screw:

$$P_{plasticizing} = \frac{\omega T_s}{1000} \qquad 4.18$$

Where $P_{plasticizing}$ is the power input provided by the drive motor (kW), ω is the angular rotational speed of the screw (rad/s), T_s is the torque of the screw (N·m).

There are chiller units for the water cooling mechanism that circulates around the barrel. The cooling power consumption in this study can be directly estimated by a linear relationship between cooling power and compounding power (Weissman et al., 2010) while the residence time for compounding process is obtained from previous experiments (Wong et al., 2012).

4.5.2 Injection moulding process

The energy requirement of injection moulding operation is reported to be low compared to material costs (Ribeiro et al., 2012). But it is still a key parameter of environmental impacts and critical to the whole sustainability strategy. Currently, few processing parameters are accessible in the product design stage, so in this study the energy requirement of injection moulding are modelled based on standard equipment applied to particular materials and part geometry. The estimation of energy consumption for injection moulded parts has been summarized into the following four steps, as shown in **Figure 4.6**. Manufacturing energy consumption is discussed followed by estimation of injection moulding cycle time.

i. Determine a runner system and shot volume based on the part geometry.
ii. Estimate the moulding machine parameters based on the processing requirement, e.g., shot volume, projected area and clamping force.
iii. Estimate the moulding cycle time in each stage and throughput based on machine parameter and part geometry.
iv. Determine energy consumption for manufacturing in each step.

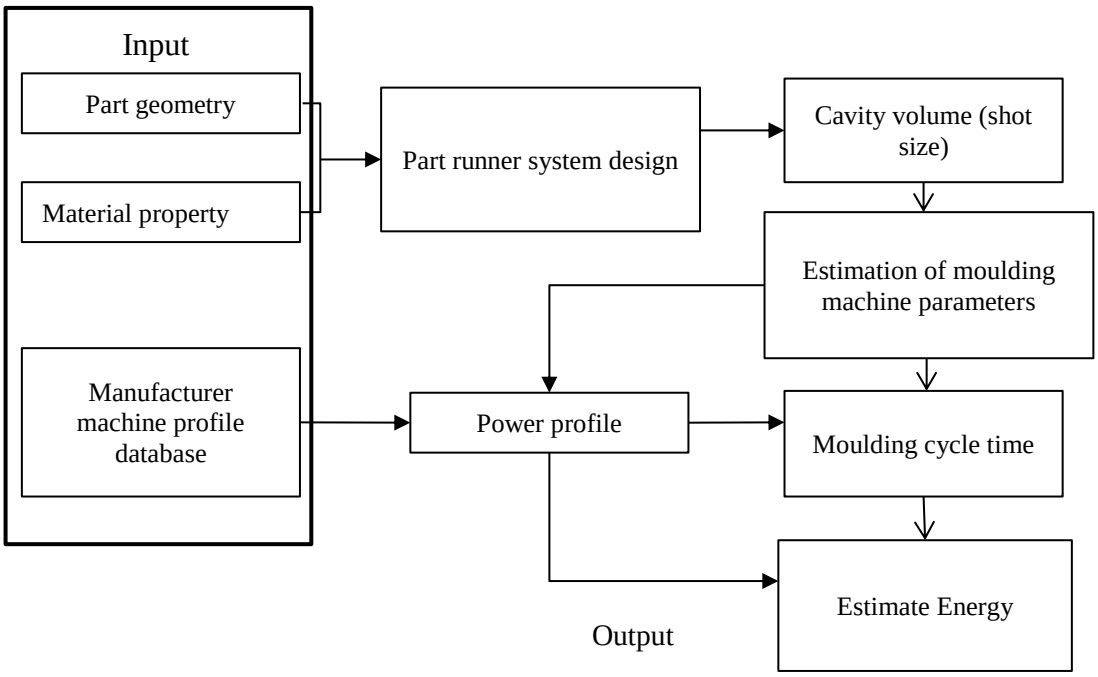

Figure 4.6. Overall approach for estimating injection moulding energy consumption.

4.5.2.1 Selection of moulding machine

First, the volume of the runner system can be determined according to the part volume calculated as given in **Table 4.2.** Also, the mould cavity volume can be determined simultaneously by the part volume and runner system.

A mean injection pressure of 140 MPa is recommended for injection moulding operation while the maximum cavity pressure is only estimated as 50% of the recommended injection pressure (Johannaber, 2008). For the selected injection moulded part, its projected area multiplied by the maximum cavity pressure enables the calculation of the clamping force required. As clamping force is used to keep the moulding in whole closed state in the total cycle time, it is a key parameter of an injection moulding machine size. Therefore, the recommended moulding

machine parameters can be selected from injection moulding machine profile accordingly (Mitsubishi Heavy Industries Plastic Technology Co. Ltd., 2016) as listed in **Table 4.3**.

Table 4.2. Runner volumes (%) for selected parts (Johannaber, 2008)

Part volume (cm^3)	Shot size (cm^3)	Runner, %
16	22	37%
32	41	27%
64	76	19%
128	146	14%
256	282	10%
512	548	7%
1024	1075	5%

Table 4.3. Injection moulding machine profile

Clamping force (kN)	Opening stroke (max) (mm)	Screw diameter (mm)	Injection capacity (cm^3)	Drive motor (kW)	Dry cycle time (s)
300	310	25	43	7.5	1.7
500	250	28	62	15	1.1
750	300	32	94	18.5	1.2
1000	350	36	143	22	1.3
1250	375	40	201	30	1.4
1800	430	45	254	37	1.5
2600	510	56	510	45	1.8
3500	610	71	982	55	2.3

4.5.2.2 Injection moulding cycle time

Total injection moulding cycle time can be divided into separate steps, i.e., injection time, plasticising time, cooling time and mould resetting time, as expressed by the equation below;

$$t = t_i + t_p + t_c + t_r \quad (4.19)$$

Where t_i is injection time required to fill the mould cavity with molten polymer (s), t_p is plasticising time to melt and deliver them for injection (s), t_c is cooling time required to cool the polymer to a temperature to solidify in the mould (s), t_r is the resetting time required to open and close the mould (termed as dry time), to eject the part from the mould and to place inserts in the mould and to apply parting agent (s).

Injection moulding machines are able to achieve the required flow rate for injection with the injection units. During injection stage, the full injection power is assumed to be utilised and the recommended injection pressure is achieved. Thus, the maximum flow rate (m^3/s) within the mould can be expressed below.

$$Q_{max} = \frac{P_i}{p_i} \quad (4.20)$$

Where P_i is injection power (W), p_i is recommended injection pressure for a specific polymer (Pa).

However, in practice, due to the flow resistance in the mould channels and the channel shrinkage from solidification of polymer against the walls, the flow rate reduces in the filling stage. Therefore, the average flow rate (Q_{avg} (m^3/s)) is calculated using equation (Boothroyd et al., 1994).

$$Q_{avg} = \frac{0.5P_i}{p_i} \quad 4.21$$

$$t_i = \frac{V_s}{Q_{avg}} = \frac{2V_{shot}p_i}{P_i} \quad 4.22$$

Where V_s is the required shot size (m^3)

Thus we can obtain a rough estimate of the polymer filling time using the cavity volume (cm^3) and the injection rate (cm^3/s). Next, depending on the thickness and complexity of the moulded product and requirements for dimensional precision, add on time for dwelling to calculate the injection time.

Note that the injection rate of a moulding machine is influenced by injection speed controls, cavity wall thickness and shape, gate cross section surface area, material grade, moulding conditions (polymer temperature, mould temperature, injection pressure) and more.

While these factors influence injection rate, the injection rate is usually 0.53-0.88 $cm^3/(s \cdot g)$ in a standard inline screw injection-moulding machine (Johannaber, 2008).

When the screw diameter and *L/D* ratio are selected for injection, key dimensions of screws for processing can be determined accordingly (Johannaber, 2008). In this study, all parameters have been shown in **Table 4.4**.

The tangential velocity at the barrel surface can be calculated based on the rotation speed and dimensions of the screw.

$$v = \frac{\pi ND}{60} \quad 4.23$$

The forward channel velocity is thus calculated

$$v = \frac{\pi ND}{60} cos\theta \quad 4.24$$

The length of the screw has already been determined by the *L/D* ratio of the selected injection moulding machine, the residence time for plasticizing can be estimated.

Table 4.4. Dimensions of the screw (Johannaber, 2008)

Screw diameter (mm)	Screw length (mm)	Channel depth (mm)	Pitch (mm)	Flight width (mm)	Channel width (mm)	Barrel diameter (mm)	Helix angle, θ (°)
25	500	3.76	25	2.5	22.66	32.51	13.75

Cooling time is reported to cover more than 50% of the whole cycle time, so it is important to get a good understanding of cooling in the mould. The molten polymer has to be cooled from injection temperature to the recommended ejection temperature. The variation of temperature across the wall thickness within the changing time follows the one-dimensional heat conduction principle in a plane-parallel plate.

$$\frac{dT}{dt} = \alpha \frac{d^2T}{dx^2} \quad 4.25$$

Where *T* is temperature (°C), *t* is time (s), *x* is the distance from centre plane of wall to the plate surface (mm), α is thermal diffusivity coefficient (mm^2/s).

Based on the above equation, the first-term solution to express the relationship between cooling time and the central temperature of the mould is given by:

$$t_c = \frac{{h_{max}}^2}{\pi^2 \alpha} ln \frac{4(T_i - T_m)}{\pi(T_x - T_m)} \quad 4.26$$

Where h_{max} is the part thickness (mm), α is thermal diffusivity coefficient (mm^2/s), α =0.08 mm^2/s, T_i is the polymer injection temperature (°C), T_x is the recommended ejection temperature (°C), T_{mol} is the recommended mould temperature (°C).

The processing data and machine parameters used for estimating cooling time are shown in **Table 4.3** (Johannaber, 2008, Boothroyd et al., 1994, Wong et al., 2012). It should be noted that the above calculation is likely to underestimate the cooling time for very thin wall mouldings. Three seconds is suggested to be the minimum cooling time despite a smaller value obtained from **eq 4.26**.

Resetting time is defined as the sum of time required to open and close the mould and eject the part from the cavity. It depends on the part separation movement from the mould cavity and upon the time to clear the part from the mould plates.

To obtain the estimation of resetting time, the maximum clamp strokes and dry cycle time are introduced. The time required for injection unit operation and the mould opening and closing at the maximum clamp stroke is referred to as the dry cycle time. The dry cycle time can be obtained for a selected machine, as shown in **Table 4.3**.

It is assumed that mould opening time is 40% of closing speed and the moulded part falls during a dwell of 1s between the plates. Therefore, for a given injection moulding machine, the mould resetting time can be expressed (Boothroyd et al., 1994)

$$t_r = 1 + 1.75t_d \left(\frac{2D + 5}{L_s}\right)^{\frac{1}{2}} \quad 4.27$$

Where t_d is the dry cycle time (s), D is the part depth (mm), L_s is the maximum clam stroke (mm).

4.5.2.3 Injection moulding energy estimation

Energy consumption profiles for various hydraulic injection moulding machines has been reported by several studies (Krishnan et al., 2009b, Krishnan et al., 2009a, Gutowski et al., 2006, Ribeiro et al., 2012, Thiriez, 2006, Mattis et al., 1996, Kanungo and Swan, 2008, Madan et al., 2014, Elduque et al., 2014). We assume that energy consumption per unit of time on a given machine is constant for a given part of the cycle. The total amount of energy an injection moulding machine consumes consists of melting and injecting resin and additional sub-process energy for opening, closing and ejecting mould and clamping action, as shown below

$$E_{total} = E_{melt} + P_{plasticizing}t_p + E_{injection} + P_{cool}t_c + E_{reset} \quad 4.28$$

Where E_{melt} is the energy used to melt the resin (MJ), $P_{plasticizing}$ is the energy used to drive the screw during the period for plasticizing (kW), t_p is plasticizing time to melt and deliver them for injection (s), $E_{injection}$ is the energy required to inject the molten polymer (MJ), P_{cool} is the

energy used to cool the mould to return it to a solid state (kW), t_c is cooling time required to cool the polymer to a temperature to solidify within the mould (s), E_{reset} is the resetting energy, including the energy consumed to hold the mould during injection, the energy needed to open and close the mould and to eject the part from the mould (MJ). E_{melt} and $P_{plasticizing}$ can be calculated using the same method as in compounding process (**eq 4.16** and **eq 4.18**).

The energy required to inject the molten polymer to the mould can be calculated by summing the injection pressure $p_{injection}$ multiplied by the volume of the cavity $V_{injection}$ as shown below.

$$E_{Injection} = \frac{p_{injection} V_{injection}}{\eta_{eff}} \qquad 4.29$$

Where η_{eff} is 80% which is within the efficiency interval of the injection machines found in literature (Ribeiro et al., 2012).

In the injection system, there are chiller units for the water cooling mechanism that circulates around the barrel. The cooling power consumption in this study can thus be directly estimated by a linear relationship between cooling power and injection machine power, which is 10.4 kW for a 165 kW machine (Weissman et al., 2010, Ribeiro et al., 2012).

The resetting energy is the sum of energy to open and close the mould and to eject the part, accounting for about 25% of the energy consumed in the total process (Mattis et al., 1996, Madan et al., 2014).

4.5.3 Validation

The injection moulding cycle time and total energy consumption value have been compared with literature values (2.0-7.9 MJ/kg composites) to ensure the model is representative (Thiriez and Gutowski, 2006, Spiering et al., 2015, Kent, 2008, Johannaber, 2008, Gutowski et al., 2006). Cooling time dominates the injection moulding process (>50% of the total time) and the resin melting step consumes the majority of the total moulding process energy although the energy values vary depending on processing specifications and part geometry.

CHAPTER 5 ENVIRONMENTAL ASPECTS OF USE OF RECYCLED CARBON FIBRE COMPOSITES IN AUTOMOTIVE APPLICATIONS

5.1 Introduction

The high cost and energy intensity of vCF manufacture provides an opportunity to recover substantial value from CFRP wastes: rCF could reduce environmental impacts relative to vCF production, and the potentially lower cost of rCF could enable new markets for lightweight materials. To support the development of rCF markets, technology demonstrators (e.g., rCF seatback demonstrators- aircraft seatback (36% aligned rCF volume fraction with PPS matrix) and automobile seat base (42% aligned rCF volume fraction with PP resin)) have established the commercial viability of CFRP recycling processes and composite manufacturing from rCF for aerospace and automotive applications (University of Nottingham, 2009, University of Nottingham, 2005) . However, there is still limited understanding of the life cycle environmental impacts associated with CFRP recycling, reuse of rCF in composite manufacture, and potential uses of the resulting materials.

Life cycle assessment (LCA) is a standardised method that can be used to quantify the environmental impacts of a product over its complete life cycle, including raw material production, product manufacture, use and end-of-life waste management according to the ISO 14040/14044 standards (International Organization for Standardization, 2006a, International Organization for Standardization, 2006b). Previous studies have applied LCA methods to investigate vCF for lightweight vehicle applications but insights of these studies are not consistent as noted in Chapter 2. Prior life cycle studies of CF recycling are limited by the

availability of relevant data for recycling and rCFRP manufacturing processes and, to date, none has considered the use of rCFRP as lightweight materials in automotive applications.

In this chapter, life cycle models are developed to assess the performance of CF recycling, via fluidised bed process, and reuse in automotive applications. A set of rCFRP manufacturing approaches (compression moulding; injection moulding) are considered and material production and its use are evaluated in a vehicle over its full lifetime. Case study automotive components are considered under different design constraints. The results are then compared with conventional automotive materials (steel) and competitor lightweight materials (aluminium, vCFRP) to identify opportunities where rCF can achieve a net environmental benefit.

5.2 Method

The goal of this study is to assess the life cycle environmental impacts of CFRP recycling and use of rCF for composite manufacture for automotive applications. Activities included within the life cycle model are shown in **Figure 5.1**, beginning with collected CFRP waste and including all subsequent activities related to CFRP recycling, rCF processing, rCFRP manufacture, and use phase. Recycled CF is assumed to be recovered from a fluidised bed recycling process, as analysed in Chapter 3 and 4. Three rCFRP production pathways are considered:

1) Random structure – Compression Moulding: rCF is processed by a wet papermaking process prior to impregnation with epoxy resin and compression moulding. Fibre volume fractions of 20%, 30%, and 40% are considered.

2) Aligned – Compression Moulding: rCF is processed by a fibre alignment process prior to compression moulded with epoxy resin. Fibre volume fractions of 50% and 60% are considered.

3) Random structure – Injection Moulding: rCF is processed by wet papermaking and subsequently chopped prior to compounding with polypropylene (PP); rCF-PP pellets are subsequently injection moulded. Fibre volume fraction is 18%.

The rCFRP production routes are compared with similar composite materials produced from vCF, specifically:

1) Woven – Autoclave: bi-directionally woven vCF is autoclave moulded with epoxy resin; fibre volume fraction is 50%.

2) Chopped – Injection Moulding: chopped, unaligned fibres are compounded with PP; vCF-PP pellets are subsequently injection moulded. Fibre volume fraction is 18%.

CF-based materials are also compared with mild steel, as a conventional automotive material, and aluminium, a potential lightweight metal.

Upstream activities preceding the CFRP becoming a waste material are excluded from the analysis. For the vCF-based materials and metals (steel, aluminium), life cycle models include all activities from initial resource extraction (e.g. CF feedstock production; ore mining), material production, component manufacture, and use.

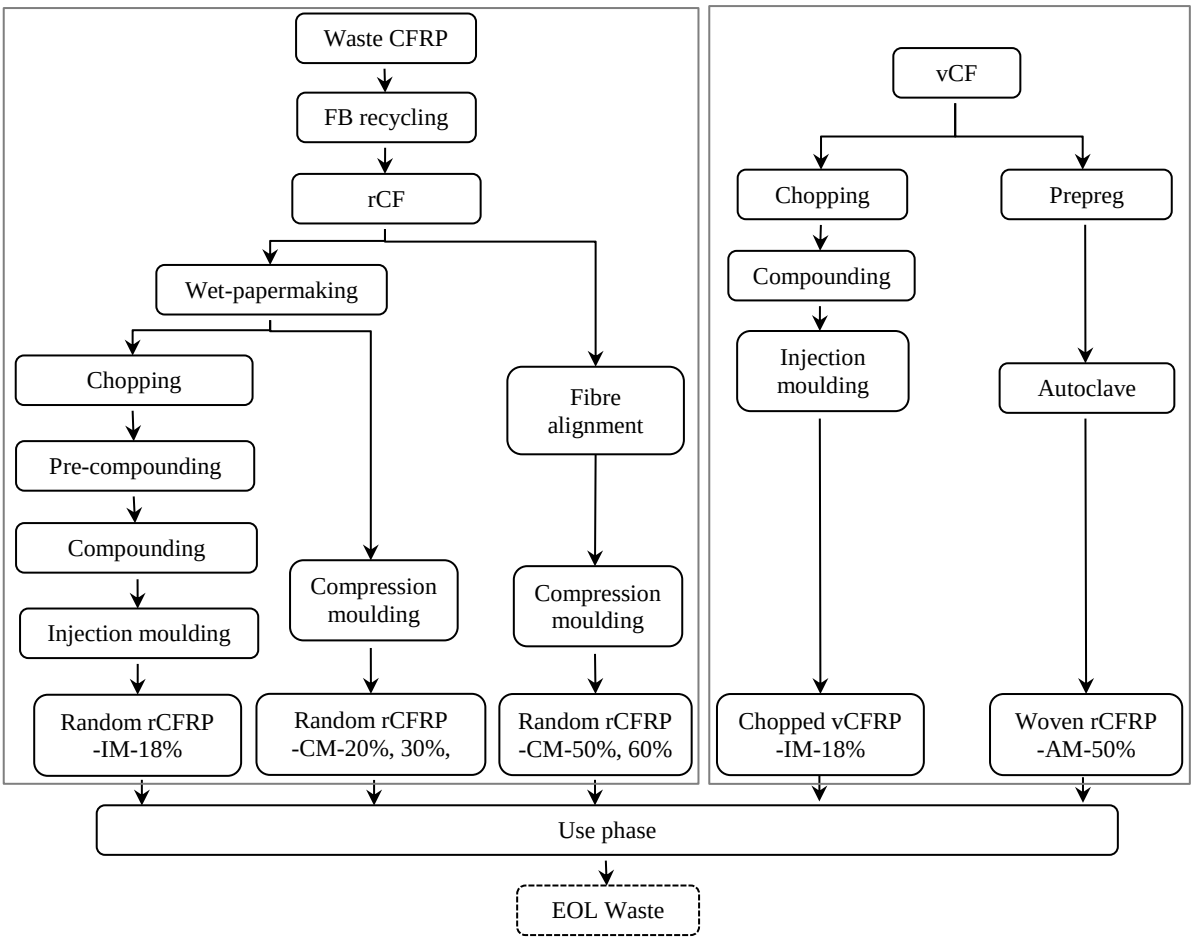

Figure 5.1. Overview of pathways and processes for manufacture of automotive components from recycled and virgin carbon fibre.

Process models of the fluidised bed recycling, rCF conversion to an intermediate material (i.e., wet-papermaking/ fibre alignment) and the subsequent CFRP manufacture (i.e., compression moulding/ injection moulding) are developed to estimate the energy and material requirements of commercially operating facilities. This data is supplemented with databases to estimate impacts of producing and using material and energy inputs (e.g., Gabi (Gabi, 2014) Ecoinvent (Wernet et al., 2016)) assuming all activities to occur in the UK. Additional details related to

waste CFRP recycling, rCF processing, and CFRP manufacture are included in the subsequent subsections.

Life cycle models are developed to assess the environmental implications of substituting steel with rCF materials and competing lightweight materials. Two environmental metrics are considered: primary energy demand (PED); and global warming potential (GWP), based on the most recent IPCC 100-year global warming potential factors to quantify GWP in terms of CO_2 equivalents (CO_2 eq.) (Solomon, 2007). A general approach is taken to ensure functional equivalence of producing automotive components from the set of materials based on the design material index (λ), a variable which is specific to the design criteria for any specific component. For further details see the review papers by Patton et al. and Ashby (Patton et al., 2004, Ashby, 2005). The component thickness is treated as a variable that is adjusted based on each material's properties and the specific applications design material index (see Section 5.2.5 for further details). Analysis results are presented on a normalised basis (relative to the mild steel reference material), and can thereby be easily applied to subsequent analyses that are undertaken for specific components where the material design index is known.

5.2.1 Carbon fibre recycling

A fluidised bed process is considered for the recycling of CFRP waste in this study. In the fluidised bed reactor, the epoxy resin is oxidised at a temperature in excess of 500 °C. The gas stream is able to elutriate the released fibres and transport out of the fluidised sand bed for subsequent separation by cyclone. After fibre separation, the gas stream is directed to a high-temperature combustion chamber to fully oxidise the polymer decomposition products. Energy is recovered to preheat inlet air to the bed. Mass and energy models of the fluidised bed process

under varying conditions (e.g., annual throughput, CFRP feed rate) and insights regarding process energy efficiency and are presented in Chapter 3 and the main results of process models have been shown in Section 5.3. For the current analysis, a plant capacity of 500 t rCF/yr and feed rate of 9 kg rCF/hr-m^2 are considered corresponding to energy requirements of 1.9 MJ natural gas/kg rCF and 1.7 kWh electricity/kg rCF

Although the full chemical formulation of the epoxy resin is not available, for the purposes of stoichiometry calculations, it is assumed to be made of Diglycidyl ester of bisphenol A (DGEBA) in 87 % wt and Isophorone Dianmine (IPD) in 13 % wt. CO_2 emissions resulting from the oxidation of the epoxy matrix material are calculated on a stoichiometric basis assuming all carbon is fully oxidised to CO_2 and all nitrogen is emitted as NO_2 (see **eqs 5.1-5.2**) Data on other potential GHG emissions (methane) are not available and are assumed to be negligible.

$$C_{10}H_{22}N_2 + 17.5O_2 \rightarrow 10CO_2 + 11H_2O + 2NO_2 \quad 5.1$$

$$C_{21}H_{24}O_4 + 25O_2 \rightarrow 21CO_2 + 12H_2O \quad 5.2$$

5.2.2 Virgin carbon fibre manufacture

The manufacture of vCF is modelled based on existing literature data. The life cycle inventory data input to our LCA models information is described previously (Meng et al., 2017) and comprises data from literature and life cycle databases, with parameters selected based on literature consensus, expert opinion and results from a confidential industrial dataset. Publicly available data on vCF manufacture is limited and, in many cases, is lacking in key details that should be incorporated into LCA studies, in particular variations in CF mechanical properties (high strength vs intermediate modulus) and corresponding energy requirements/

environmental impacts. The implications of the data source on results are discussed in Section 5.4.3. In this research, high strength vCF is assumed to be manufactured from a polyacrylonitrile (PAN) precursor followed by subsequent stabilisation, carbonisation, surface treatment and sizing processes. Based on a literature value for mass efficiency of 55%-62% (Griffing and Overcash, 2010, Duflou et al., 2009), a representative mass yield is assumed to be 58%. All inventory data have been recalculated relative to 1 kg CF and the total actual energy consumption is estimated to be 149.4 MJ electricity, 177.8 MJ natural gas and 31.4 kg steam. Direct process emissions are estimated based on available data (Griffing and Overcash, 2010) and adjusted to reflect the mass efficiency assumed in the current assessment.

5.2.3 Carbon fibre conversion process

Two processes are considered to convert rCF to a form suitable for composite manufacture: wet papermaking process to produce a random oriented mat (Wong et al., 2009a), and fibre alignment process to produce a unidirectional fibre mat (Wong et al., 2009b). Mass and energy balances of these two rCF processing methods are established based on key processing parameters presented in Chapter 4.2 and summarized as described below.

To form a random mat via the wet-papermaking process, CF is first dispersed in a viscous liquid to form a fibre suspension (assumed here to be a fibre volume content of 0.1% to avoid agglomeration of fibres (Turner et al., 2015)) by stirring for 24 hours at a rotational speed of 800 rpm. The fibres are then deposited on a conveyor and dried to produce a random mat. Energy requirements of each associated activity are estimated based on experimental data, parameter optimisation to minimise energy consumption (see Section 5.3.2) and, where available, energy efficiency data of standard equipment (Kemp, 2012, Ghosh, 2011). A fibre

alignment process is also considered wherein the fibre suspension is injected onto a mesh screen inside a rotating drum and the nozzle filters and aligns the fibres prior to dewatering/drying. This fibre alignment process is still under development, and so energy consumption is estimated based on a target for technology development (22 MJ/kg rCF mat). Due to confidentiality of the process in the development, limited details of the fibre alignment process can be given (see Chapter 4.3). The implications of this assumption on results are discussed in Section 5.4.

5.2.4 Composite manufacturing processes

5.2.4.1 Compression moulding

Compression moulding production of CFRP requires CF mats (random or aligned mats from rCF; prepreg from vCF) and epoxy resin film to be cut to size required to fit into the mould with cutting energy use of 0.37 MJ/kg (Witik et al., 2012). Before applying compression pressure, a standard vacuum bagging procedure is implemented to reduce air entrapment during ply collation and thus to reduce the void content inside the composite (Wong et al., 2009a). For random rCFRP, the mould is subsequently compressed under pressure of 2 to 14 MPa depending on fibre volume fraction required, with higher fibre fraction components requiring higher pressures (Wong et al., 2009a). For aligned rCFRP, the compression pressure is lower (8 MPa) (Liu et al., 2015). During compression moulding, materials are heated to 120 °C for curing. A detailed description of compression moulding energy models is presented in Chapter 4.4.

5.2.4.2 Injection moulding

Injection moulding has been successfully demonstrated to be an efficient way to process rCF into CFRP materials (Wong et al., 2012) and is capable of achieving similar mechanical properties to materials produced from vCF . First, the CF is compounded with a thermoplastic matrix (polypropylene) to produce composite pellets for input to the injection moulding. To produce rCF-PP pellets, randomly aligned rCF mat (100 g/m^2) is chopped to pellets 4 mm wide and 6 mm long. This may not be the efficient method to manufacture rCF-PP pellets but will be optimised where available in the future study. To ensure bonding between the rCF and PP matrix, PP is first compounded with a coupling agent (maleic anhydride grafted polypropylene coupling agent, 5% by weight) via a screw extrusion process at 210 °C with a screw rotational speed of 80 rpm and a residence time of 130 s. The rCF pellets are subsequently compounded with the PP pellet at 18% volume fraction (30% weight fraction) by screw extrusion (210 °C, 50 rpm, and 150 s residence time). For vCF, a coupling agent is assumed to be not required and so vCF-PP pellets can be produced by a single compounding step with chopped vCF and PP granules (18% fibre volume; 30% fibre mass) is required and is operated under the same conditions as the rCF-PP compounding step described above. For injection moulding of CF-PP pellets to form the automotive components, recommended parameters are presented before (Wong et al., 2012).

Compounding energy consumption is calculated accounting for polymer melting, screw driving, and cooling and combined with output of the compounder obtained by the function of solid flow rate and simulation of factors. Injection moulding energy requirements are calculated to account for specific component geometry (mould cavity volume, projected area). Moulding machine parameters, specifically the clamping force, injection pressure/ temperature, ejection

temperature, and screw drive rotational speed, are used to determine power requirements and combined with cycle time to estimate total energy requirements, based on relationships developed in prior studies (Boothroyd et al., 1994, Madan et al., 2014). Further details on the injection moulding model development and parameters are given in Chapter 4.5.

5.2.4.3 Autoclave moulding

Autoclave moulding is commonly utilised by the aerospace industry where heat and pressure are applied to prepreg laminates in a pressure vessel. It enables the manufacture of CFRP components with high fibre volume fractions and low void contents but requiring intensive energy and high costs of both initial acquisition and use. In general, CF is pre-impregnated with a thermoset resin before being laminated and curing under typical pressure of 0.6- 0.8 MPa. Energy consumption for composite manufacture is substantially affected by processing parameters (e.g., curing temperature and time, degree of packing of the autoclave, etc.) which are associated with the geometry and size of the component. Due to the complexity of component design and autoclave process, industrial data and best available literature data are gathered to assess the environmental energy. Energy requirements of prepreg production (4 MJ/kg) and the subsequent autoclave moulding (29 MJ/kg) are used in this study based on literature sources (Song et al., 2009, Scelsi et al., 2011, Suzuki and Takahashi, 2005).

5.2.5 Functional unit

The functional unit chosen for this study is a generic automotive component, assumed to be produced from mild steel, and allocated a normalised thickness and mass of 1. When evaluating alternative materials, functional equivalence is maintained by considering the design material

index (λ) and varying component thickness to account for differences in each material's mechanical properties according to (Ashby, 2005, Patton et al., 2004, Li et al., 2005):

$$R_t = \frac{t}{t_{ref}} = \left(\frac{E_{ref}}{E}\right)^{\frac{1}{\lambda}} \quad 5.1$$

Where R_t is the ratio of component thicknesses between the proposed lightweight material (t) and the reference (mild steel, t_{ref}), E is the modulus of the two materials (GPa), and λ is the component-specific design material index. The normalised component mass is calculated based on the relative thickness and density of alternative materials.

Depending on design purposes, the parameter λ value may vary between 1 and 3. λ=1 is appropriate for components under tension loading (e.g., window frame), λ=2 is for columns and beams under bending and compression conditions in one plane (e.g., vertical pillar) and λ =3 is suitable for plates and flat panels when loaded in bending and buckling conditions in two planes (e.g., car bonnet). Actual component designs require a finite element analysis to identify the material design index that would ensure design constraints are met. Based on finite element simulation, vehicle structural components, for example, between the roof and vertical pillars, can have a λ value range of 1.2-2.0 (Patton et al., 2004) while other car body structural members, such as floor supports, have been shown to have a λ value range of 1.21-2.4 (Cui et al., 2011). The present analysis considers λ values ranging from 1 to 3 to assess the environmental viability of rCF applications under different design constraints. Insights from this analysis can subsequently be applied to specific components where the exact design constraints are known.

Mechanical properties of vCFRP and random rCFRP were obtained from the previous experiments (Wong et al., 2009a) and manufacturers (PlastiComp Inc., 2016, GoodFellow,

2016). Properties of aligned rCFRP were calculated using a micromechanics model to estimate resulting CFRP properties (Berthelot, 2012, Daniel et al., 1994). Data for other materials (mild steel, aluminium, magnesium) are from online databases (MatWeb, 2016, Kelly et al., 2015, ASM Aerospace Specification Metals Inc., 2015). Material properties and corresponding relative thicknesses of component materials are summarised in **Table 5.1**.

Table 5.1. Material properties of general engineering materials selected for LCA study

Material	Matrix	Manufacture	Density, g/cm3	Modulus, GPa	Strength, MPa	References
Mild steel	-	Stamping	7.81	207.00	350.00	(MatWeb, 2016)
Magnesium	-	Die-casting	1.81	45.00	150.00	(Kelly et al., 2015)
Aluminium	-	Wrought	2.70	69.00	276.00	(ASM Aerospace Specification Metals Inc., 2015)
Random rCF 20%	Epoxy resin	Compression moulding	1.32	27.57	259.88	(Wong et al., 2009a)
Random rCF 30%	Epoxy resin	Compression moulding	1.38	37.14	341.44	(Wong et al., 2009a)
Random rCF 40%	Epoxy resin	Compression moulding	1.44	39.84	301.70	(Wong et al., 2009a)
Aligned rCF 50%	Epoxy resin	Compression moulding	1.50	60.84	-	calculated
Aligned rCF 60%	Epoxy resin	Compression moulding	1.56	73.89	-	calculated
Woven vCF 50%	Epoxy resin	Autoclave moulding	1.60	70.00	570.00	(GoodFellow, 2016)
Random rCF 18%	PP	Injection moulding	1.17	16.26	125.20	(Liu et al., 2015)
Chopped vCF 18%	PP	Injection moulding	1.07	16.21	117.00	(PlastiComp Inc., 2016)

5.2.6 Use phase analysis

During the use phase, the automotive components will impact vehicle fuel consumption due to their weight and corresponding mass-induced fuel consumption. In-use energy consumption is calculated with the Physical Emission Rate Estimator developed by the US Environmental Protection Agency (Nam and Giannelli, 2005) and the mathematical model (Kim et al., 2015) for mass induced fuel consumption. In brief, this method estimates vehicle power demand, which is impacted by total vehicle weight, and integrates over a standard driving cycle. Model parameters for a set of production vehicles are available, in this research, a Ford Fusion is selected as a representative mid-size light duty vehicle. Mass induced fuel consumption is calculated based on the differences in vehicle mass from utilising lightweight materials assuming no effect of material substitution on the vehicle aerodynamics and no powertrain resizing. As a base case, a typical vehicle life of 200,000 km (Helms and Lambrecht, 2007, Witik et al., 2011) is considered, but the sensitivity of results to this key parameter are evaluated.

5.3 Results of process modelling

5.3.1 Carbon fibre recycling

5.3.1.1 Feed rate

Carbon fibres can be recovered from CFRP with energy expenditure as little as 6 MJ/kg for the fluidised bed operating parameters considered. **Figure 5.2** shows the energy balance of the recycling process, including energy inputs (natural gas, electricity), energy release from resin oxidation, and heat losses, for a FB plant with 100 t/yr of annual throughput of rCF. The energy requirements of the fluidised bed recycling process are primarily dependent on two factors: the

feed rate of CFRP processed per unit bed area (kg CF/hr-m^2), and the in-leakage of ambient air. At lower feed rates, relatively more air needs to be heated and transferred through the system per kg of CF recovered, leading to greater natural gas demand for thermal energy and electricity for the fans. At higher feed rates, thermal energy requirements are significantly reduced to the extent that most process heat can be provided by resin oxidation. Beyond a feed rate of 5kg/hr-m^2, energy efficiency gains are minor as the resin energy input is fully exploited in heating the fluidised bed to 550 °C and there is a minimum gas quantity required to raise the oxidiser temperature to 750 °C. Air exhaust from the system following the oxidation and heat recovery stage is the primary mode of heat loss from the fluidised bed system. The quantity of heat that can be recovered to the recycling process is limited due to the temperature mismatch between the oxidiser (750 °C) and the fresh air leaving the heat exchanger (531 °C to 409 °C for feed rates 3 to 12 kg/hr-m^2 based on the energy model results). We arrange the heat recovery system to give the maximum practical heat recovery but that nevertheless the exhaust gases from the stack where exhaust temperatures range from 98 °C to 208 °C across parameters considered in this study. Heat recovery from the stack for other process uses could therefore improve overall efficiency.

While we identify energy efficiency gains achievable by increasing feed rate, there are potential trade-offs in terms of resulting rCF properties. To avoid agglomeration in the recycling process at high feed rates, fibre length must be reduced (Jiang et al., 2005). However, fibre length may also affect the downstream composite manufacturing process and resulting composite product properties. It is expected that fibre lengths in the range of 1-10 mm will be preferred for balancing fluidised bed performance and recovered CF properties for composite manufacture; however, this is a topic of ongoing research.

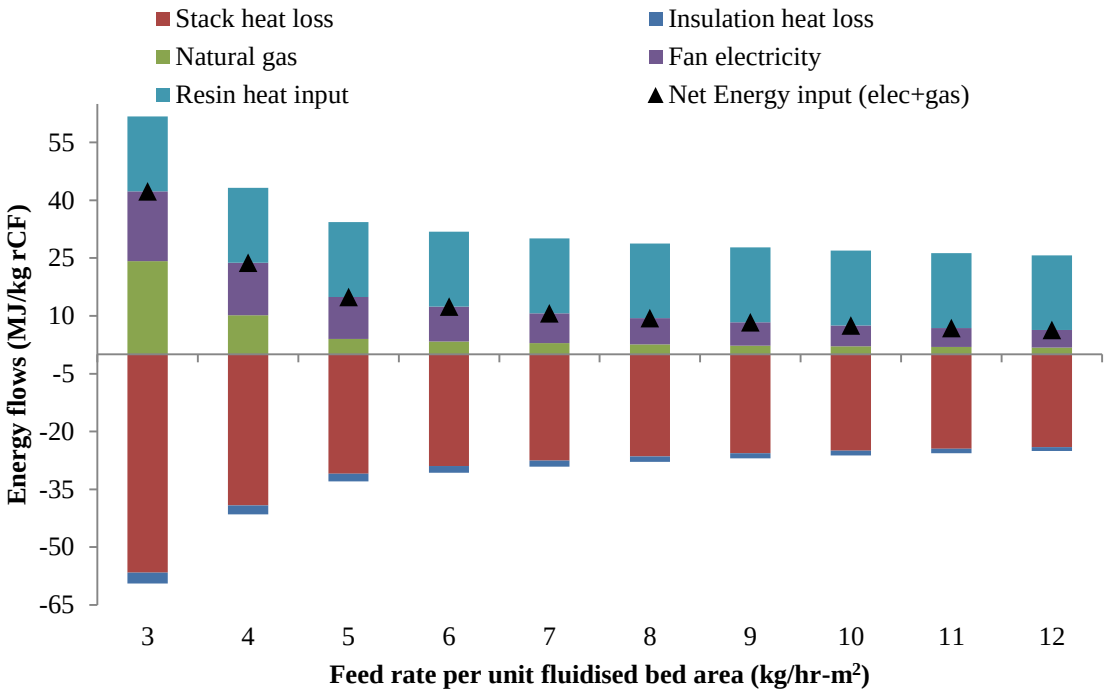

Figure 5.2. Energy flows including heat losses from each component and energy value from resin and energy supply for plant corresponds to mass flow per unit area of bed.

5.3.1.2 Annual throughput

Inefficiency arises in the process from in-leakage of air from the system to the ambient due to the operation of the system below atmospheric pressure. **Figure 5.3** shows the results obtained from the FB plant at various feed rates per unit fluidised bed area with no air in-leakage for annual throughputs of 50, 200 and 800 tonnes rCF per annum to investigate the effects of feed rate and plant capacity. The overall energy input decreases largely as the feed rate per unit bed area increased. It is noted that the plant capacity does not have a significant impact on the total energy requirement, which varies by only 6% for annual capacities ranging from 50 t/yr to 500

t/yr for 3 kg/hr-m^2 feeding rate. This is because volume of air required to process the CFRP is negatively correlated to the feed rate per unit bed area rather than annual capacity.

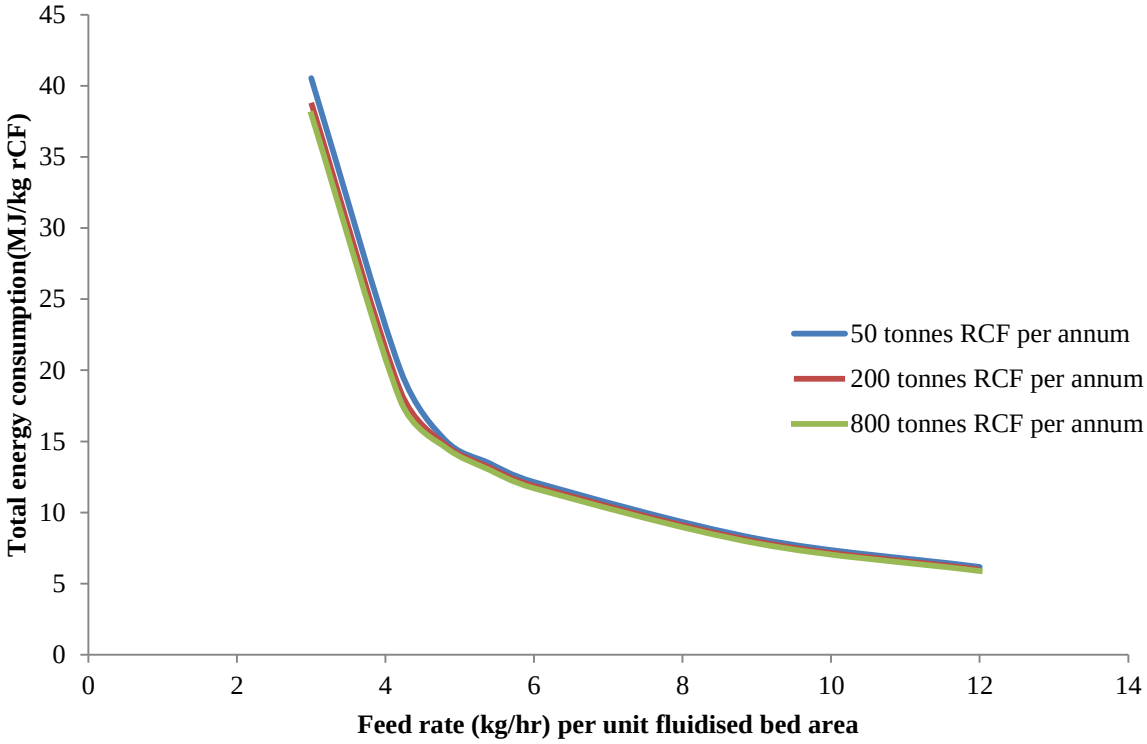

Figure 5.3. Total energy consumption (electricity + natural gas) for plant corresponds to various annual outputs of recovered carbon fibre and mass flow per unit area of bed with 0% air in-leakage rate.

5.3.1.3 Air in-leakage rate

As described before, there is air leakage at pipework joints and in particular at shaft seals in the fans in the system because of the negative pressure. The air in-leakage rate impacts the thermal energy requirements as this introduces a mismatch in mass flow rate: additional air must be heated to 750 °C at the oxidiser, thereby resulting in greater exhaust heat losses. Air leakage also places an impact on fan power consumption by changing the mass flow rate. We

evaluate air in-leakage rates up to 10%, finding that natural gas and electricity requirements increase by up to 340% and 1% respectively while stack heat loss rises by up to 165% (see **Figure 5.4**). The insulation heat losses remain almost unchanged with varied leakage rate as the thermal resistance is independent of air in-leakage. Though we could reduce or avoid the air in-leakage if not operating at negative pressure, emission of epoxy decomposition products would have to be mitigated in some way for environmental issues.

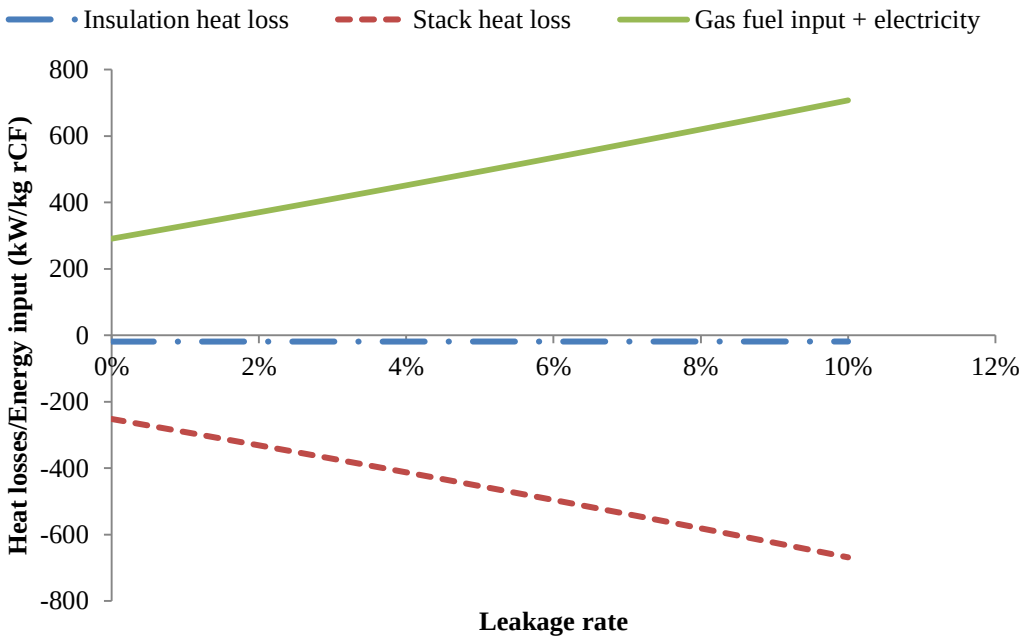

Figure 5.4. Heat losses from insulation and exhaust stack respectively and total gas input energy with respect to leakage rate (6 kg/hr-m^2 bed of feeding rate and 500 t/yr of annual throughput).

5.3.1.4 Optimization of Pipe insulation

Figure 5.5 shows net present value of insulation in fluidised bed recycling plant with respect to various insulation materials and thicknesses. It can be clearly seen that pyrogel as insulation

materials has the lowest total pipework cost for the fluidised bed plant with 6 kg/hr-m^2 bed feeding rate and annual throughput of 100 t/yr. For the selected plant, the lowest cost occurs at an insulation thickness of 0.52 m. Further financial analysis of different plant capacities shows that the best insulation thickness varies with the annual throughput of the plant: 0.52 m for lower throughput of 100 t/yr, 0.62 m for medium throughput of 500 t/yr and 0.66 m for higher throughput of 1000 t/yr, respectively. This is because the cost of pipework increases with the increased length of pipework associated with annual throughput.

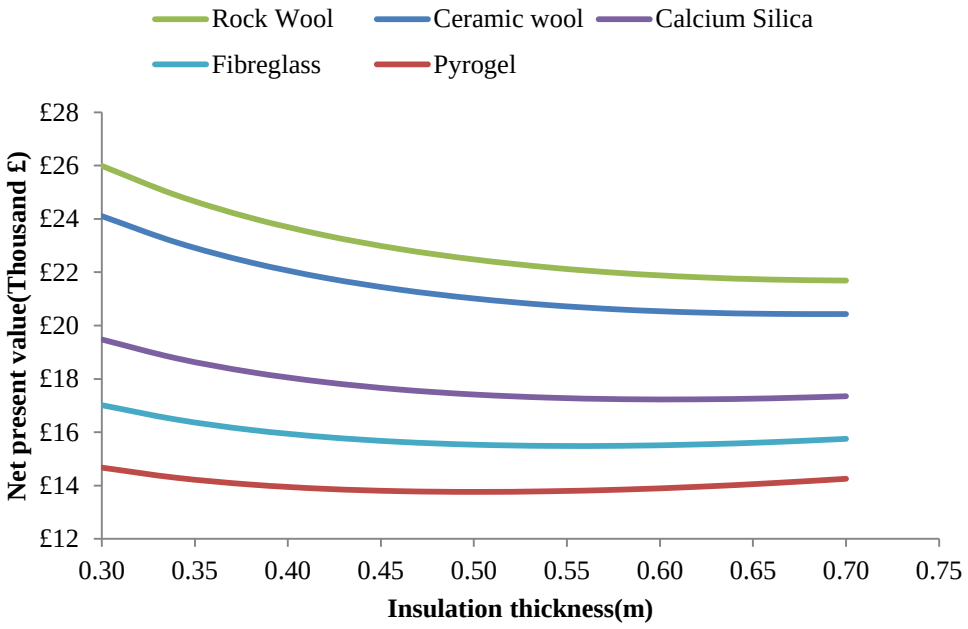

Figure 5.5. Net present value of insulation with respect to various insulation materials and thicknesses (6 kg/hr-m^2 bed of feeding rate and 100 t/yr of annual throughput).

5.3.2 Recycled carbon fibre conversion process

Direct energy requirements for one of the rCF conversion processes (i.e., papermaking) are presented in this section. These results are presented on a mass basis of the rCF mat based on

the processing model of the lab-scale wet papermaking process using representative operating conditions as in Chapter 4. Model parameters for fibre dispersion and drying affect energy requirements of the process; an assessment of the sensitivity of results to variations in these parameters and insights are presented below.

5.3.2.1 Fibre dispersing

The geometry of a stirrer and its insertion into a reactor influences the characteristics of a stirring system. The stirrer in this study which is a propeller type stirrer produces a recirculation axial flow with the vessel. As described before, the power consumption is a function of shear rate, density and viscosity of the fluid and the volume of the fluid (assumed to be the tank volume). For a given tank, the geometry is constant, thus the shear rate is determined by the rotational speed of the motor. Therefore, the growth of the rotational speed increases the dispersion energy by changing the shear rate (see **Figure 5.6**).

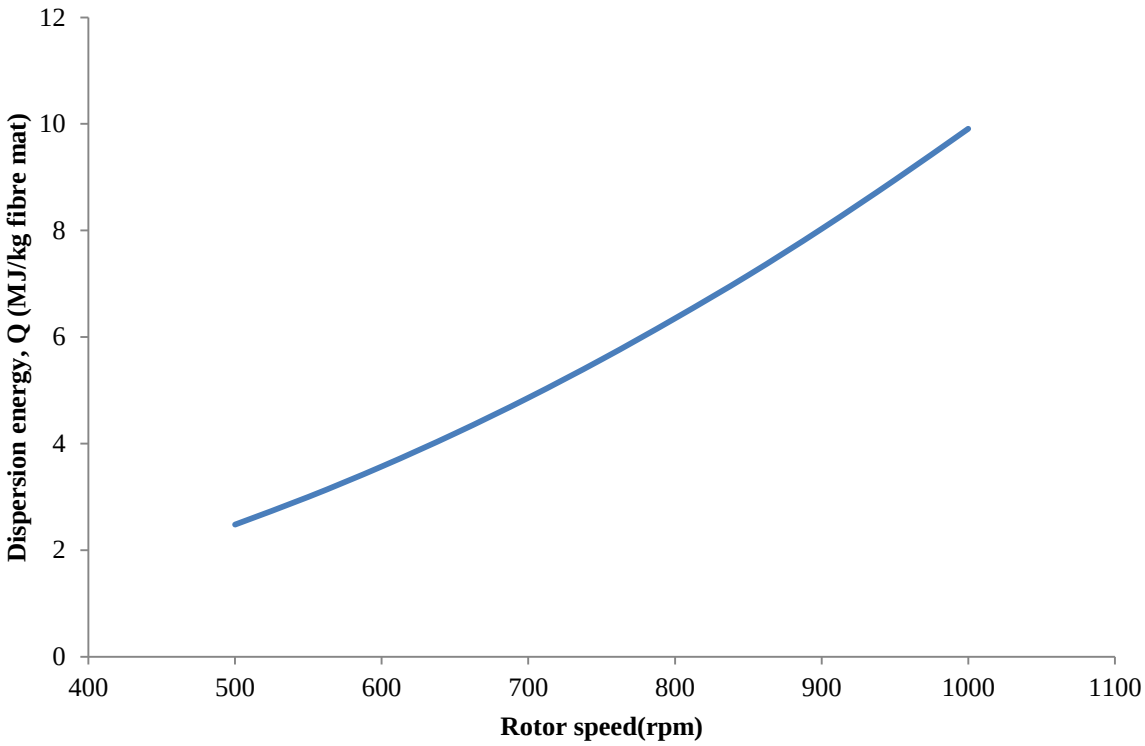

Figure 5.6. Dispersion energy vs rotor speed.

Dynamic viscosity of 0.219 kg/(m·s) has shown a good dispersing performance for rCF. However, as the dispersion energy increases from 1.78 MJ/kg to 41.88 MJ/kg with the dynamic viscosity of the dispersion liquid (0.06-1.41Pa.s), further evaluation would be best to focus on opportunities to optimise the dispersion of rCF and the energy requirement – e.g., by reducing dynamic viscosity but perhaps achieving adequate dispersion.

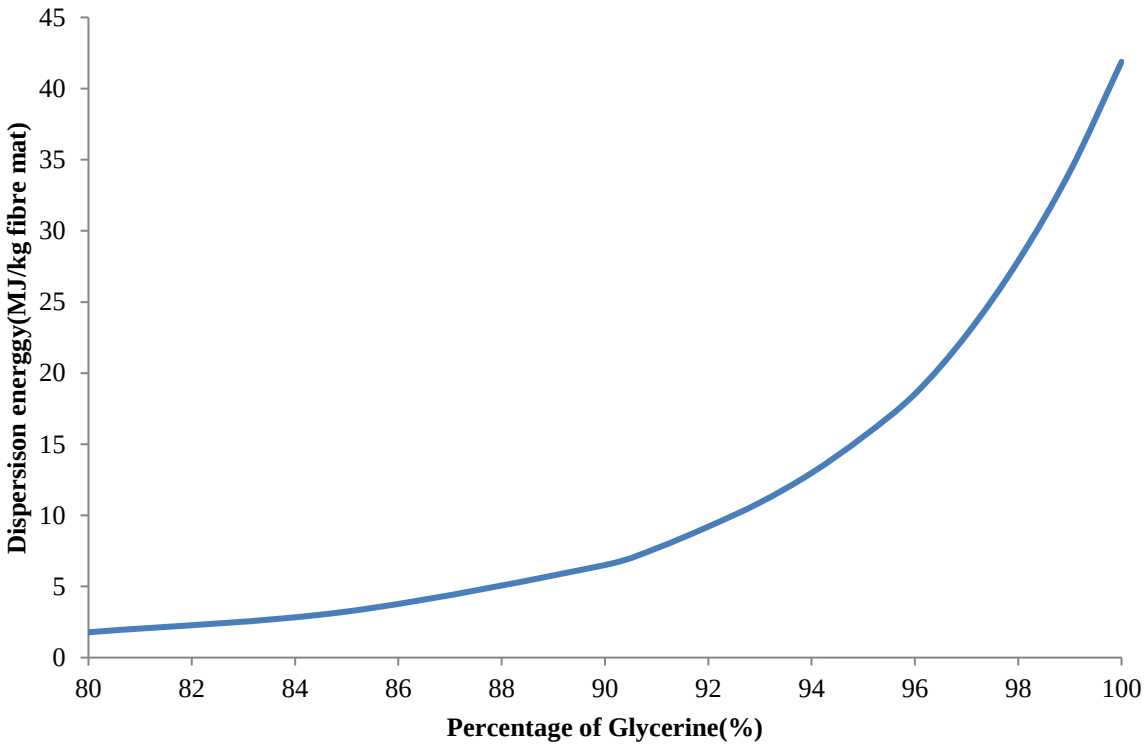

Figure 5.7. Dispersion energy corresponds to various contents of glycerine.

In addition, the fibre volume content mixed in the stirred tank is only 0.1% as there might be agglomeration of fibres at too high fibre volume. Current research is investigating how high fibre volume fraction can be achieved considering possibility of changing geometry of tank and impeller to reduce agglomeration.

The current model assumes a rotational speed of 810 rpm for 24 hours, dynamic viscosity of 1.41Pa.s based on the best performance shown in previous experiments (Wong et al., 2014), giving an optimised fibre dispersion energy consumption of 6.51 MJ/kg. Fibre dispersion energy consumption will be revised once further experimental data is available.

5.3.2.2 Vacuum and thermal drying

Two drying methods are considered in combination – vacuum and thermal and assessed to deliver the lowest total energy consumption for parameters selection in subsequent LCA study. Moisture content of the fibre mat can be reduced by vacuum drying, thermal drying, or a combination of both. The unit vacuum drying energy consumption per $kg \cdot hr \cdot m^2$ is constant at 1.77 $MJ/(kg \cdot hr \cdot m^2)$ under various conditions of belt speed and cross sectional area of the vacuum surface slots (vacuum area).

Mass air flow rate is proportional to vacuum area, having an impact on the actual time experiencing vacuum drying. Therefore, the energy consumption for vacuum drying increased from 1.54 to 30.71 MJ/kg fibre mat with the growth of vacuum area from 1 to 17 cm^2 (belt speed is 60 mm/s). In the meantime, the energy for thermal drying decreases from 6.65 to 1.05 MJ/kg fibre mat within the range. As shown in **Figure 5.8**, if there is no vacuum drying step (vacuum area =0), the total drying energy would be quite high at 40 MJ/kg fibre mat. Totally, with the vacuum area of 3.4 cm^2, the combination of vacuum and thermal drying delivers the lowest energy consumption of 8.19 MJ/kg fibre mat.

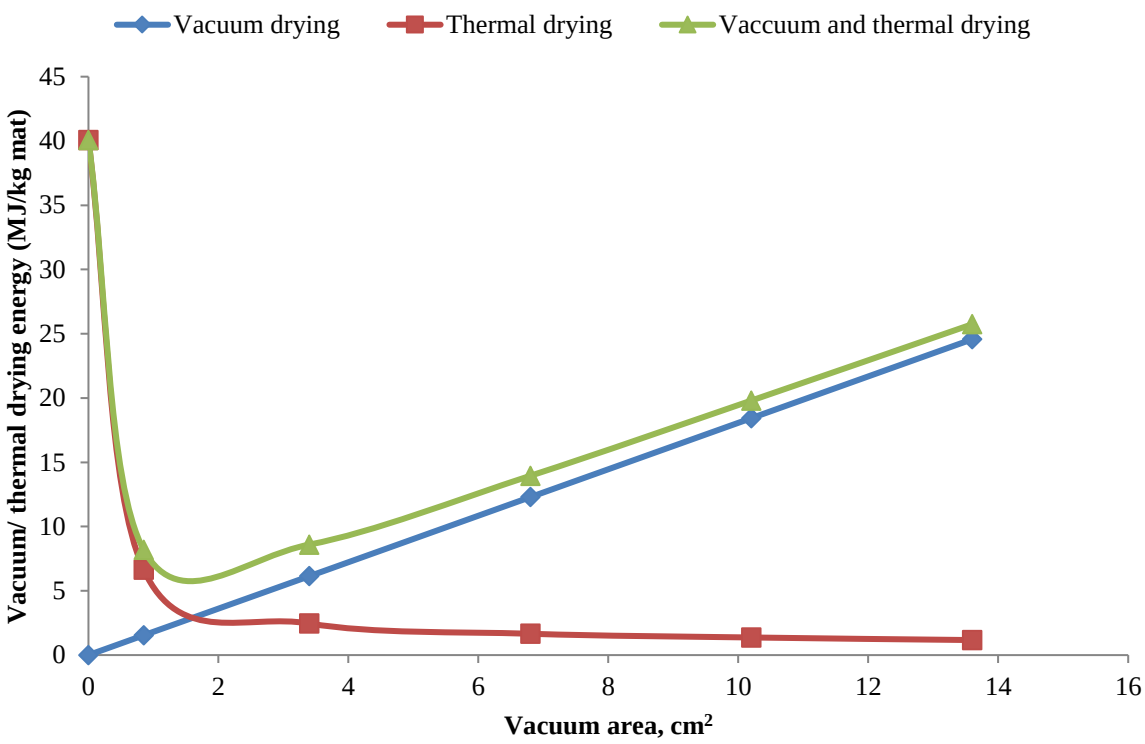

Figure 5.8. Relationship between vacuum/ thermal drying energy and vacuum area.

On the other hand, belt speed also influences the energy consumption of vacuum drying and thermal drying with the similar mechanism (vacuum area of 3.4 cm^2) (see **Figure 5.9**). Higher belt speed reduces the time for vacuum drying, thus moisture content reduction is less compared to lower belt speed. Therefore, the energy consumption for vacuum drying reduces against the growth of belt speed. However, the thermal drying energy increases due to the increase of moisture content. The total energy in the two steps follows a power trend towards the belt speed, suggesting the benefits of increased belt speed if allowed. However, there is a limit for the belt speed as the fibre dispersion has to be pumped onto the belt with a certain flow rate and at too high belt speed makes it not appropriate to shape the fibre mat. In this study, we assume the belt speed to be 80 mm/s. Future investigation is suggested to evaluate how a

higher belt speed achieved with the continuity and steady operation of the fibre dispersion pumping and mat formation.

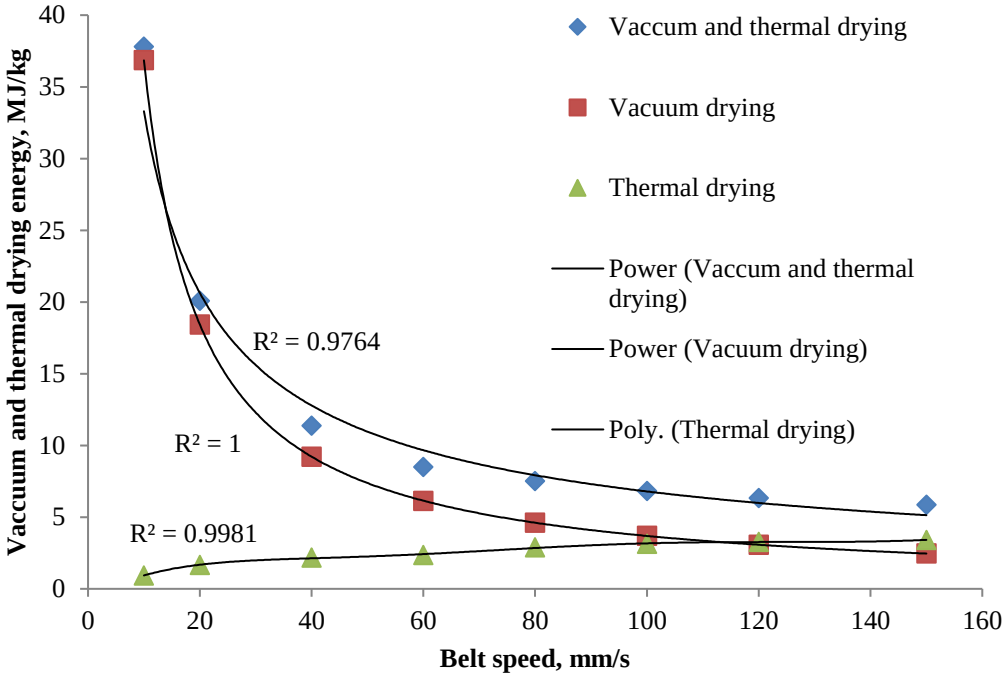

Figure 5.9. Relationship between vacuum/ thermal drying energy and belt speed.

The literature value of efficiency of a dryer is 48.9%-79.4% while the actual thermal energy is calculated based on the efficiency and latent heat of water evaporation. Therefore, the thermal drying energy can be varied from 4.4 to 2.8 MJ/kg fibre mat with respect to various thermal efficiencies in the range of 50 %-80 %. Thermal efficiency can be increased with improved thermal energy supply as well as good insulations to reduce heat losses.

5.4 Life cycle environmental impacts

5.4.1 Component production

Direct energy requirements for component manufacture of different pathways have been estimated from process models or from literatures under different design constraints (i.e., λ=1, 2, 3). We only present direct energy consumption results for automotive components for λ=2 in this section although results under other design constraints can be analysed in the same way. The total energy consumption of compression moulding processes has been reported to be 7.2-14.3 MJ/kg (Suzuki and Takahashi, 2005, Das, 2011) for composites, while the value for random rCFRP manufacture under equivalent stiffness here is estimated as high as 15.9 MJ/kg for a 3.5 mm rCFRP beam under λ=2. This is because an additional vacuum bagging procedure (approximately 35% of total energy consumption) was implemented for 30 mins at room temperature before applying the compression pressure to reduce the void content as described before (Wong et al., 2009a).

In compression moulding pathways, as shown in **Figure 5.10**, the actual manufacturing energy requirement per rCFRP part is 73- 89% of that of woven vCFRP respectively. Recycled CF conversion processes (i.e., papermaking and fibre alignment) account for a large part of energy intensity for the manufacture (20%-60% of the total) and the higher fibre volume fraction, the higher rCF conversion energy consumption. In compression moulding energy, the heating stage accounts for the majority of the energy consumption of the compression moulding process (20%-60% of total). The compression moulding energy decreases with the increase of part thickness; therefore, random rCFRP with higher fibre volume fraction (e.g., 40% vf) has higher energy requirement than lower fibre volume fraction (e.g., 20% vf).

As reported (Bolur, 2000), cooling time takes up over 65% of the total cycle time and in this research, for instance, the total injection moulding cycle time is estimated at 447s with t_c=433s under λ=2. In the material substitution, the component thickness is treated as a variable that is adjusted based on each material's mechanical properties, resulting in different cooling time and associated different energy consumption (e.g., cooling energy). The total energy consumption of injection moulding can be estimated at 2.1 MJ/kg for injection moulded rCFRP under λ=2 corresponding to the reported value of 2.0-7.9 MJ/kg composites (Johannaber, 2008, Thiriez, 2006, Kent, 2008, Spiering et al., 2015).

In random structure-injection moulding pathways, as shown in **Figure 5.10**, rCF processing (i.e., papermaking) accounts for 44% of the total energy to manufacture rCFRP with 18% fibre volume fraction. In comparison, vCF processing (i.e., prepreg production) consumes only 12% of total energy for woven vCFRP production mainly due to the relatively higher energy-intensive autoclave moulding process (87% of the total). The energy intensity between injection moulded- vCFRP part (24 MJ/part) and - rCFRP part (54 MJ/part) to displace mild steel also varies due to their different thicknesses and densities and rCFRP requiring an additional pre-compounding process to prepare PP/coupling agent pellets.

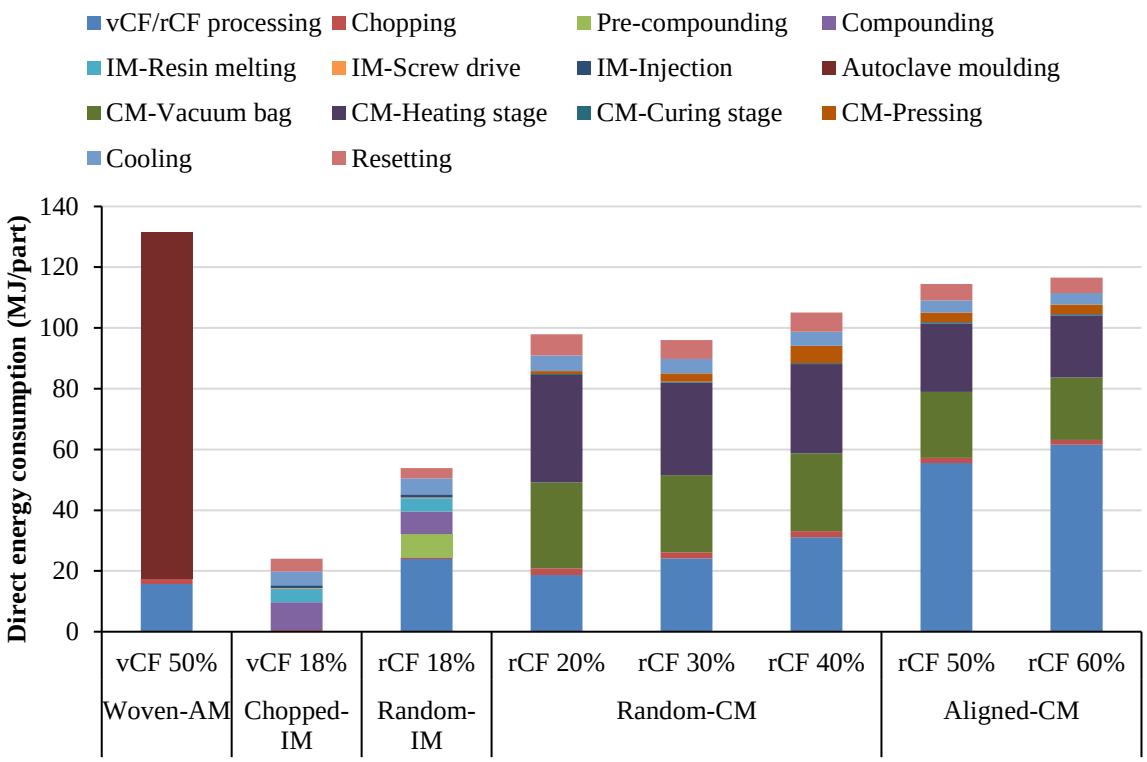

Figure 5.10. Direct energy data of each step in CFRP manufacture of various fibre volume fractions.

The normalised component mass and primary energy demand and greenhouse gas emissions associated with component production (excluding the vehicle use phase) for a component with material design index λ=1, 2 and 3 are shown in **Figure 5.11**. As previous studies (Patton et al., 2004, Li et al., 2005, Kelly et al., 2015, Farag, 2008) have indicated, the weight reduction achieved with lightweight materials is strongly dependent on the material design index: at a higher λ value, lightweight substitution materials can provide more weight reduction while at lower λ values, substitution materials present a less weight reduction or, in some cases, result in higher component weight. For material design indices of 2 and 3, alternative materials are capable of significantly reducing component weight relative to steel (normalised mass = 1). CFRP materials produced via compression moulding and autoclave moulding achieve the

greatest weight reductions relative to steel. Increasing the fibre volume fraction in the rCF materials can be beneficial in achieving greater component mass reductions: significant weight reductions are seen in increasing the fibre content of random rCFRP from 20% to 30%. However, benefits of further increases in rCF content are minimal for the randomly-oriented materials (e.g., 40% rCF volume fraction) due to fibre damage during the manufacturing process and corresponding degradation of material properties (Wong et al., 2009a). Achieving high fibre volume fractions of 50% and 60% requires fibre alignment and results in significant reductions in component weight; this demonstrates the importance of developing cost-effective techniques for aligning rCF. Similar to the aligned rCFRP, woven vCFRP achieves very low component weight. CFRP production via injection moulding produces the heaviest CFRP components due to the low fibre volume fraction that is achievable (18%). However, injection moulded CFRP components can still reduce component weight by 47% relative to steel (λ=2). Aluminium can also achieve significant weight reductions benefits compared to steel (40% and 50% weight reduction for λ=2 and 3, respectively). In contrast, for λ=1 only aligned rCFRP and woven vCFRP can reduce weight relative to steel; aluminium and random rCFRP have similar weight while injection moulded rCFRP components have approximately double component weight relative to steel (see scatter plots in **Figure 5.11**).

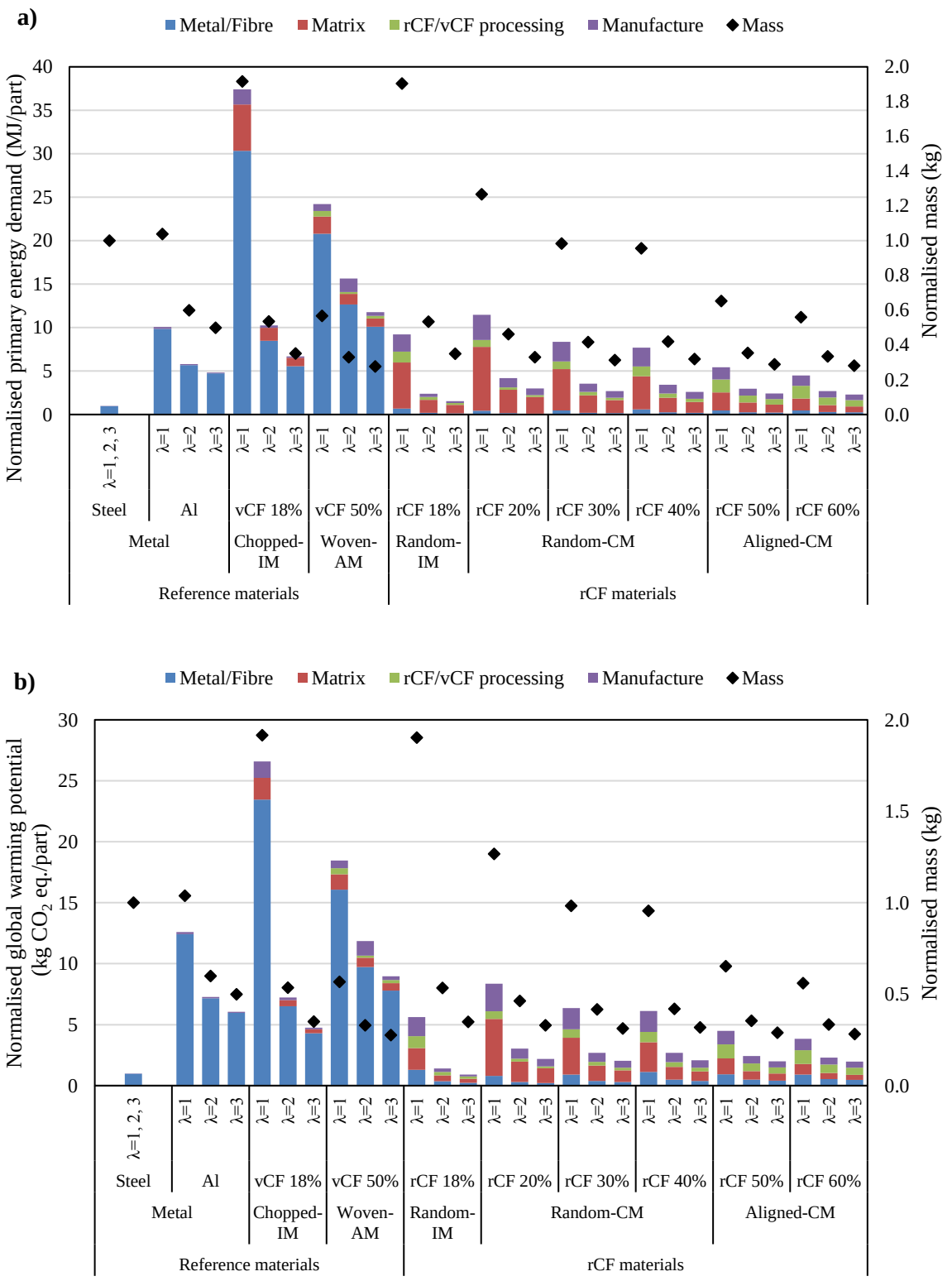

Figure 5.11. Normalised production a) PED and b) GWP and mass of components to satisfy component design constraints for λ=1, 2, 3.

Note: CM=compression moulding, AM=autoclave moulding, IM=injection moulding

GHG emissions and primary energy demand (PED) associated with component manufacture are proportional to component mass and, as such, follow similar trends to the relative mass results. For material design indices of λ=2 and λ=3, GHG emissions associated with the production of rCFRP components are generally less than those of other lightweight materials and, in some cases, represent only a minor increase relative to the reference steel component. Recovery of rCF from waste CFRP is very energy efficient and, correspondingly, is associated with very low GHG emissions. Production of matrix material, rCF processing, and final part manufacture represent the largest shares of production emissions. Increasing the fibre volume fraction serves to reduce the production impacts of rCFRP components, as production of rCF is less GHG-intensive than the epoxy matrix material. But rCFRP components cannot achieve weight reductions relative to the reference steel component (λ=1), production emissions significantly exceed those of the steel component by factors of 4 to 8 (see **Figure 5.11** b)).

The very high GHG intensity of vCF manufacture results in relatively high vCFRP component production GWP, representing 82% and 90% of emissions for the manufacture of compression moulded and injection moulded vCF components, respectively. Manufacture of components from rCF is associated with GWP of 17 to 26% that of the woven vCFRP component produced via autoclave moulding. Similarly, aluminium has embodied GHG emissions approximately an order of magnitude greater than the reference steel component, primarily due to the energy-intensive manufacture of the raw materials.

The PED results exhibit very similar trends to the GWP analysis, showing production PED decreases with the increasing fibre volume fraction for compression moulding pathways of rCFRP (see **Figure 5.11**). This can be attributed to PED reduction from the reduced content of epoxy resin mitigating the increase of PED associated with the CF recycling and manufacturing,

whereby 1 kg epoxy resin of 138 MJ versus 1 kg rCF of 35 MJ for rCF recycling and manufacturing.

In the injection moulding pathways, rCFRP component with 18% rCF volume fraction shows lower normalised PED requirement of 2.39 MJ/part while the vCFRP component presents quite high normalised PED burdens primarily due to the high environmental impacts of vCF manufacture (10.27 MJ/part).

5.4.2 Life cycle energy use and greenhouse gas emissions

Components manufactured from rCF can, in some cases, achieve significant reductions in PED and GWP relative to steel and other lightweighting materials over the full life cycle including vehicle use (**Figure 5.12**). However, the environmental benefits from substitution are dependent on the specific component design constraints and corresponding material design index (λ): at higher λ values, greater weight reductions are achieved, resulting in lower mass-induced fuel consumption during the vehicle use phase as well as lower material requirements during manufacture.

For design constraint λ =2, which is typical for components under bending and compression conditions in one plane (vertical pillars, floor supports), rCFRP components can significantly reduce PED and GWP relative to steel over the full life cycle. Impacts associated with rCFRP components vary depending on the production route and fibre volume fraction. Random structure, compression moulded rCFRP components can reduce PED relative to steel by 33% (20% rCF volume fraction) to 43% (40% volume fraction); similar trends are seen in GHG emissions. Injection moulded rCFRP components have slightly lower energy use and GHG emissions compared to compression moulded random rCFRP materials, primarily due to the

low energy intensity of injection moulding process (3 MJ/kg) and matrix material production (polypropylene for injection moulding versus epoxy resin for compression moulding). Achieving higher fibre fractions through alignment can deliver further PED reductions of up to 56% for the highest fibre content considered here (60% fibre volume fraction), demonstrating the potential advantages to be seen from developing alignment techniques. This finding, however, is dependent on alignment technologies meeting the development target energy consumption of 22 MJ/kg. As actual fibre alignment energy requirements may be more or less than this target, the break-even alignment energy consumption for aligned rCFRP materials are calculated to retain superior life cycle environmental performance over the best-case randomly-aligned rCFRP material. This breakeven point is found to be 95 MJ/kg and 110 MJ/kg to achieve similar life cycle PED and GWP impacts respectively. This result suggests that, should technology development objectives be achieved, then aligned rCFRP would be a promising low life cycle environmental impact material for automotive applications.

In contrast, the energy- and GHG-intensive manufacture of vCF precludes significant reductions in life cycle PED and GWP in all but the most promising substitution scenario (λ=3). In agreement with previous analyses (Witik et al., 2011, Suzuki and Takahashi, 2005), results indicate that although woven vCFRP components can achieve the lowest mass of all alternative materials considered in this research, in-use fuel savings can be counteracted by the impacts of vCF manufacture. In comparison, rCFRP components benefit from the low energy-intensity of CF recovery (compared to vCF manufacture) and can thereby achieve significant reductions in life cycle energy use and GHG emissions.

The lightweight aluminium components also present significant reductions in PED and GWP relative to steel mainly due to the moderate production impacts and large use phase fuel savings.

They can achieve similar PED and GWP reductions with woven vCFRP components relative to steel but still underperform rCFRP components. It should be noted that in the research, aluminium alloy is from primary materials, no recycling of input materials included. Compared with the production of primary aluminium, recycling of aluminium products needs as little as 5% of the energy and emits only 5% of the greenhouse gas. And the share of primary and recycled aluminium products is expected to be 70%:30% by 2020 (Committee, 2009). As shown in Figure 5.12 a), production of aluminium accounts for about 40% of the total life cycle PED. Therefore, considering a portion of recycled aluminium giving a 28% reduction in the combined energy intensity of aluminium production, the full life cycle PED of aluminium component can be reduced by 10%. For λ=2, before considering the portion of recycled aluminium, PED of rCFRP components is 54%-76% of aluminium. However, it should be noted that an estimated 30% recycled aluminium content in transportation applications is difficulty to achieve in current technology and for performance requirement. Therefore, rCF products still achieve superior environmental performance relative to aluminium.

For λ=1, for columns and beams under tension loadings (e.g., a window frame), there is limited scope for lightweighting with any of the materials considered in the present study. Only aligned rCFRP with high fibre volume fractions (i.e., 50% vf and 60% vf) can reduce life cycle PED and GWP relative to steel.

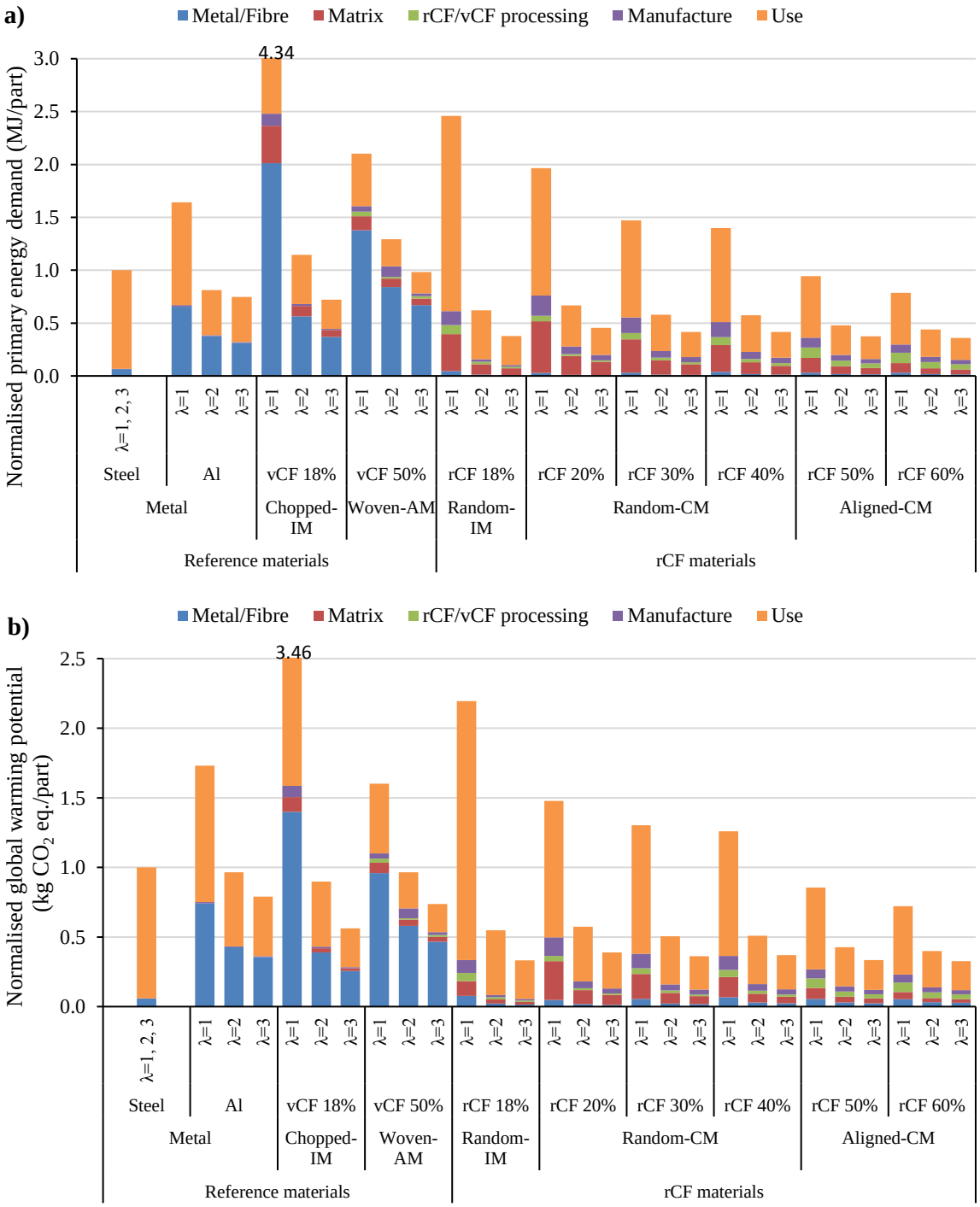

Figure 5.12. Total life cycle a) PED and b) GWP and mass of components made of different materials achieving equivalent stiffness in automotive steel components for different design constraints (λ=1, 2, 3) in an overall lifetime distance of 200,000 km.

5.4.3 Sensitivity analysis

The study results are sensitive to a number of key parameters, including material substitution assumptions, impacts of vCF manufacture, GHG-intensity of electricity inputs, impact of component weight on in-use energy consumption, and vehicle lifetime.

Uncertainty associated with vCF production impacts arise from data quality issues as well as regional variability of electricity generation sources and associated impacts.

The quality of life cycle inventory data for vCF manufacture is poor: publicly available data is limited; vCF production energy requirement and sources vary significantly (198 to 595 MJ/kg from a mix of electricity, natural gas, and steam);(Suzuki and Takahashi, 2005, Carberry, 2008, Duflou et al., 2009, Witik et al., 2013) and studies have not linked production data to CF properties despite different processing conditions required to achieve high modulus and high strength CF (between 1000-1400℃ for high modulus fibers, or 1800-2000℃ for high strength fibers). Therefore, there is inadequate information to match energy intensity to fibre properties. In this thesis, the value developed based on the literature is 149.4 MJ electricity, 177.8 MJ natural gas and 31.4 kg steam per kg vCF manufacture. But the impact of various literature values on life cycle results are assessed in low case (198 MJ/kg) and high case (595 MJ/kg) relative to the reference value used in this research (see shaded area in **Figure 5.13**). The same ratio of energy types (electricity, natural gas and steam) is assumed for low and high energy intensity of vCF production as the one for the base case. The sensitivity of vCF production energy requirement and sources accounts for the main impact on the full life cycle GHG emissions of vCF-based materials. If the lower end of production energy estimates can be achieved, the life cycle GHG emissions of vCF-based materials correspondingly decrease by

17% (**Figure 5.13** and **Figure 5.14**, for λ=2), whereas the higher energy requirement estimate would increase emissions by 36%.

Due to the low GHG intensity of 7 g CO_2 eq. per kWh electricity produced from hydro power, 1 kg vCF production only emits 29 kg CO_2 eq. compared to 68 kg CO_2 eq. using coal electricity source of which the GHG intensity is 960 g CO_2 eq. per kWh (see Figure S5). With the highest electricity intensity, the GHG emission of rCF production would be only up to 9% of vCF production compared to 5% using UK electricity mix. Since vCF production has a high energy intensity and the renewable electricity content affects the GHG emissions of vCF manufacture, more and more industries are seeking sustainable and low cost energy sources such as SGL Automotive Carbon Fibres and BMW group set up the vCF production process in Moses Lake, USA to use 100% hydro power electricity for BMW I series car manufacture. On the other hand, this result indicates markets for rCF– potential trade-off between environmental impact reductions in recycling and providing the same functional requirement with vCF.

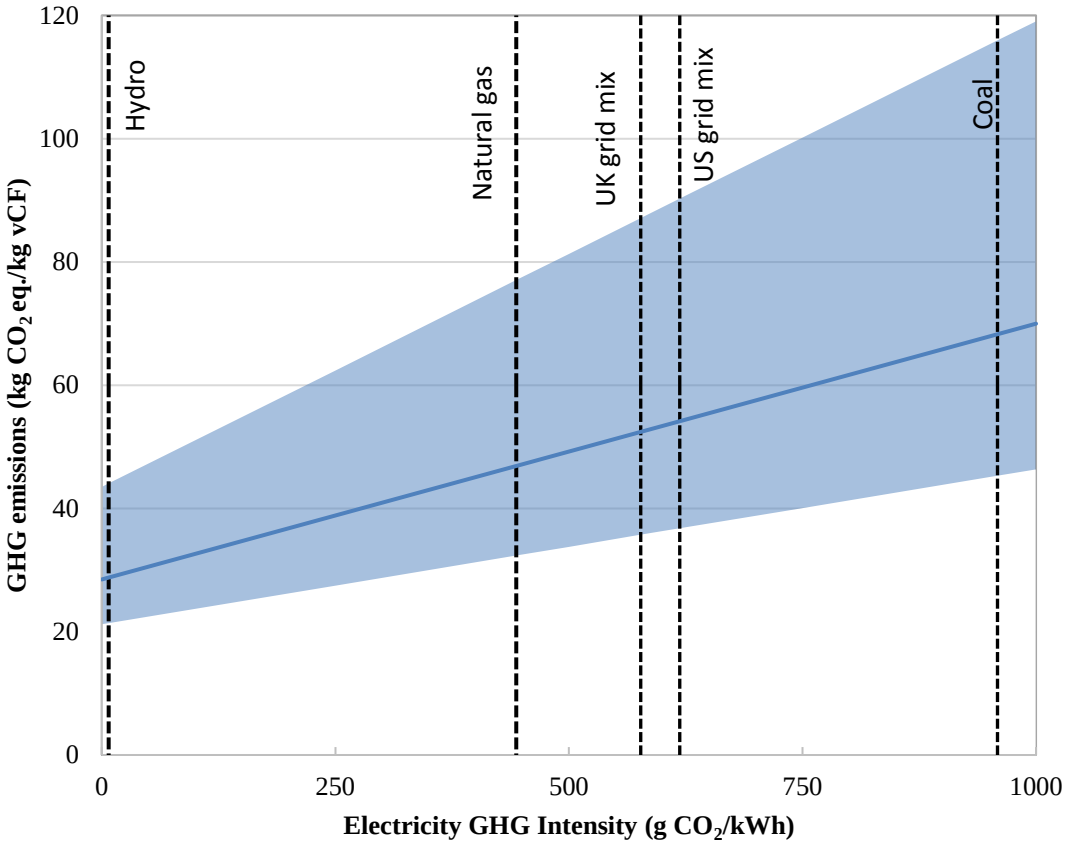

Figure 5.13. Sensitivity of total life cycle GHG emissions to manufacture 1 kg vCF to the GHG intensity of grid electricity input under λ=2.

Note: UK grid mix is based on 2013 UK average (36% coal, 27% gas, 20% nuclear, 14.9% renewables and other sources; US grid mix is based on 2013 US average (38% hard coal, 27% gas, 19% nuclear, 13.3% renewables and other sources); natural gas generation is from a combined cycle facility.

Life cycle GHG emissions are sensitive to the generation mix of input electricity; however, regardless of electricity source, components manufactured with rCF achieve the lowest emissions of all materials considered in this study (**Figure 5.14**). By utilising hydroelectric power to produce the CF-based materials, life cycle GHG emissions can be reduced by 35% (woven vCF; aligned rCFRP) and 20% (random rCFRP) relative to the base case electricity

source (UK grid mix). With increasing non-renewable content of electricity, the ability of alternative materials to reduce GHG emissions relative to steel declines. As such, on-going decarbonisation of the electricity sector seen recently in many countries will serve to improve the relative performance of lightweight materials relative to conventional steel materials.

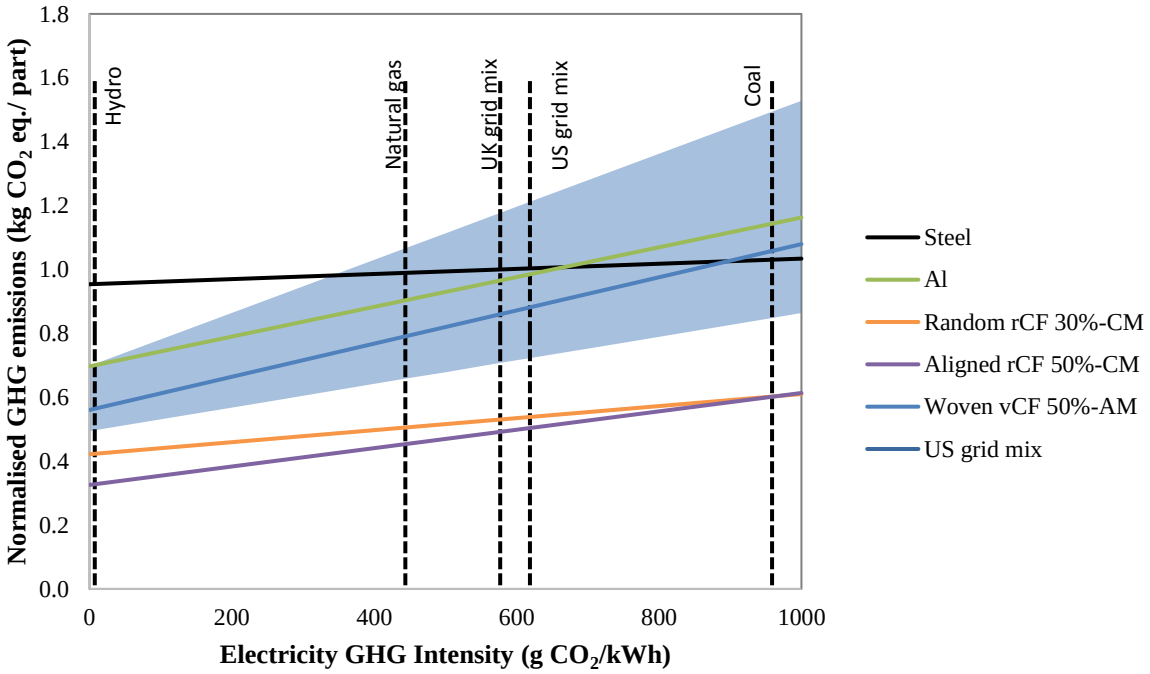

Figure 5.14. Sensitivity of life cycle GHG emissions of automotive component materials to the GHG intensity of grid electricity input to material production and uncertainty in energy requirements of vCF production (λ=2).

Note: CM=compression moulding.

Uncertainty in vehicle life does not alter the finding that rCFRP components achieve the lowest life cycle PED and GWP impact (see **Figure 5.15**). As expected towards 300,000 km, advantages of lightweight materials become more pronounced. With increase of travel distances, the ability of rCFRP materials to reduce life cycle PED and GWP relative to steel

increases. In particular, aligned rCFRP components reduce GHG emissions relative to steel by up to 94%; vCF components become favourable to steel when vehicle life exceeds 250,000 km (λ=2). Conversely, shorter vehicle life reduces in-use fuel savings and is therefore detrimental to the performance of lightweight materials. However, rCF components can reduce PED and GWP relative to conventional steel components even with very short distances travelled (<50,000 km). The traditional lightweight aluminium starts to show environmental benefits at a medium travelling life distance of about 150,000 km.

Uncertainty in vehicle fuel consumption considered for different brands of mid-size light duty vehicles with the value of 0.26-0.44 L/ (100km·100kg) similarly impact the performance of lightweight materials (see **Figure 5.16**). Life cycle GHG emissions of rCFRP materials are more sensitive to the mass induced fuel consumption than vCFRP material and lightweight aluminium. However, across the range of values considered in the study, rCFRP materials maintain the lowest life cycle environmental impact. It is also noted that woven vCFRP and aluminium could show significant GHG emission reduction in light of relatively high mass-induced fuel consumption assumed.

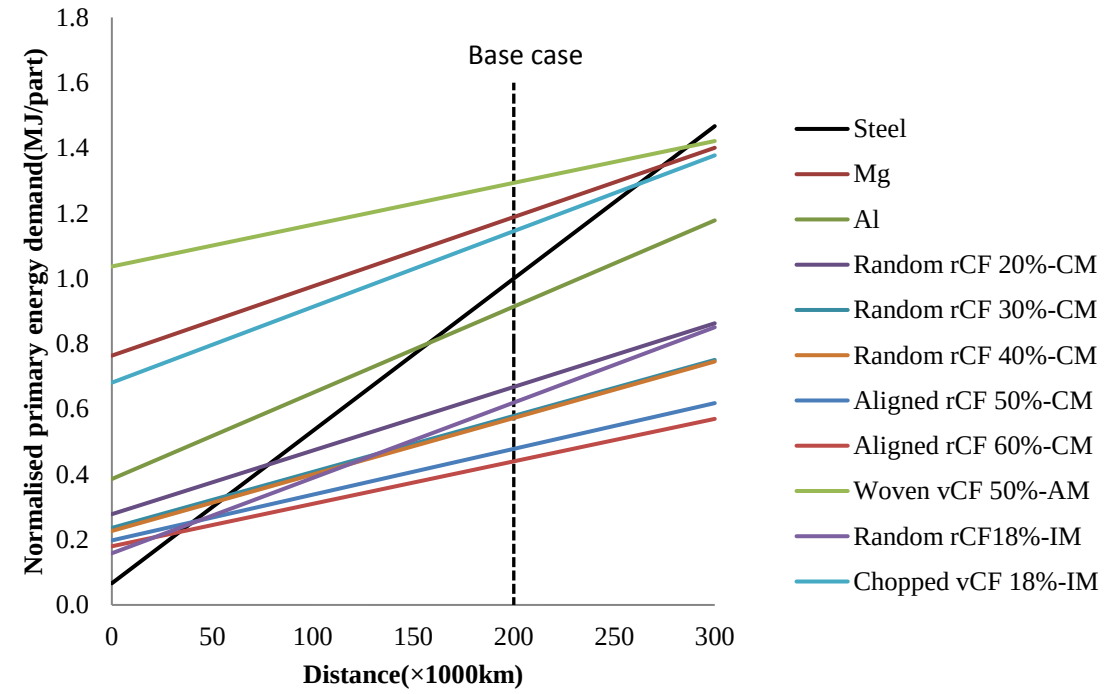

a)

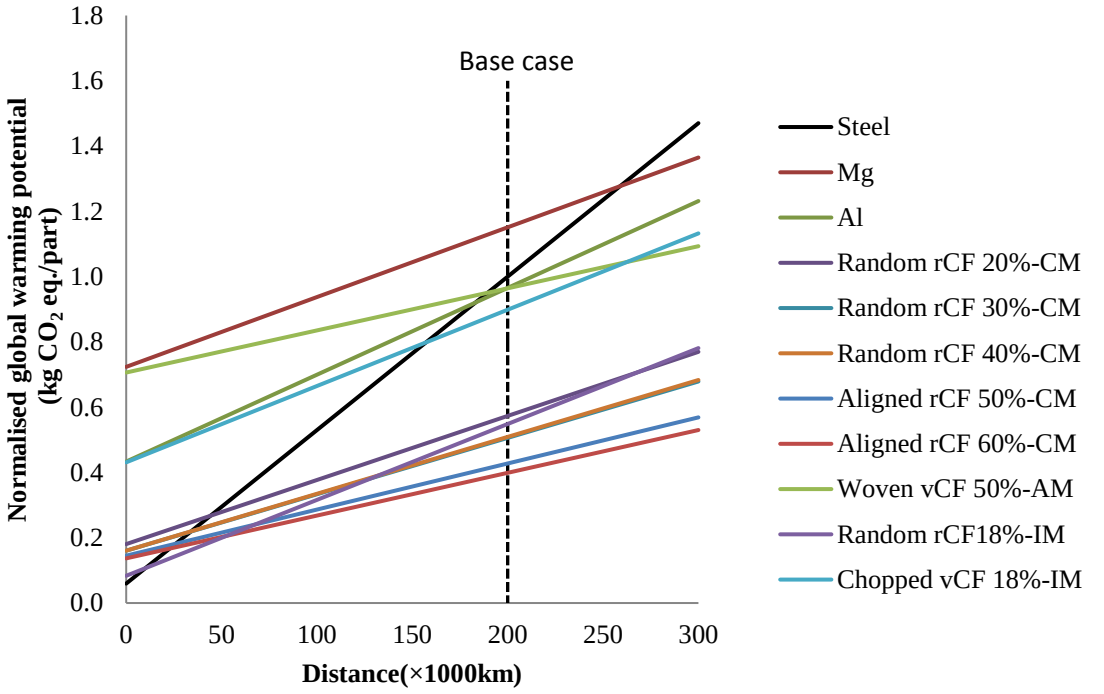

b)

Figure 5.15. Sensitivity of a) life cycle PED and b) life cycle GHG emissions as a function of the vehicle distance travelled under λ=2.

Note: CM=compression moulding, IM=injection moulding, AM= autocalve moulding.

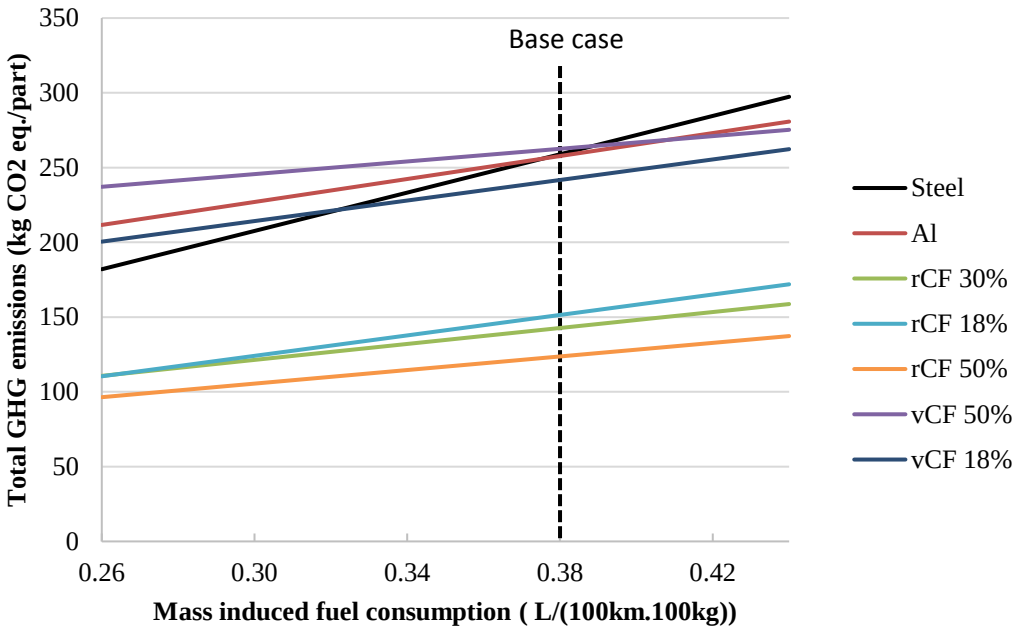

Figure 5.16. Sensitivity of total normalised GHG emissions with varied mass induced fuel consumption under λ=2

5.5 Discussion

Lightweight materials for automotive applications can reduce in-use environmental impacts and enable alternative transmissions (e.g., range extension for electric vehicles). However, weight saving is not a reliable indicator of environmental performance as this single metric ignores the impacts associated with material production. Cost and embodied energy barriers associated with the production of lightweight metals and vCF materials can, in some cases, outweigh weight reduction and environmental benefits associated with reduced fuel use during the vehicle life. In the current study, we demonstrate the advantages of rCFRP materials for automotive applications compared to competing lightweight materials (aluminium, vCF).

Components produced from rCFRP can achieve similar or greater weight reductions to competing lightweight materials while substantially reducing the impacts of production due to the low energy intensity of recycling and rCF processing activities. Moreover, the use of rCFRP results in significant reduction in GWP and PED relative to conventional steel components is primarily attribute to large use phase fuel savings.

The finding supports the commercialisation of CF recycling technologies and identifies significant potential market opportunities in the automotive sector. It has the potential to inform industry and policy-makers regarding environmental impacts related to CFRP recycling technologies and the development of relevant policies to encourage suitable utilisation of rCF materials. By adjusting model values, the model can be used to evaluate environmental impacts of other jurisdictions, co-location scenarios, co-production scenarios.

Recycled CF materials demonstrate significant environmental benefits for material selection processes and empowers eco-friendly lightweighting strategies in the automotive sector. Identifying specific components where rCFRP materials can achieve substantial weight reductions is critical to maximising their potential environmental benefits. In the current study, a range of design material constraints are considered. Further investigations must extend these methods that efficiently link component design criteria to life cycle environmental impact to integrate this approach with finite element analysis and whole-vehicle design considerations in order to identify the most promising applications

While the environmental performance of rCFRP materials is presently demonstrated, there is less certainty as to the financial viability of their production and application in the automotive sector. The next chapter focuses on the financial analysis of the recycling process and the

subsequent manufacture of rCFRP and combined with LCA method to support material design and investigate applications of rCFRP for best trade-offs between environment impact and cost. Also of concern is the mismatch between rCF availability (estimated at 50,000 t/yr in 2017(Witik et al., 2013)) and potential demands in the automotive sector, which produced in excess of 95 million vehicles globally in 2015 (European Automobile Manufacturers Association, 2017), and other potential applications of rCF materials. It will therefore be essential to identify optimal rCF utilisation opportunities that maximise net environmental and financial benefits. Environmental assessment and further life cycle cost analysis will thus play a crucial role in identifying suitable waste management strategies to address the emerging waste burden of end-of-life and manufacturing scrap CFRP materials and to determine beneficial uses of rCF in automotive sector or in other applications.

CHAPTER 6 FINANCIAL ANALYSIS OF CLOSED LOOP OF FLUIDISED BED RECYCLED CARBON FIBRE

6.1 Introduction

Vehicle lightweighting is a potentially effective method to reduce energy consumption in the transportation sector. Due to its low density and high mechanical performance, CF has been widely used in lightweighting applications. The global demand for CFRP in automotive industries values $2.4 billion in 2015 and is expected to increase to $6.3 billion by 2021 with an average increase of 17.5% (Mazumdar, 2016). However, compared to conventional steel and aluminium, the high cost of the manufacture of vCF has constrained the net benefits of lightweighting and is a barrier that needs to be overcome. It is estimated that the global demand of vCF would be 1.23 million tonnes if it was available at $11/kg (Mazumdar, 2016); however recent prices are estimated in the range of $33-66/kg (Carberry, 2008). Recycled CF can potentially provide similar lightweighting performance as vCF at a lower cost; however there is limited understanding of the overall financial viability of producing automotive components from rCF.

The generation of CFRP-based wastes is correspondingly increasing along with the increasing demand of CFRP, arising from manufacturing, where up to 40% of the CFRP can be waste arising during manufacture (Witik et al., 2013, Pickering, 2006, Pimenta and Pinho, 2011) and end-of-life products/components. For instance, 6,000-8,000 commercial aircraft are expected to come to their end-of-life by the year of 2030 (McConnell, 2010, Carberry, 2008). Treatment of CFRP waste must account for environmental and cost impact. Conventional methods to treat the CFRP wastes, such as landfilling and incineration, incur costs while recovering little value

and are discouraged by policies aimed at reducing waste sent to landfill (European Council, 1999) and increasing the recovery and recycling of materials from end-of-life products, including automobiles under the End-of-life Vehicle Directive (European Council, 2000). Opportunities to recover CF could thus extract greater value from CFRP waste streams while contributing to a range of policy objectives.

There is very little publicly available cost information regarding the performance of commercial-scale/ pilot-scale facilities associated with fibre recovery rate or other processing details. Mechanical recycling is a mature technology but is only employed at commercial scale to recycle glass fibre reinforced plastics (Oliveux et al., 2015). Commercial-scale pyrolysis plants have been built in Japan, Europe, and US with CFRP waste processing capacities of 1,000- 2,000 t/yr (Carbon Conversions, 2016, KARBOREK RCF, 2016, CFK Valley Stade Recycling GmbH and Co KG, 2016, ELG Carbon Fibre Ltd, 2016). In contrast, the fluidised bed and chemical processes (supercritical fluid; subcritical fluid) are still transitioning from lab scale to pilot plant, including a 50 t rCF/yr fluidised bed pilot plant developed at the University of Nottingham. This recycling technology is particularly suitable for dealing with end-of-life CFRP wastes which are likely to be contaminated with other materials (Yip et al., 2002, Pickering, 2006). Energy related cost data for CFRP recycling is either based on hypothesis or literatures for lab-scale operation. This results in uncertainties/limitations of the financial results as a comprehensive assessment of recycling processes can only be implemented when high quality data is available.

The knowledge gap is also existing in the subsequent manufacturing processes of rCFRP in considering the rCFRP applications. Recycled CF are typically in a discontinuous and filamentised form with random orientation and low bulk density but without tow structures.

Therefore, it is difficult in handling and processing compared to vCF with a continuous tow form, which has limited the penetration of rCF into vCF markets so far. Moreover, gaps exist in current understanding of rCF conversion techniques for opportunities to produce high performance rCFRP materials in a cost-effective ways (e.g. processing time, temperatures, pressures, capacity) and no cost analysis has been conducted previously to the best of our knowledge.

Limited studies have examined the viability of CFRP recycling and utilisation of rCF. Materials produced from rCF can significantly reduce key environmental impacts (greenhouse gas emissions, fossil energy use) in automotive applications when used in place of conventional materials (steel) and alternative lightweighting materials (vCF, aluminium) (Chapter 5). However, there is little understanding of the financial performance of recycling and remanufacturing routes to assess CFRP technologies capable of producing rCF suitable for vCF displacement. To date, only one study (Li et al., 2016)) evaluated the financial viability of mechanical recycling of CFRP waste and use of rCF in place of virgin glass fibres, finding that this low value use of rCF provided insufficient revenue to compensate for the costs of CFRP waste collection and CF recovery.

For the full implications of any use of rCF to be considered, technical and financial viability of utilising rCF-based composite materials needs to be evaluated for automotive component manufacture. In this chapter, a techno-economic analysis is undertaken to determine the financial viability of producing automotive components from rCF. The analysis considers: 1) the minimum rCF selling prices based on key operating parameters of a fluidised bed recycling process; 2) cost of manufacturing automotive components from rCF, competitor lightweight materials (vCF, aluminium) and conventional materials (steel); and 3) in-use fuel costs due to

mass-induced fuel consumption in a typical light duty passenger vehicle. Comparisons with conventional and competitor lightweight materials are made to assess financial viability and provide insights to rCF use in automotive applications.

6.2 Methods

Techno-economic models are developed to assess the feasibility of rCF use in automotive applications. The techno-economic analysis includes cost modelling of: 1) CF recycling by the fluidised bed process, 2) processing of rCF, 3) manufacture of rCFRP automotive components, and 4) mass-induced fuel consumption. A set of rCFRP manufacturing routes are considered:

1) Random structure – Compression Moulding: rCF is processed by a wet papermaking process prior to impregnation with epoxy resin and compression moulding. Fibre volume fractions (vf) of 20%, 30%, and 40% are considered.
2) Aligned – Compression Moulding: rCF is processed by a fibre alignment process prior to compression moulding with epoxy resin. Fibre volume fractions of 50% and 60% are considered.
3) Random structure – Injection Moulding: rCF is processed by wet papermaking and subsequently chopped prior to compounding with polypropylene (PP); rCF-PP pellets are subsequently injection moulded. Fibre volume fraction is 18%.

The overall life cycle cost of rCFRP components are compared to conventional material (steel) and competitor lightweight materials (aluminium, vCFRP) to assess the relative financial performance of utilising rCF for automotive component manufacture while meeting the same component design criteria (see Section 6.2.6). The first considers autoclave moulded vCF material typical of high-performance applications wherein bi-directionally woven vCF is

autoclaved moulded from prepreg with epoxy resin with a fibre volume fraction of 50%. A second, similar process wherein chopped, unaligned fibres are compounded with PP and vCF-PP pellets are subsequently injection moulded with a fibre volume fraction of 18%. The CF-based materials are also compared with mild steel manufactured by stamping process, as a conventional automotive material, and potential lightweight materials (aluminium manufactured via casting process) as described in Section 6.2.5. Vehicle assembly is excluded in this study as costs are assumed to be similar for all materials considered. The end of life stage is also excluded.

The techno-economic models are developed to account for capital cost (CAPEX) such as equipment and financing, and operational cost (OPEX) such as fixed operating and maintenance, utilities costs (e.g., energy), depreciation and overheads. Taxes, subsidies, and profit margins are not included in the analysis. The minimum rCF selling price is determined based on estimated costs of CFRP recycling and key operating parameters of a fluidised bed process (see Section 6.2.2). Overall life cycle costs of manufacturing automotive components and their in-use fuel costs are calculated for all materials to determine the relative financial performance of rCF-based materials.

The comparison analysis is taken to ensure functional equivalence of producing automotive components from the set of materials based on the design material index (λ) (Patton et al., 2004, Ashby, 2005) in order to broadly understand the financial viability of rCF materials in potential applications. The component thickness is variable and is adjusted based on each material's mechanical properties and the specific design material index (see Section 6.2.6 for further details). Financial results are presented on a normalised basis (relative to the mild steel

reference material), and can thereby be easily applied to subsequent analyses that are undertaken for specific components where the material design index is known.

Table 6.1. Summary of the cost model input data.

Items		**Values**
CAPITAL COSTS		
Fixed capital, C_{FC}		C_{FC}=Purchase cost $(1+f_{10}+f_{11}+f_{12})$
Working capital, C_{WC}		C_{WC}=15% C_{FC}
Total capital investment, C_{TC}		$C_{TC}=C_{FC}+C_{WC}$ /available data
OPERATIONAL COSTS		
Direct		
Raw materials	Steel	\$0.43/kg[a]
	Aluminium	\$1.65/kg[b]
	vCF	\$41/kg[c]
	Epoxy resin	\$16/kg[d]
	Polypropylene	\$1.35/kg[e]
Utilities	Electricity cost	£0.09 (\$0.14)/kWh[f]
	Natural gas cost	£0.007(\$0.011)/MJ[f]
Maintenance		5-10% of fixed capital (6% used)
Operating labour	Labour costs	£18.20 (\$27.70) per hour[g]
	Working days per year	250
	Shifts	8 h/3 per day
Indirect		
Plant overheads		60% of operating labour
Insurance		0.5% of the fixed capital
General expenses		
Administrative costs		25% overhead
Distribution and selling costs		5% of total expense
Research and development		5% of total expense
Production volume		50,000 parts/yr
Production period		10 yrs
Depreciation time		10 yrs (estimated machine lifetime)
Use		Premium unleaded gasoline in 2015: \$1.70/litre[h]

[a] Source: Ref. (MEPS (International) LTD, 2016) [b] Source: Ref. (InfoMine, 2016)
[c] Source: Ref. (Warren, 2011) [d] Source: Ref. (Easy Composites Ltd, 2016)
[e] Source: Ref. (MRC Ltd, 2016)
[f] Source: Ref. (Dempsey et al., 2015)
[g] Source: Ref. (UK Department of Energy & Climate Change, 2015)
[h] Source: Ref. (Eurostat Statistics Explained, 2015)

6.2.1 Capital and operational costs

The CAPEX estimation is undertaken for hypothetical CFRP recycling, rCF processing, and rCFRP manufacturing facilities. Equipment costs are estimated with insights from the Nottingham fluidised bed demonstration plant (50 t/yr capacity) and laboratory-scale processes developed for rCF processing (papermaking, fibre alignment). Installed costs are estimated for standard equipment, sized to required capacity, and non-standard equipment with indicative cost data from the demonstration plant, using the factor method (Ulrich, 1984, Gerrard, 2000) as shown in **Table 6.1**. All major equipment items are designed and costed based on the process information described in Section 6.2.2-6.2.5. Costs are then extrapolated to year 2015 costs based on the Chemical Engineering Plant Cost Index (Chemical Engineering, 2015) (**eq. 6.1**). An exponential relationship as shown in **eq. 6.1** is used to estimate equipment capital costs for different plant capacities. Normalised annual CAPEX is calculated assuming a 15% of return tax rate for a plant life of 10 years (Pickering et al., 2000) where needed for part cost prediction.

$$C_{p,v,2015} = C_{p,u,r}\left(\frac{v}{u}\right)^{n}\left(\frac{I_{2015}}{I_r}\right) \qquad 6.1$$

Where $C_{p,v,2015}$ is the equipment CAPEX with capacity v in the year of 2015, $C_{p,u,r}$ is the reference equipment cost at capacity u in year r, I_{2015} is cost index in the year of 2015., I_r is cost index in year r. A scaling factor (n) of 0.6 is assumed.

The annual operational cost is calculated as the sum of operating costs (labour, material, utility), plant overheads, and maintenance cost as shown in **Table 6.1** but OPEX information is updated based on actual component of pilot plant or standard equipment where available. The labour

cost is estimated based on an hourly pay rate of £18.20 ($27.70) in 2015 (Eurostat Statistics Explained, 2015) for plant operation requirement of 3 shifts per day across 250 days per year (see **Table 6.1**). Other operational costs including materials, utilities, plant overheads and maintenance are obtained from publicly available data and, where appropriate, are adjusted to the plant capacities considered in this study.

Techno-economic modelling is highly sensitive to the accuracy of the input data, but a sensitivity analysis as in this paper can be performed where uncertainties exist to evaluate the impact of input parameters.

6.2.2 CF recycling

The overall fluidised bed process consists of two main sub-processes, waste CFRP size reduction (shredder, hammer mill) process and a fluidised bed process. In the fluidised bed reactor, the epoxy resin is oxidised at a temperature in excess of 500 °C. The gas stream is able to elutriate the released fibres and transport them out of the fluidised bed for separation by cyclone. After fibre separation, the gas stream is directed to a high-temperature oxidiser to complete oxidation of resin decomposition products. Energy is recovered to preheat inlet air to the fluidised bed. Process models of the fluidised bed recycling plant have been developed in Chapter 3 and are used in this study to calculate utilities cost. The rCF minimum selling price is calculated for a set of operational parameters such as plant capacity (50 to 6,000 t/yr) and feed rate per fluidised bed area (3 to 12 kg/hr-m^2).

The capital and operational costs associated with rCF are estimated for a fluidised bed plant with a hypothetical throughput of 1,000 t/yr as a base case while a range of 100-6,000 t/yr is considered in the sensitivity analysis. The main components of the fluidised bed plant are

shown in **Figure 3.1**. Cost for shredding (shredder) is estimated for processing particle size to 25-100 mm and finally to 5-25 mm (Ulrich, 1984, Gerrard, 2000). An indicative oxidiser fixed cost is obtained based on the pilot plant. Fixed costs for all other equipment are estimated based on processing parameters (e.g., flow rate, temperature and pressure) for best operation of the pilot plant using appropriate cost indices, installation factors and other costing factors given by (Ulrich, 1984). All capital costs are adapted for required capacity in the year of 2015 and normalised to annual capital costs.

The OPEX of the selected recycling plant is calculated based on a nominal operating labour of 3 persons per shift, utility inputs (natural gas, electricity) calculated in Chapter 3, and costs associated with maintenance, supervision and indirect costs as detailed in Section 6.2.1. Heat recovery from the exhaust stream is assumed to provide additional revenue by displacing natural gas used for an onsite/offsite heating system. The financial value of recovered heat is assumed to be 80% that of the avoided natural gas consumption to account for costs of a heat recovery system. Heat recovery, however, depends on having a customer for the heat; this is discussed further in the results section.

A discounted cash flow analysis is used to determine the rCF minimum selling price (MSP) ($/kg) to achieve a net present value of zero:

$$MSP = \frac{OPEX + ACAPEX - OR}{AO} \qquad 6.2$$

Where OPEX is the operational cost ($/yr), ACAPEX is annualised capital cost ($/yr), OR is other revenue ($/yr), e.g. heat sales, and AO is annual rCF output (t/yr)

6.2.3 Processing of rCF

Due to its discontinuous, filamentised form and low bulk density, rCF cannot be directly manufactured into CFRP. Currently, there are two methods to convert rCF into intermediate mats: wet papermaking process for random rCF mats and fibre alignment process for aligned rCF mats. The main equipment of papermaking process consist of mixer, belt conveyer, vacuum dryer and thermal dryer. Capital costs are estimated based on standard equipment, sized to required capacity and non-standard equipment with processing parameters from lab-scale plant. Plant capacity required can be related to quantity of rCF required in final CFRP part manufacture volume. An energy analysis of the papermaking process has been performed based on the processing parameters in Chapter 4 and used for energy cost estimation in this study (4 kWh/kg). Viscosity modifier cost is estimated assuming a recycling rate of 99.5%, which can be achieved by complete recovery during vacuum drying and minor losses during thermal drying. The papermaking process is assumed to need 1.5 labourers per operational shift.

Fibre alignment processes are under development and show promise to allow rCF to be manufactured into CFRP with high fibre volume fraction for high value applications (Wong et al., 2009b). As the alignment process is under development, no cost information is available for fibre alignment rig yet while there is a target cost that aligned rCF intermediate materials must achieve to compete with competitor materials and randomly oriented rCF materials. Additional alignment costs could be acceptable due to the improved mechanical performance that can be achieved from aligned, high volume fraction rCFRP materials relative to unaligned materials. Target fibre alignment costs are determined in order for aligned rCFRP materials to achieve the same life cycle cost as a conventional steel component and the best performing

randomly aligned rCFRP material. To see if target cost is reasonable, energy cost is considered based on research estimates of hypothetical commercial process.

6.2.4 Component manufacture

After rCF processing, rCF can be manufactured into the final CFRP products by either compression moulding or injection moulding from random/aligned rCF mats.

A compression moulding method has been utilised to produce rCFRP components from either random or aligned CF at lab scale. In this process, CF mats and epoxy resin film are cut to fit into the mould. The main equipment consists of a compression moulding press and a trimming machine of which fixed capital is $1.88 million for a 200 t/yr plant (Witik et al., 2011) and scaled up to the required capacity of component production and extrapolated to 2015. Energy analysis of the process (i.e. heating stage, curing stage, pressure build-up stage and finishing stage) based on heat transfer and force analysis has been performed in Chapter 4 and used for utilities estimation. The process is assumed to require 1.5 labourers per operational shift.

Injection moulding is also an efficient way to process rCF leading an outstanding mechanical performance when compared to vCF counterparts (Wong et al., 2012). The CF is compounded with polymer matrix to produce pellets for injection moulding. The injection moulding facility is made up of compounding, injection and trimming machines and the equipment capital cost ($24.8m for a 144 t/yr plant) (Witik et al., 2011) and scaled up to the required capacity of component production and extrapolated to 2015. Operational cost is based on material requirements as in the discussion of material substitution under equivalent stiffness, manufacturing energy use (based on previously presented models of energy consumption in Chapter 4). This process is assumed to require 1.5 labourers per shift.

Table 6.2. Summary of cost data of manufacturing routes (normalised to 2015)

Items		Steel	Aluminium	CFRP		
Manufacture type		Stamping	Casting	IM	CM	AM
Part manufacture	Equipment	$18.2m[a]	$6.24m[a]	$24.8m[a]	$1.96m[a]	$4.50m[b]
	Plant capacity	460 t/yr	210 t/yr	144 t/yr	200 t/yr	210 t/yr
	Energy	0.34 MJ/kg	18.43 MJ/kg	3-4 MJ/kg	15-20 MJ/kg	33 MJ/kg
	Labour	4	2	1.5	1.5	2

Note: CM=compression moulding, IM=injection moulding, AM=autoclave moulding

[a] source: Ref (Witik et al., 2011) [b] source: Ref (Witik et al., 2012)

The reference component is assumed to be made of hot rolled steel coil. The manufacturing devices are assumed to include a coil handling and a stamping equipment (CAPEX is $18.2m for a 460 t/yr plant) and the manufacturing energy is 0.34 MJ/kg (Witik et al., 2011). Aluminium is assumed to be manufactured by wrought methods including casting, punching and machining units (CAPEX is $6.24m for a 210 t/yr plant) and the total energy requirement is 18.43 MJ/kg (Sullivan et al., 2010). Virgin CF is either manufactured by autoclave moulding (CAPEX is $4.50m for 210 t/yr (Witik et al., 2012)) into woven vCFRP or by injection moulding into chopped vCFRP similar as for rCFRP. Publicly available operational cost data including materials, labour and utilities for these manufacturing processes, are obtained from process models, literature and online database (Sullivan et al., 2010, Ingarao et al., 2016, InfoMine, 2016, Witik et al., 2012).

6.2.5 Use phase

In the use phase, the automotive part will influence vehicle fuel consumption due to its weight. Mass-induced fuel consumption is calculated for a typical midsize passenger vehicle (Ford, Fusion) with the Physical Emission Rate Estimator model (US EPA, 2016). A typical vehicle

life of 200,000 km (Helms and Lambrecht, 2007, Witik et al., 2011) is assumed. Fuel prices are regionally dependent; as a base case we consider the average 2015 UK petrol price (£1.11/litre or approximately $1.70/litre) (UK Department of Energy & Climate Change, 2015) but consider a range of fuel costs in typical of other jurisdictions. To compare with upfront costs, use phase fuel costs are converted to a present value assuming a 5% discount rate and a vehicle life of 10 years.

6.2.6 Automotive component design criteria

Automotive components produced from different materials must meet the same design criteria in order to be suitable for their application. In this research, a generic automotive component, assumed to be produced from mild steel, is selected as the reference component and allocated a normalised thickness and mass of 1. When evaluating alternative materials, it is ensured that each meets the component design criteria by considering the design material index (λ) and varying component thickness to account for differences in each material's mechanical properties. Properties of rCFRP materials, vCFRP materials, mild steel, and aluminium are obtained from experiments (Wong et al., 2009a) and online databases (MatWeb, 2016, Kelly et al., 2015, ASM Aerospace Specification Metals Inc., 2015, GoodFellow, 2016). The mass and thickness ratio among components made of different materials is expressed below:

$$\frac{m_2}{m_1} = \frac{\rho_2}{\rho_1}\left(\frac{E_1}{E_2}\right)^{\frac{1}{\lambda}} \tag{6.3}$$

$$\frac{t_2}{t_1} = \left(\frac{E_1}{E_2}\right)^{\frac{1}{\lambda}} \tag{6.4}$$

Where E_1, t_1, ρ_1 are the tensile modulus, thickness and density of reference materials (i.e. mild steel), E_2, t_2, ρ_2 are the tensile modulus, thickness and density of replacing material, (e.g. aluminium, CFRP), λ is the component-specific design material index (more details can be found in Section 5.2.6 in Chapter 5).

The relative thickness of the components impacts costs for raw material procurement as thicker CFRP components require greater quantities of fibre and matrix materials for functional equivalence. Larger weight of components also require higher cost for manufacturing. Moreover, they impact more in-use fuel consumption associated with mass as will be discussed in the following sections.

6.3 Results

6.3.1 CF recovery

Recovery of CF from CFRP wastes can be achieved at under $5/kg across a wide range of process parameters. **Figure 6.1** shows the minimum selling price of rCF with a breakdown costs at a range of capacities between 50 and 6,000 t/yr. The cost includes all variable and fixed costs associated with the construction and operation of the fluidised bed recycling plant and revenue from heat recovery. The relative contribution of fixed and operational costs is highly dependent upon the plant capacity for recycling. At capacities in excess of 500 t/yr, an rCF minimum selling price of less than $5/kg can be achieved. Operation at smaller capacities is detrimental to financial viability: at relatively low capacity of 100 t/yr, rCF would have to achieve a market value of up to $15/kg to be financially feasible. This is primarily because of the higher relative share of fixed capital and labour costs. At all plant capacities, operational cost accounts for over 50% of the total cost of recycling. As labour cost is determined by the

operational requirement of the recycling process itself and is independent of plant capacity, its relative contribution therefore reduces when the plant capacity grows. For a fixed feeding rate (kg/hr-m^2), larger size of equipment results in lower specific capital cost ($/t-yr) due to economies of scale. Heat recovery from exhaust contributes to reducing the rCF minimum selling price by $0.17/kg for all capacities. At the base case capacity of 1,000t/yr, heat sales represent 6% of rCF recovery costs. If a customer for the heat is not available, rCF recovery cost would correspondingly increase. Sorting, dismantling and transport of waste CFRP to the facility are not included in this analysis, but this could represent significant costs, particularly if manual disassembly is required (Li et al., 2016). Transportation costs also account for a large part due to waste availability and regional factors when high capacities can be achieved. Therefore, further work is suggested to investigate types, locations and quantities of CFRP wastes to better understand these costs and their impact on financial viability.

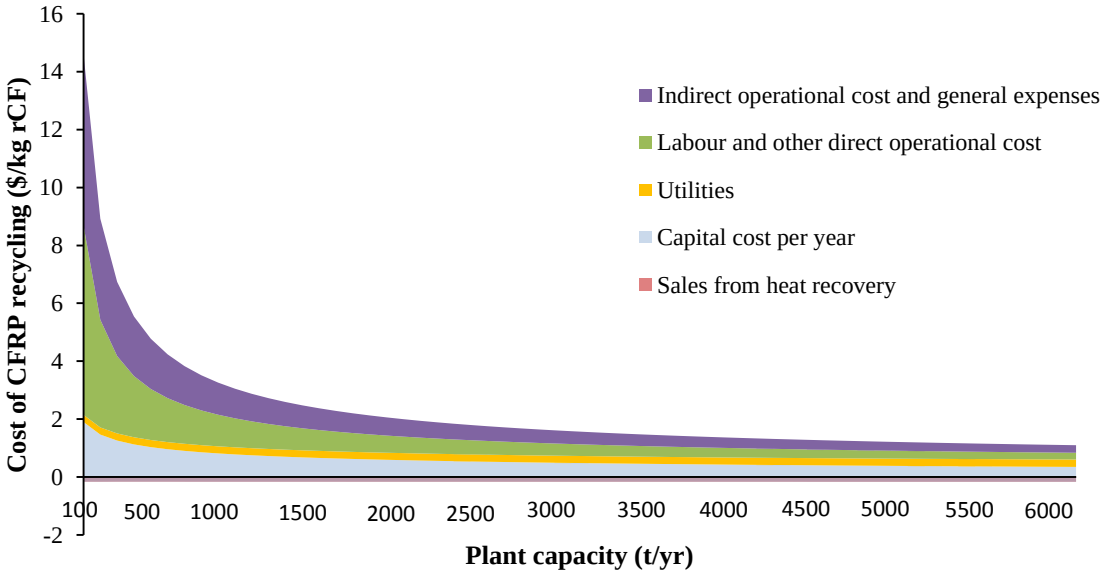

Figure 6.1. Minimum selling price of rCF and breakdown cost components for different plant capacities at feed rate of 9 kg/hr-m^2.

Table 6.3. Manufacturing costs of 1000 t/yr rCF recycling plant

Job title: Fluidised bed recycling plant		Date estimate carried out: September 2016
Location: Nottingham		Capacity: 1000 t/yr rCF
		Cost index type: Chemical Engineering in 2015
		Cost index value: 557.91
CAPITAL COSTS		
Fixed capital, C_{FC}	$4,117,108	$C_{FC}=PPC*(1+f_{10}+f_{11}+f_{12})$
Working capital, C_{WC}	$617,566	$C_{WC}=15\%\ C_{FC}$
Total capital investment, C_{TC}	$4,734,674	$C_{TC}=C_{FC}+C_{WC}$
OPERATIONAL COSTS		
Direct	$/yr	
Raw materials		CFRP waste
Miscellaneous materials		10% of maintenance
Utilities	254,914	Electricity and natural gas
Maintenance	247,026	5-10% of fixed capital (6% used)
Operating labour	499,378	from manning estimate
Supervision	74,907	15% of operating labour
Operating Supplies	24,703	10% of maintenance
Laboratory charges	49,938	10% of operating labour
Royalties		1% of the fixed capital
Total, A_{DME}	1,150,866	
Indirect		
Plant overheads	492,787	60% of operating labour
Insurance	20,586	0.5% of the fixed capital
Total, A_{IME}	554,543	
Total manufacturing expense (excluding depreciation), $A_{ME}=A_{DME}+A_{IME}$	1,725,995	
General expenses		
Administrative costs	123,197	25% overhead
Distribution and selling costs	102,733	5% of total expense
Research and development	102,733	5% of total expense
Total, A_{GE}	328,662	
Total expense, A_{TE}	2,031,785	$A_{TE}=A_{ME}+A_{BD}+A_{GE}$
Revenue from sales, As		
rCF/ $2.83/kg	2,805,710	MSP
Process steam/ $0.009/kg	169,467.66	

The impacts of feed rate per unit fluidised bed area on the minimum selling price of rCF and the breakdown of the costs for a 1,000 t/yr plant are shown in **Figure 6.2**. The minimum selling price per kg rCF varies from \$3.9 to \$2.0 with respect to feeding rate of 3 kg/hr-m^2 to 12 kg/hr-m^2. Prior analysis in Chapter 5 also shows feeding rate is a key factor for environmental impact which is correlated to the energy input. For a fixed plant capacity, with the increase of feed rate per unit bed area the size of equipment can be reduced. Therefore, the annualised capital cost reduces relative to the increase of feed rate. Also, plant with higher feeding rate consumes less energy (i.e. natural gas and electricity) and thus has less utilities cost while the other costs including labours remain unchanged. For instance, the utilities cost is \$0.73/kg (15% of the total) at 3 kg/hr-m^2 but reduces to \$0.18/kg (4% of the total) at 12 kg/hr-m^2. While cost effectiveness gains are identified to be achievable by increasing feed rate, there are potential trade-offs in terms of resulting rCF properties. To avoid agglomeration in the recycling process at high feed rates, fibre length must be reduced (Jiang et al., 2005). However, fibre length may also affect the downstream rCFRP manufacturing process and resulting rCFRP properties. The feed rate has to balance recycling cost and subsequent rCFRP properties, however; this is a topic of ongoing research.

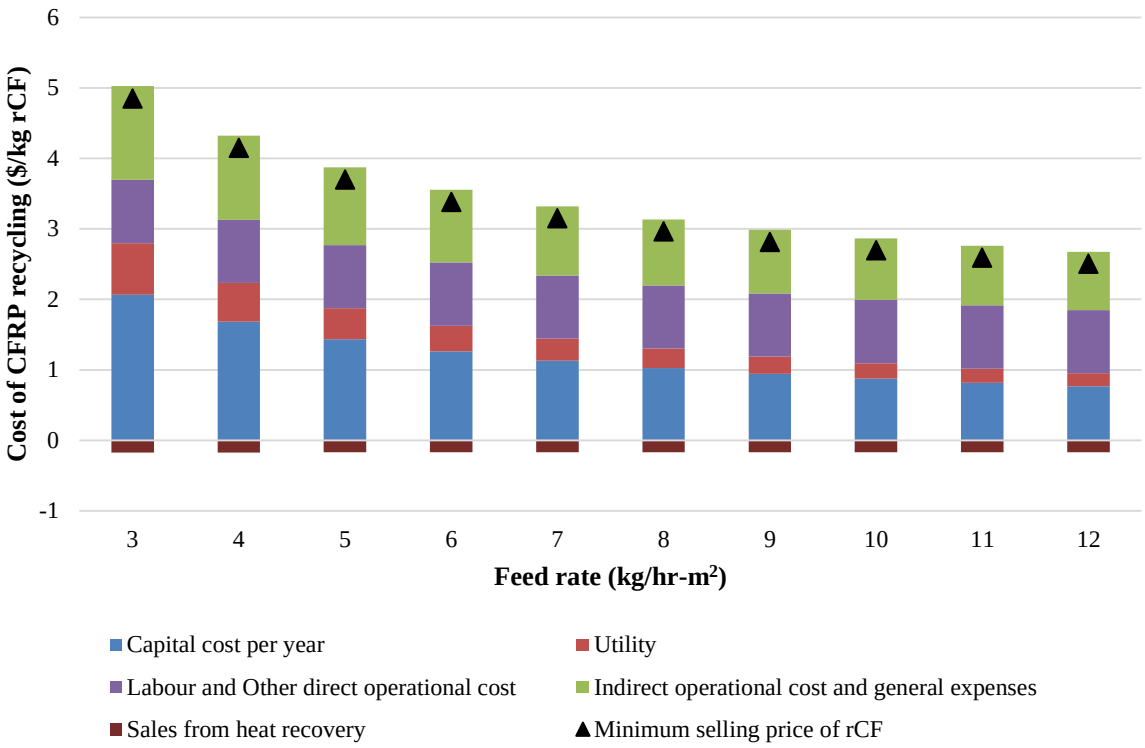

Figure 6.2. Minimum selling price and breakdown costs of rCF for different feed rates (kg/hr-m^2) for 1000 t/yr.

6.3.2 Complete life cycle cost

CFRP materials manufactured from rCF can offer cost savings and weight reductions relative to steel and competitor lightweight materials in some cases, but is dependent on the specific application, e.g., material design index, as this drives the weight reduction/in-use fuel consumption and material requirements.

With the increasing fibre content, rCFRP materials show better mechanical performance. Thus increasing the fibre volume fraction in CFRP materials is beneficial in reducing component mass for functional equivalence with steel. For design material index λ=2, for instance, significant weight reductions are seen in increasing the fibre content of random rCFRP

components from 20% vf (54% reduction) to 30% vf (58% reduction); however, further increase to higher volume fraction of 40% compromises the weight reductions due to fibre damage during the manufacturing process while it achieves the same weight reduction as for 30% vf (see scattered dots in **Figure 6.3**). Although achieving further high fibre volume fractions of 50% and 60% provides 65%-67% weight reductions, this requires new fibre alignment techniques, which are still under development.

Weight savings achieved during substitutions can lead in-use fuel saving and thus potential life cycle cost benefits. However, the net financial benefits can be compromised for high cost of raw materials. For instance, due to extremely high cost of vCF, the total life cycle cost of vCFRP does not present significant benefits especially for low fibre volume fraction ($1.6/part for vCF 18%). The normalised life cycle costs including vehicle use for material substitution under different design indices (i.e., λ=1, 2, 3) are shown in **Figure 6.3** where life cycle cost of the parts made of rCFRP and other alternative lightweight materials are compared relative to steel.

For design index λ =2, which is typical for components under bending and compression conditions in one plane (vertical pillars, floor supports), rCFRP components show slight cost reductions relative to steel over the full life cycle. For random rCFRP parts with different fibre volume fractions, total normalised cost varies between $1.12/part for 20% vf, $0.98/part for 30% vf and $0.98/part for 40% vf. It is noted that for random rCFRP, from 30% vf to 40% vf, the life cycle cost is not expected to be reduced as from 20% to 30%. This is primarily because of different weight reductions achieved between 20%- 30% and 30%- 40% as discussed above. Raw material costs account for a large part of the life cycle cost (23%-29%) primarily due to the high cost of epoxy resin. On the contrary, although use phase cost of random rCFRP parts

is 42%-46% that of steel part, these benefits do not compensate the material and manufacturing cost.

Compression moulding random rCFRP part costs only 61%-70% of that for injection moulded random rCFRP part in the full life cycle. Compression moulding random rCFRP part with higher fibre volume fraction (20% - 40%) shows better mechanical performance than injection moulded part, which results in greater weight reductions relative to steel. Therefore, injection moulded random rCFRP part with 18% vf has less fuel savings and as such higher life cycle cost compared to compression moulded rCFRP part.

For a panel loaded in bending and buckling conditions in two planes (λ=3), following similar trends as for λ=2, larger weight savings for rCFRP in replacement of steel are observed and as such more fuel savings can be achieved in the use phase. For random rCFRP components, normalised life cycle costs are \$0.84/part for 20% vf, \$0.78/part for 30% vf and \$0.79/part for 40% vf, respectively.

For λ=1, for columns and beams under tension conditions (e.g., a window frame), there is limited scope for lightweighting with any of the materials considered in this study. Even though, fibre alignment could still potentially improve financial performance of rCFRP provided that the target value of \$1.5/kg for fibre alignment technique is met.

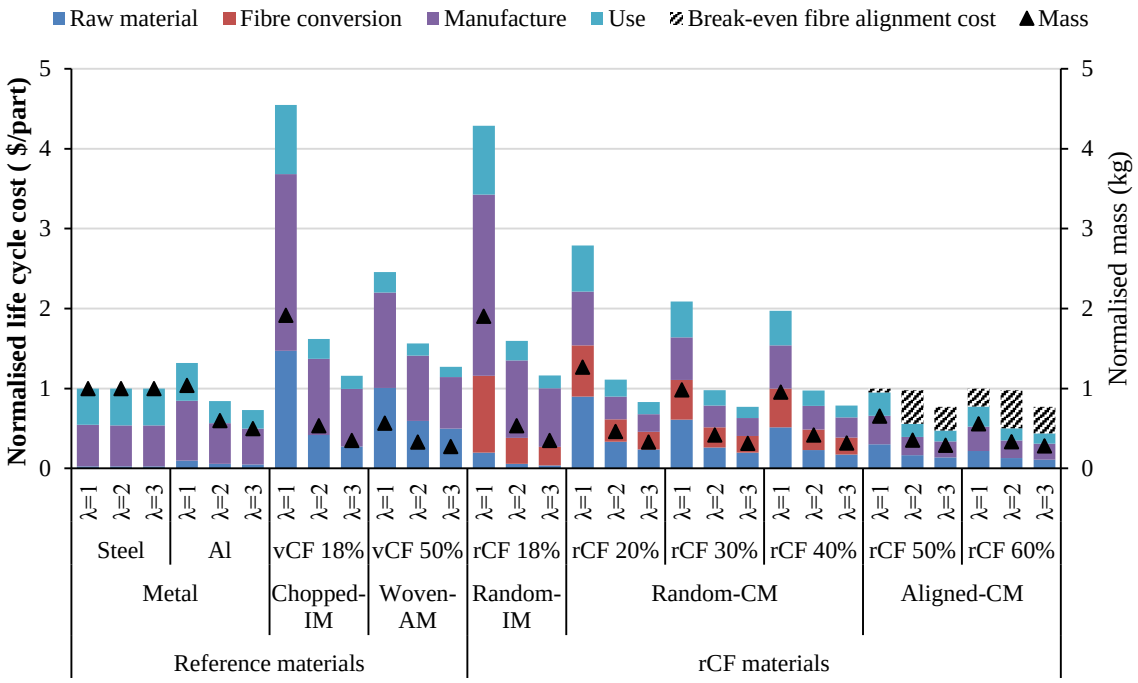

Figure 6.3. The normalised life cycle cost of the automotive components made of steel and substitution materials under different design indices (i.e. λ=1, 2, 3).

Note: Hatched columns represent fibre alignment cost range allowed to breakeven with conventional steel components and randomly oriented rCF components competitors.

6.3.2.1 Cost target for fibre alignment

To achieve high rCF fibre volume fraction, which is necessary to achieve similar mechanical performance as woven vCFRP, fibre alignment is necessary. The life cycle cost results are used to set targets for the development of fibre alignment technologies that are currently under development. Hatched columns on **Figure 6.3** show the target cost that aligned rCF intermediate materials must achieve to compete with best available random rCFRP (i.e. rCFRP with 30% vf) for λ=2 and λ=3 or with steel for λ=1. Therefore, for instance, life cycle cost for aligned rCFRP component is assumed to be \$0.78/part, giving a corresponding target alignment cost of \$0.31/part for 50% vf and \$0.34/part for 60% vf respectively (λ=3). If rCF can be

produced at a cost of $3/kg at an annual throughput of 1,000 t/yr as discussed in Section 3.1, higher processing costs (i.e., fibre alignment cost) could be accommodated for high quality aligned rCFRP products to achieve the same cost level as the random rCFRP products or steel under different design constraints in the full life cycle. The target fibre alignment cost is $21.2/kg aligned rCF mat compared to $11.6/kg random rCF mat via papermaking process under λ=2, 3 while the target value has to be as low as $1.5/kg in order to achieve the same life cycle cost with steel under λ=1.

In **Figure 6.4**, the magnitudes of life cycle cost of rCFRP against weight savings are compared to that of steel and other substitution alternative materials for design criteria index λ=1, 2 and 3 in **Figure 6.4** a), b), and c), respectively. Cost data for members of a particular group of material (e.g. vCFRP, rCFRP) cluster together and can be enclosed by an envelope. As previously discussed, greater weight and life cycle cost reductions can be achieved at higher design criteria indices. With the increase of lambda values, using rCF materials to replace steel show more life cycle cost reductions as well as weight reductions. This demonstrates the more appropriate cost effective applications of rCF materials in beam/panel part manufacture under bending conditions. Results also indicate larger cost savings together with weight savings can be achieved by using high-fibre-volume-fraction rCFRP. Compared to vCFRP, providing the same weight reduction, aligned rCFRP materials potentially lead to larger life cycle cost reductions in replacement of steel in automotive parts. This demonstrates fibre alignment could potentially improve financial performance provided technology development targets are met.

Figure 6.4. The weight saving for panels against normalised cost target relative to steel baseline for a) λ=1, b) λ=2, c) λ=3.

6.3.3 Sensitivity analysis

The cost analysis entails uncertainties as not all costs of stages of the life cycle are known in the design process. Variation in key parameters (in-use fuel consumption, vehicle lifetime, fuel price, raw material price) in the life cycle would have an impact on results.

Uncertainty associated with mass-induced fuel consumption and vehicle lifetime does not alter the finding that rCFRP components significantly reduce the life cycle cost among the lightweight substitution materials from a life cycle perspective (see **Figure 6.5**). Mass-induced fuel consumption is estimated to be 0.26-0.44 L/ (100 km·100 kg) for different brands of mid-size light duty vehicles. Mass-induced fuel consumption of 0.38 L/ (100 km·100 kg) for Ford Fusion vehicle in 2015 is selected as the base case for life traveling distance of 200,000 km as presented in **Figure 6.5**. Across the range of values considered in the study, rCFRP materials maintain the lowest life cycle cost impact. Aligned rCFRP materials offer possibilities for further life cycle cost savings than random rCFRP and weight reductions while maintaining good mechanical properties but fibre alignment technique is still under development. It is also noted that due to the high energy intensity of vCF production, vCFRP with low fibre volume fraction (18%) only exhibit cost savings when the mass induced fuel consumption is larger than 1.48 L/ (100 km·100 kg).

Similarly, life cycle cost increases with traveling distance, depending on the mass of the substitution alternatives, the initial cost of raw material and part manufacturing. At extended vehicle lifetime (up to 300,000 km), cost advantages of lightweight materials become more pronounced. Aligned rCFRP components reduce life cycle cost relative to steel by up to 60% excluding fibre alignment; fibre alignment could potentially improve financial performance

(see dashed lines in **Figure 6.5**) provided technology development targets are met, demonstrating lowest cost from use of high volume fraction rCFRP. CFRP components from vCF become favourable to steel when vehicle life exceeds 566,000 km (λ=2). Conversely, shorter vehicle life reduces in-use fuel savings and is therefore detrimental to the performance of lightweight materials. However, rCF components can reduce life cycle cost relative to conventional steel components even with relatively short distances travelled (~180,000 km). Conventional lightweight aluminium also show cost reductions from the very start of the life.

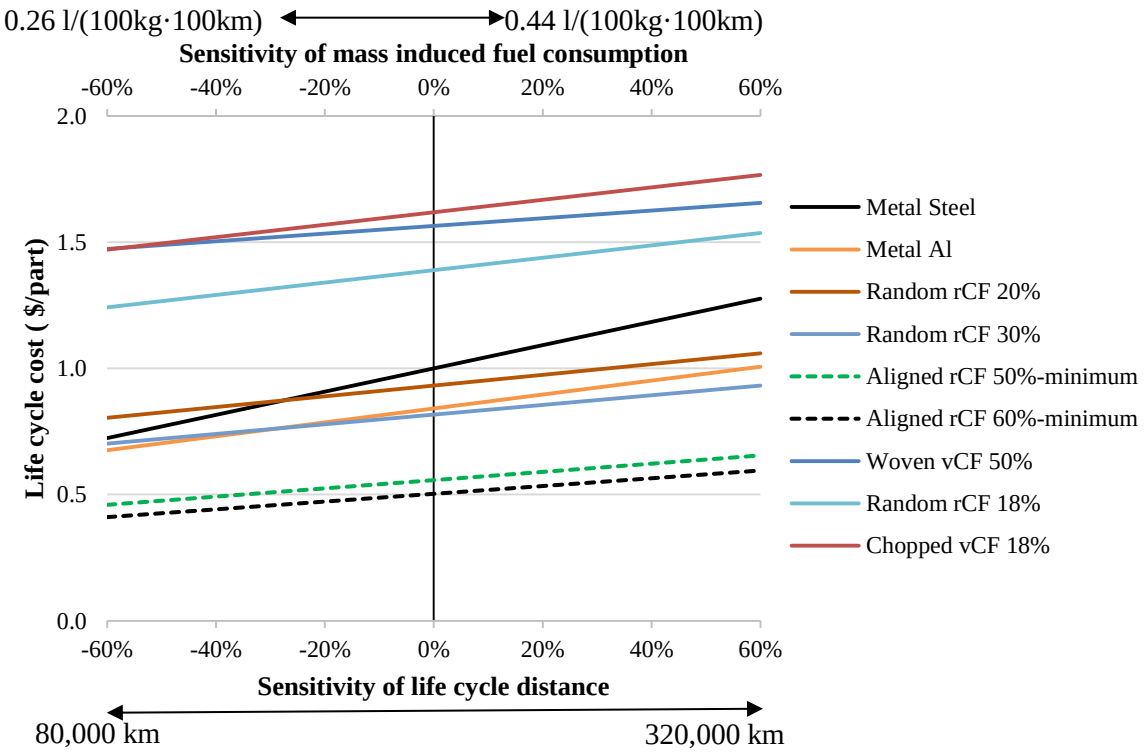

Figure 6.5. The life cycle cost of automotive component materials with varied life cycle distances and mass induced fuel consumption (λ=2).

Life cycle costs are sensitive to fuel price similar with the variations in mass-induced fuel consumption (see **Figure. 6.6**). Life cycle cost shows linear relationships with fuel price but

rCFRP materials continue to show significant cost reductions across the range of values considered in this study. For each material type, cost variations between -60% and +30% is shown. This is based on historic fuel price range of $1.22-2.07/litre (£0.8-1.35/litre) in UK from 2000 to 2015 (UK Department of Energy & Climate Change, 2015) with a reference price of $1.70/litre (£1.11/litre) in 2015. Considering proportional relationship between the fuel consumption and the part mass, for functional equivalence, weight savings mean cost reductions in the replacement and therefore fuel price directly impact quantities of fuel savings. The total life cycle cost varies 4-6% for rCF 30% compared to 10-13% for steel relative to the base case ($1.70/litre) mainly due to larger mass-induced fuel consumption for steel part. Results are compared for regional variations amongst US, Canada, EU average and Netherlands due to different fuel prices in 2015. Because of regional variations in transport fuel tax rates, rCFRP show variations in net cost savings relative to steel, for instance, the net cost saving of using rCFRP to replace steel in US is smaller than that in Netherlands.

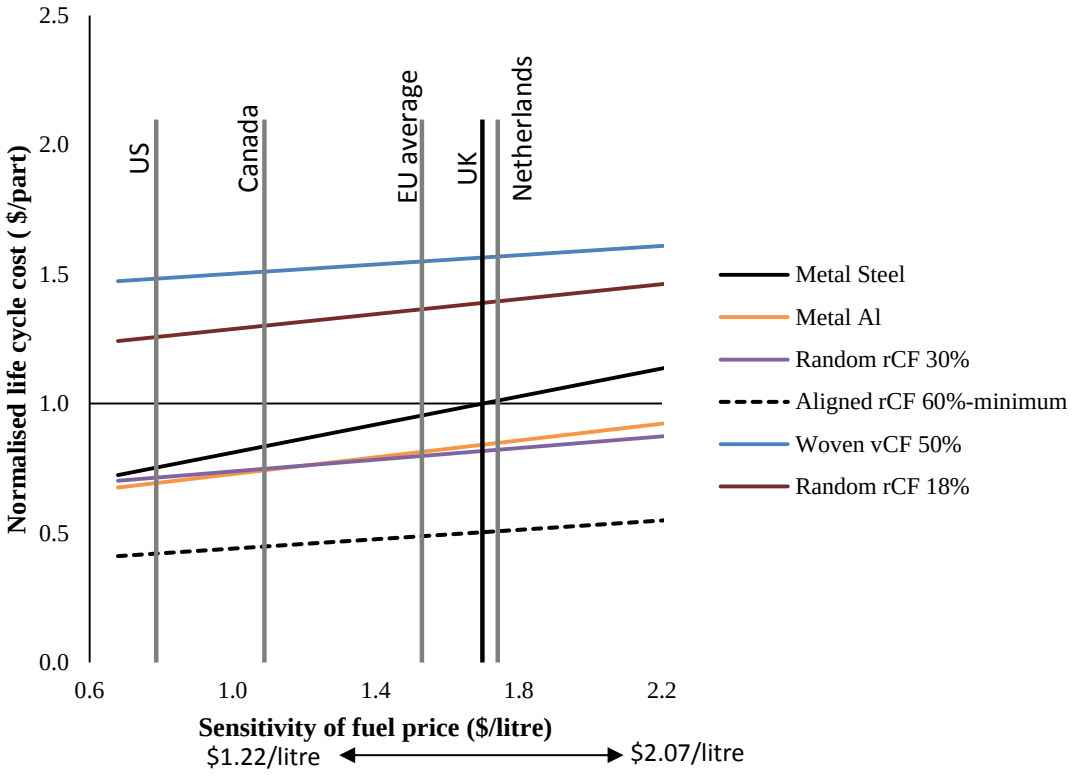

Figure 6.6. The life cycle cost of automotive component materials with varied fuel prices (λ=2).

Uncertainty in raw material prices brings sensitivity of life cycle cost results depending on the material types (**Figure 6.7**). The price range is mostly considered under historic figures from 2000 to 2015. For rCF, the prices vary depending on the plant capacities and feeding rate as discussed in Section 3.1 in the region of $1.2-5/kg under common industrial scales (500 - 6000 t/yr). As raw material costs account for a relatively small part, the total life cycle cost of steel part has only -0.2%~+0.2% variations corresponding to variations of -13%~+13% for the steel price. Variations of rCF price also have an impact on the total life cycle cost of rCFRP components: -58%~+78% variations of rCF price result in -6%~+7% variations for random rCFRP with 30% vf. Excluding alignment cost, life cycle costs for aligned rCFRP components

is sensitive to rCF price showing relatively high variations of -5%~+6% with high rCF content (50%). Virgin CFRP components are sensitive to vCF prices (-25%~+25% variations) that the life cycle cost shows -10%~+8% variations for woven vCFRP primarily due to the large proportion of vCF production cost in the full life cycle.

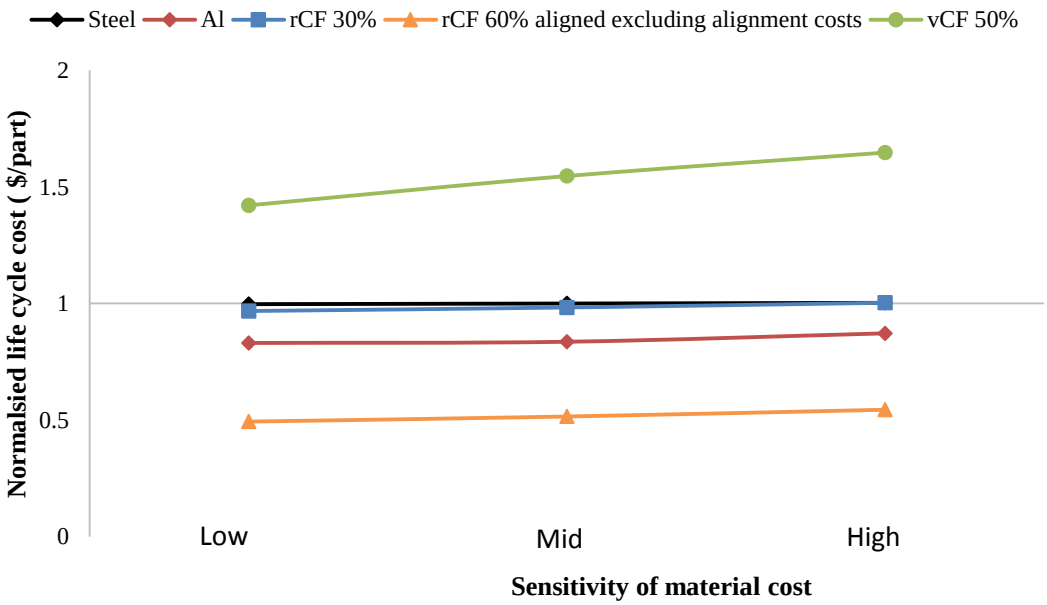

Figure 6.7. The life cycle cost of automotive component materials with varied raw material prices (low, medium and high) (λ=2).

6.4 Discussion

The need for a systematic identification of the utilisation of rCF materials in order to reduce life cycle costs has been addressed. In the chapter, techno-economic models have been developed for cost impact assessment of a hypothetical commercial-scale fluidised bed recycling plant and rCFRP manufacturing technologies to identify the market opportunities for rCF. Recovery of CF from CFRP wastes can be achieved at $5/kg or less across a wide range of key process parameters including plant capacity and feeding rate per unit bed area. The

manufacture of rCFRP is selected for case studies in terms of material selection and substitution for steel under different design indices. Case studies are used to assess the life cycle cost performance of rCFRP which is required to be addressed before it is used widely in applications in automotive industries.

The comparative assessment showed that rCFRP can be a competitive material that can replace conventional metal materials and vCFRP materials in automotive applications. It is observed that significant weight savings are achieved by rCFRP materials, especially the aligned rCFRP, in substituting steel materials while providing the same mechanical properties. Random rCFRP shows significant life cycle cost reduction for λ=3, no cost savings for λ=2 and cost increase for λ=1. Financial credits are primarily from the vehicle in-use fuel cost savings due to mass-induced fuel consumption associated with mass reduction. The cost is already competitive with the conventional steel component, prior to monetising the environmental benefits of rCF materials (e.g. social cost of carbon (i.e., a term represents the economic cost caused by an additional ton of carbon dioxide emissions or its equivalent)). Further cost analyses to include social cost of carbon indicates replacement of conventional steel by rCFRP materials achieve significant cost savings for λ=2 and 3.

Injection moulded rCFRP parts cost more than those manufactured by compression moulding. However, injection moulding process allows for close tolerances in small parts with complex geometries at high production rates and it requires little post-production work as parts have finished shape after ejection, which is very suitable for CF/matrix part formation. There is limited scope of materials in this study such as other matrices and fibres to compare over the life cycle as it is outside of current scope.

Aligned rCFRP as the lightest substitution alternative could potentially improve financial performance provided technology development targets are met. Although there are higher manufacturing energy consumption, emissions and costs than steel, full life cycle cost is largely reduced primarily due to the significant fuel savings in the use phase.

This is one of a few studies on CFRP recycling that offers financial assessment of CFRP recycling and reutilisation of rCF. It offers an extensive list of environmental and financial impact categories and offers a set of valuable data to cover some gaps of data availability for the CFRP recycling process. While developed to assess financial viability of fluidised bed recycling process in automotive application, the method could be applied to any CFRP recycling technologies and reutilisation of rCFRP materials in other structural and/or non-structural applications.

The findings of this chapter together with previous life cycle assessment results provide insight for decisions makers seeking to use rCF composite materials during material selection and design processes, especially considering for reductions in weight, energy intensity, greenhouse gas emissions and life cycle costs.

CHAPTER 7 CONCLUSIONS

Carbon fibre reinforced plastic recycling and the reutilisation of the recovered carbon fibre can compensate for the high impact of vCF production. The focus of this thesis is on evaluating the life cycle primary energy demand, greenhouse gas emission and financial impacts of CFRP recycling technologies, in particular the fluidised bed CF recycling process and reutilisation of rCF in the automotive sector. The overall evaluation framework involves the integration of a number of analytical methodologies and adaptation of experimental data that are also collected for emerging technologies to assess hypothetical commercial-scale deployment of recycling and manufacturing technologies. The comprehensiveness of this approach is beyond the current understanding as presented in literature. The framework presented here is relevant for a wide range of materials for evaluating the viability as lightweight automotive materials from environmental and financial perspectives.

This study provides a complete life cycle assessment and life cycle costing of fluidised bed recycling of CFRP materials including: a comparative study of rCF and vCF; a comparative study of production processes of rCFRP; and case studies in which environmental and financial performance of reutilisation of rCF in substitution of current materials under different design constraints are evaluated. It contributes to filling the gaps in environmental and cost data availability for CFRP recycling and CFRP manufacturing technologies. Compared with studies found on the subject, this for the first time presents an analysis based on process modelling of pilot plant and data measured experimentally rather than assumptions and simplified, aggregated, and non-specific data that has been provided by industry sources in some limited cases.

Process, LCA, and techno-economic models of CFRP recycling developed in this thesis enable industry and policy makers to comprehensively understand the environmental and financial impacts in comparison with conventional material groups in particular at product design stage for lightweighting applications. The development of mathematical models for these recycling techniques is significant for researchers to better understand and optimise emerging technologies that can address barriers to CFRP recycling and rCFRP manufacture. The same modelling and analytical methodologies developed in this thesis can be applied for other recycling and manufacturing processes and other potential rCF markets.

In Chapter 3 and Chapter 4, detailed process modelling of fluidised bed CF recycling technology and composite manufacturing technologies (rCF processing; manufacture of rCFRP product) are undertaken based on thermodynamic principles, established modelling techniques for optimization calculations and the experimental operation of pilot plant. The process models assist researchers to understand how the performance of fluidised bed recycling process is affected by the different process parameters. As CFRP recycling processes are in transitions from lab scale/pilot scale to commercial scale, the models significantly identify optimization opportunities to reduce energy intensity of CFRP recycling and rCFRP manufacturing techniques while maintaining high performance of rCFRP materials. This level of detail is not found in any other literature while understanding these details of the carbon fibre recycling process is critical as energy inputs will be majors factor for environmental impacts of the recycling process, as well as important operating cost for evaluating financial viability.

In Chapter 5, life cycle assessment models are developed to quantify the environmental primary energy demand and global warming potential impacts of hypothetical CFRP recycling system configurations and producing rCF-based materials as substitutes for conventional and proposed lightweight materials (e.g., steel, aluminium, virgin carbon fibre) in automotive applications. The rCF component can substantially reduce life cycle primary energy demand and global warming potential relative to steel and other conventional lightweight materials (aluminium, vCFRP) while achieving higher fibre volume fractions through alignment offers potential to further reduce PED and GWP. The result demonstrates the potential environmental viability of rCF materials, supporting the emerging commercialisation of CF recycling technologies and identifying significant potential market opportunities in the automotive sector. It also has the potential to inform industry and policy-makers regarding environmental impacts related to CFRP recycling technologies and the development of relevant policies to encourage suitable utilisation of rCF materials. By adjusting model values, the model can be used to evaluate environmental impacts of other jurisdictions, co-location scenarios, co-production scenarios.

In Chapter 6, financial analysis and identification of market opportunities for recycled carbon fibres are performed by estimating the capital and operational costs and the net present value associated with minimum selling price. Cost impacts of using rCF as a substitute for conventional materials are also assessed in the full life cycle, making use of data from energy and cost models, manufacturers and existing cost databases. The total financial analysis results show that rCF composites bring substantial cost reductions due to the weight reductions for functional equivalence. While developed to assess financial viability of fluidised bed recycling process in automotive application, the method could be applied to any CFRP recycling technologies and reutilisation of rCFRP materials in other structural and/or non-structural

applications. The findings of this study provide insight for decisions makers seeking to use rCF composite materials during material selection and design processes, which reduce the risks of sub-optimisations and trade-offs of reductions in weight and financial impact.

The following limitations, however, should be noted in interpreting the results from the research:

- Only limited environmental metrics were considered in the study, primarily renewable and non-renewable primary energy demand and 100-year global warming potential.
- Results from the LCA and financial analyses are only as robust as the data and assumptions that are employed. The models are based on and validated with process parameters from best-performance experimental operations of the lab-scale/pilot plant but there is an associated uncertainty as we do not have data to validate at 10x or 100x pilot plant capacity. Actual performance in commercial facilities such as the fluidising velocity, air flow rate and the size of waste materials for larger plant scales may differ and could impact the results presented here. Therefore this as an important future research topic as the FB technology moves closer to commercial deployment.
- The thesis considers emerging rCF processing processes, especially fibre alignment technique. However, as it is a new technique under development, obtaining necessary data to undertake a life cycle based environmental and financial study is particularly difficult due to limited availability, confidentiality and representativeness of process data that yet have to be commercialised.
- This thesis specifically considers the fluidised bed recycling process while there are other methods for recycling, processing rCF, manufacturing rCFRP, and different

applications for the materials. These could have very different financial and environmental implications, which are yet to be assessed.

Summarising, this is the few study on CFRP recycling that offers a whole gate-to-gate or gate-to-grave life cycle assessment on CFRP recycling and reutilisation of rCF. It offers a list of environmental and financial impact categories and offers a set of valuable data to cover some gaps of data availability for the CFRP recycling process. Moreover, it offers an analysis on possible commercial-scale fluidised bed CFRP recycling and subsequent manufacturing processes.

7.1 Future work

The recycling process is more likely to have impacts rather than in GHG. Decomposition products from (amine/amide) epoxy resin are likely to include NO_x, and potential for dioxins if chlorine is present dependent on fluidised bed temperature. NO_x has potential implications in acidification, aquatic- and human-toxicity (and eventually eutrophication) and therefore additional environmental impact metrics such as land use, acidification, ozone depletion, human and eco-toxicity can be included in future analysis. Air emissions are also very relevant for transport, so further work could compare the emissions from CFRP recycling with reductions during use phase from reduced fuel consumption. Emissions of the recycling process could also be better understood where measurement data is available as it was based on stoichiometric balances of carbon in the current research.

For the fluidised bed recycling process, the most important optimisation is to reduce the energy consumption and the associated environmental and cost impacts, by minimising the heat losses and maximising the recovery of heat. More studies are needed to understand the reactors

mechanism which would help in estimating the optimum quantities of materials and energy inputs required to maximise the output and in reducing wastes, emissions and cost. Such information would also be of importance to improve the quality and precision of the LCA study presented. Moreover, as energy recovery from the exhaust heat is not considered in the pilot plant, further impact reductions need to be evaluated by investigating the recovery practice and use of heat where data is available.

Impacts of geographical location of electricity generation on environmental and cost results can be seen from sensitivity analysis sections. A more detailed assessment is required in what future recycling systems would look like in terms of waste CFRP availability and location, which would impact plant capacity as well as location and regional factors.

This research provides methods to evaluate between CFRP recycling technologies and associated environmental and financial impacts. Evaluations go for questions such as how these methods can help both industry and government in dealing with CFRP wastes. Reutilisation opportunities of rCF in wide lightweighting and non-lightweighting applications should be extensively evaluated to identify market opportunities for rCF. The work on optimal and high-performance application of rCF such as fibre alignment to improve the quality to manufacture rCFRP products with high fibre volume fraction is scarce or still in development. The more comprehensive analysis of feasibility, environment and cost impact of these technologies are crucial in composites field where information is available in its development stage. Meanwhile, optimisation modelling needs to be applied in the rCF conversion and manufacturing techniques to ensure they are in a cost-effective and environmentally friendly manner.

Assessment of different recycling methods (mechanical, pyrolysis, chemical recycling) by mathematical modelling and experimental assessment will be significant in the development of CFRP recycling resource databases. In comparison to fluidised bed process, pyrolysis process can recover epoxy resin composition as chemical products while chemical recycling process can recover epoxy resin for reuse in other sectors but inventory data on these technologies and associated environmental and financial data are lacking in the current research. Once the data are available, a critical assessment can be performed to identify the most appropriate technology for different CFRP waste streams and for development of optimised waste management policies.

In the higher level of recycling hierarchy (waste reduction > reuse > recovery > disposal), efforts for post-use systems are rare reuse: vessel/body structure – components – materials. For example, 747 Wing House directly reuses the aircraft wing structure as the roof of house. However, the markets for reuse of CFRP is limited as thermoset polymers cannot be melted down and remoulded like thermoplastics that it has to be maintained in its original formation. Therefore, there are indeed opportunities for reuse of CFRP wastes but required to find emerging and efficient use to keep its value in the future.

Waste reduction at the highest level of waste management hierarchy is still the most demanding option. In aerospace industry, the 'buy-to-fly' ratio (the ratio of materials weight procured to the weight of the finished product) is a key concern and lots of efforts at reducing manufacturing waste generation are in progress. It includes the manufacturing technology developments such as out of autoclave and novel curing. Moreover, high performace fibre reinforced thermoplastic composites and more sustainable single-polymer-composites have been developed for aircraft industries. As they are recyclable via melting while proving great

mechanical performance in forms of sandwich panels, they can be considered in replacing the high-cost and high-energy-intensity fibre reinforced thermoset composite materials to some extent and this will be the on-going technologies under development.

As this study did not consider specific design requirements in material substitution, more feasibility studies have to assess in more details on specific automotive applications, including details such as car safety and other generic aspects (surface quality, etc.) but also considering particular issues when in use (e.g., durability, expected lifetime) and issues at end of life (e.g., recyclability of rCFRP materials) for future whole vehicle design.

In light of applications of rCFRP, not restricted to automotive industries, future research could evaluate in more details for wide applications of rCFRP materials, such as aerospace, wind energy and sporting industries. Their environmental and financial impacts could be assessed for a creation of reutilisation pathway databases and trade-off strategies for waste management of CFRP wastes.

REFERENCES

ABBOTT, R. 2000. 6.09 - Composites in General Aviation. *In:* KELLY, A. & ZWEBEN, C. (eds.) *Comprehensive Composite Materials.* Oxford: Pergamon.

ABEYKOON, C., KELLY, A. L., BROWN, E. C., VERA-SORROCHE, J., COATES, P. D., HARKIN-JONES, E., HOWELL, K. B., DENG, J., LI, K. & PRICE, M. 2014. Investigation of the process energy demand in polymer extrusion: A brief review and an experimental study. *Applied Energy,* 136**,** 726-737.

AIRBUS. 2014. *An Airbus working group sets out a composites recycling roadmap* [Online]. Available: http://www.airbus.com/newsevents/news-events-single/detail/an-airbus-working-group-sets-out-a-composites-recycling-roadmap/ [Accessed December 2016].

ASHBY, M. F. 2005. *Materials Selection in Mechanical Design(third edition)*. Butterworth-Heinemann, Oxford, UK. 0 7506 6168 2.

ASM AEROSPACE SPECIFICATION METALS INC. 2015. *Aluminum 6061-T6* [Online]. Available: http://asm.matweb.com/search/SpecificMaterial.asp?bassnum=MA6061t6 [Accessed December 2015].

ASMATULU, E. 2013. *End-of-life analysis of advanced materials.* Doctor of Philosophy, Wichita State University.

ASPEN AEROGELS. 2015. *Pyrogel® xt-e: flexible insulation for hot work* [Online]. Available: http://www.aerogel.com/products-and-solutions/pyrogel-xt-e/ [Accessed March 2015].

BADER, M. G. 2000. 6.01 - The Composites Market. *In:* KELLY, A. & ZWEBEN, C. (eds.) *Comprehensive Composite Materials.* Oxford: Pergamon.

BAGG, G. E. G., COOK, J., DINGLE, L. E., EDWARDS, H. & ZIEBLAND, H. 1977. *Manufacture of composite materials*. US, US 20130264521 A1.

BAGG, G. E. G., DINGLE, L. E., JONES, R. H. & PRYDE, A. W. H. 1971. *Process for the manufacture of a composite material having aligned reinforcing fibers*. US, US 3617437 A.

BELL, J., PICKERING, S., YIP, H. & RUDD, C. 2002. Environmental Aspects of the Use of Carbon Fibre Composites in Vehicles –Recycling and Life Cycle Analysis. *End of Life Vehicle Disposal--Technical, Legislation, Economics (ELV 2002).* Warwick, UK: .

BERTHELOT, J.-M. 2012. *Composite materials: mechanical behavior and structural analysis*, Springer Science & Business Media. New York. 1461205271.

BMW GROUP. 2016a. *BMW i3 and i8 series car* [Online]. Available: https://www.bmw.co.uk/en/index.html [Accessed June 2016].

BMW GROUP. 2016b. *BMW, Boeing to cooperate on carbon fiber recycling* [Online]. Available: https://www.press.bmwgroup.com/ [Accessed July 2016].

BOEING 2014. The Boeing Company 2013 Environmental Report.

BOEING. 2017. *Boeing 787 Dreamliner* [Online]. Available: http://www.boeing.com/commercial/787/ [Accessed March 2017].

BOLUR, P. C. 2000. *A guide to injection moulding of plastics*, Allied Publishers Limited. India. 81-7764-000-3.

BOOTHROYD, G., DEWHURST, P. & KNIGHT, W. A. 1994. *Product design for manufacture and assembly / Geoffrey Boothroyd, Peter Dewhurst, Winston Knight*, Marcel Dekker. 0824791762.

BRONDSTED, P., LILHOLT, H. & LYSTRUP, A. 2005. Composite materials for wind power turbine blades. *Annu. Rev. Mater. Res.,* 35**,** 505-538.

BROOKS, R. 2000. 6.16 - Composites in Automotive Applications: Design. *In:* KELLY, A. & ZWEBEN, C. (eds.) *Comprehensive Composite Materials.* Oxford: Pergamon.

CARBERRY, W. 2008. Airplane Recycling Efforts benefit boeing operators. *Boeing AERO Magazine QRT,* 4**,** 6-13.

CARBON CONVERSIONS. 2016. Available: http://www.carbonconversions.com/ [Accessed June 2016].

CENGEL, Y. A. & BOLES, M. A. 1998. *Thermodynamics : an engineering approach*, McGraw Hill. 0071152474.

CFK VALLEY STADE RECYCLING GMBH AND CO KG. 2016. Available: http://www.cfk-recycling.com [Accessed July 2016].

CHEMICAL ENGINEERING 2015. Chemical Engineering's Plant Cost Index.

CLIFFORD, M., SIMMONS, K. & SHIPWAY, P. 2009. *An introduction to mechanical engineering: Part 1*, CRC Press. London: Hodder Education, An Hachette UK Company. 1466585455.

COMMITTEE, G. A. R. 2009. Global aluminium recycling: a cornerstone of sustainable development. London: International Aluminium Institute.

CONNOR, M. L. 2008. *Characterization of recycled carbon fibers and their formation of composites using injection molding.* Master degree, North Carolina State University.

CUI, X., ZHANG, H., WANG, S., ZHANG, L. & KO, J. 2011. Design of lightweight multi-material automotive bodies using new material performance indices of thin-walled

beams for the material selection with crashworthiness consideration. *Materials & Design,* 32**,** 815-821.

CUNLIFFE, A. M., JONES, N. & WILLIAMS, P. T. 2003. Recycling of fibre-reinforced polymeric waste by pyrolysis: thermo-gravimetric and bench-scale investigations. *Journal of Analytical and Applied Pyrolysis,* 70**,** 315-338.

DANIEL, I. M., ISHAI, O., DANIEL, I. M. & DANIEL, I. 1994. *Engineering mechanics of composite materials*, Oxford University Press New York.

DAS, S. 2001. The cost of automotive polymer composites: A review and assessment of DOE's lightweight materials composites research. *American Department of Energy: Springfield, VA,* 1-47.

DAS, S. 2011. Life cycle assessment of carbon fiber-reinforced polymer composites. *International Journal of Life Cycle Assessment,* 16**,** 268-282.

DAVIDSON, J. F., CLIFT, R. & HARRISON, D. 1985. *Fluidization*, Academic Press. Orlando, Fla. 0122055527

DELHAES, P. 2003. *Fibers and composites*, CRC Press. 0203166787.

DEMPSEY, N., BARTON, C. & HOUGH, D. 2015. Energy prices- Commons Briefing papers SN04153.

DHILLON, B. S. 2009. *Life Cycle Costing for Engineers*, Taylor & Francis. 9781439816882.

DOE 2015. Chapter 6: Innovating Clean Energy Technologies in Advanced Manufacturing Technology Assessments. *Quadrennial Technology Review 2015.*

DOE OFFICE OF ENERGY EFFICIENCY AND RENEWABLE ENERGY 2014. "Clean Energy Manufacturing Innovation Institute for Composite Materials and Structures," Funding Opportunity Announcement (FOA) Number DE-FOA-0000977, issued 2/265/2014.

DUFLOU, J. R., DE MOOR, J., VERPOEST, I. & DEWULF, W. 2009. Environmental impact analysis of composite use in car manufacturing. *CIRP Annals-Manufacturing Technology,* 58**,** 9-12.

DUFLOU, J. R., DENG, Y., VAN ACKER, K. & DEWULF, W. 2012. Do fiber-reinforced polymer composites provide environmentally benign alternatives? A life-cycle-assessment-based study. *MRS Bulletin,* 37**,** 374-382.

EASY COMPOSITES LTD. 2016. *EL2 Epoxy Laminating Resin* [Online]. Available: http://www.easycomposites.co.uk/#!/resin-gel-silicone-adhesive/epoxy-resin/EL2-epoxy-laminating-resin.html [Accessed September 2016].

EBERLE, R. A. F., H. 1998. Modelling the Use Phase of Passenger Cars in LCI. *SAE Total Life-cycle Conference.* Graz Austria: SAE Technical Paper 982179

EDWARDS, H. & EVANS, N. 1980. A method for the production of high quality aligned short fibre mats and their composites. *ICCM-3, Paris***,** 1620-35.

ELDUQUE, A., JAVIERRE, C., ELDUQUE, D. & FERNÁNDEZ, Á. Sensitivity Analysis of the Environmental Impact of Polymer Injection Molding Process. The 4th World Sustainability Forum, 2014. Multidisciplinary Digital Publishing Institute.

ELG CARBON FIBRE LTD. 2016. Available: http://www.elgcf.com/ [Accessed September 2016].

EUROPEAN AUTOMOBILE MANUFACTURERS ASSOCIATION. 2017. *World Production* [Online]. Available: http://www.acea.be/statistics/tag/category/world-production [Accessed February 2017].

EUROPEAN COMMISSION-INTELLIGENT ENERGY EUROPE 2006. Reduced energy consumption in plastics engineering- European best practice guide. Smithers Rapra Technology Ltd United Kingdom.

EUROPEAN COUNCIL 1999. Directive 1999/31/EC on the landfill of waste. *Off J Eur Union L,* 182**,** 1-19.

EUROPEAN COUNCIL 2000. Directive 2000/53/EC of the European Parliament and of the Council on end-of-life vehicles. *Off J Eur Union L,* L.269**,** 34-269.

EUROSTAT STATISTICS EXPLAINED. 2015. *Estimated labour costs for the whole economy in EUR, 2015* [Online]. Available: http://ec.europa.eu/eurostat/statistics-explained/index.php/Main_Page [Accessed July 2016].

FABRYCKY, W. J. & BLANCHARD, B. S. 1991. *Life-cycle cost and economic analysis,* Prentice Hall. 0135383234.

FARAG, M. 2008. Quantitative methods of materials substitution: application to automotive components. *Materials & Design,* 29**,** 374-380.

FRANCIS, D., TOWERS, M. & BROWNE, T. 2002. Energy cost reduction in the pulp and paper industry. *Montreal, QC: Pulp and Paper Research Institute of Canada*.

FRIEDRICH, K. & ALMAJID, A. A. 2013. Manufacturing Aspects of Advanced Polymer Composites for Automotive Applications. *Applied Composite Materials* 20**,** 107-128.

GABI 2014. Gabi Extension Database VII Plastics.

GERRARD, A. 2000. *Guide to capital cost estimating,* IChemE. 0852953992.

GHOSH, A. K. 2011. *Fundamentals of Paper Drying-Theory and Application from Industrial Perspective,* INTECH Open Access Publisher. 953307583X.

GIMBUN, J., CHUAH, T. G., FAKHRU'L-RAZI, A. & CHOONG, T. S. Y. 2005. The influence of temperature and inlet velocity on cyclone pressure drop: a CFD study. *Chemical Engineering and Processing: Process Intensification,* 44**,** 7-12.

GOODFELLOW. 2016. *Technical Information - Carbon/Epoxy Composite* [Online]. Available: http://www.goodfellow.com/ [Accessed August 2016].

GRIFFING, E. & OVERCASH, M. 2010. Carbon fiber HS from PAN [UIDCarbFibHS]. *1999-present.* Chemical Life Cycle Database www.environmentalclarity.com.

GUTOWSKI, T., DAHMUS, J. & THIRIEZ, A. Electrical energy requirements for manufacturing processes. 13th CIRP international conference on life cycle engineering, 2006.

HEDLUND, A. 2005. *Model for End of Life Treatment of Polymer Composite Materials.* Doctoral thesis, Royal Institute of Technology.

HELMS, H. & LAMBRECHT, U. 2007. The potential contribution of light-weighting to reduce transport energy consumption. *The International Journal of Life Cycle Assessment,* 12**,** 58-64.

HENRIKKE BUMANN, A.-M. T. 2004. *The Hitch Hiker's Guide to LCA,* Studentlitteratur AB. Lund, Sweden.

HODGKIN, J. H., SIMON, G. P. & VARLEY, R. J. 1998. Thermoplastic toughening of epoxy resins: a critical review. *Polymers for Advanced Technologies,* 9**,** 3-10.

HOWARTH, J., MAREDDY, S. S. R. & MATIVENGA, P. T. 2014. Energy intensity and environmental analysis of mechanical recycling of carbon fibre composite. *Journal of Cleaner Production,* 81**,** 46-50.

ILG, P., HOEHNE, C. & GUENTHER, E. 2016. High-performance materials in infrastructure: a review of applied life cycle costing and its drivers – the case of fiber-reinforced composites. *Journal of Cleaner Production,* 112**,** 926-945.

IMPROVE YOUR PLASTIC INJECTION MOLDING BUSINESS. 2015. *Plastic Injection Molding Process - Energy Saving Techniques* [Online]. Available: http://www.improve-your-injection-molding.com/ [Accessed December 2015].

INCROPERA, F. P., BERGMAN, T. L. & LAVINE, A. S. 2013. *Foundations of Heat Transfer,* Wiley. 9780470646168.

INFOMINE. 2016. *Charts and Data for the Mining Industry* [Online]. Available: http://www.infomine.com/ChartsAndData/ [Accessed August 2016].

INGARAO, G., DENG, Y., MARINO, R., DI LORENZO, R. & LO FRANCO, A. 2016. Energy and CO2 life cycle inventory issues for aluminum based components: the case study of a high speed train window panel. *Journal of Cleaner Production,* 126**,** 493-503.

INTERNATIONAL ORGANIZATION FOR STANDARDIZATION 2006a. *ISO 14040: Environmental Management: Life Cycle Assessment: Principles and Framework*.

INTERNATIONAL ORGANIZATION FOR STANDARDIZATION 2006b. *ISO 14044: Environmental Management, Life Cycle Assessment, Requirements and Guidelines*.

JACOB, G. C., FELLERS, J. F., SIMUNOVIC, S. & STARBUCK, J. M. 2002. Energy Absorption in Polymer Composites for Automotive Crashworthiness. *Journal of Composite Materials,* 36**,** 813-850.

JAMES, P. N. 1968. *Improvements in or relating to methods of aligning fibres*. United Kingdom, WO 1990008024 A1.

JEC GROUP 2011. A number of investments announced for carbon fibres. *JEC Composites,* 23**,** 28-29.

JEON, S. 2015. An investigation on innovative green lightweight composite for the next generation heavy-duty trucks. *CAMX 2015.*

JIAMJIROCH, K. 2012. *Developments of a fluidised bed process for the recycling of carbon fibre composites.* Doctor of Philosophy Ph.D. dissertation, University of Nottingham.

JIANG, G., PICKERING, S. J., LESTER, E. H., TURNER, T. A., WONG, K. H. & WARRIOR, N. A. 2009. Characterisation of carbon fibres recycled from carbon fibre/epoxy resin composites using supercritical n-propanol. *Composites Science and Technology,* 69**,** 192-198.

JIANG, G., PICKERING, S. J., WALKER, G. S., WONG, K. H. & RUDD, C. D. 2008. Surface characterisation of carbon fibre recycled using fluidised bed. *Applied Surface Science,* 254**,** 2588-2593.

JIANG, G., WONG, K., PICKERING, S., WALKER, G. & RUDD, C. 2006. Alignment of recycled carbon fibre and its application as a reinforcement. *SAMPE Fall Technical Conference and Exhibition, Dallas, November.*

JIANG, G., WONG, W., PICKERING, S., RUDD, C. & WALKER, G. 2005. Study of a fluidised bed process for recycling carbon fibre from polymer composite. *7th world congress for chemical engineering, Glasgow, UK.*

JOB, S. 2010. Composite recycling-summary of recent research and development-Materials KTN Report.

JOHANNABER, F. 2008. *Injection molding machines*, Hanser Munich. 0029494206.

KANUNGO, A. & SWAN, E. 2008. All Electric Injection Molding Machines: How Much Energy Can You Save? *13th Industrial Energy technology Conference.* New Orleans, LA.

KARBOREK RCF. 2016. Available: http://www.karborekrcf.it/home/en/ [Accessed July 2016].

KELLY, J. C., SULLIVAN, J. L., BURNHAM, A. & ELGOWAINY, A. 2015. Impacts of Vehicle Weight Reduction via Material Substitution on Life-Cycle Greenhouse Gas Emissions. *Environmental science & technology,* 49**,** 12535-12542.

KEMP, I. C. 2012. Fundamentals of energy analysis of dryers. *Modern Drying Technology, Energy Savings.* Wiley-VCH Weinheim, Germany.

KENT, R. 2008. Energy management in plastics processing—framework for measurement, assessment and prediction. *Plastics, Rubber and Composites,* 37**,** 96-104.

KIM, H. C., WALLINGTON, T. J., SULLIVAN, J. L. & KEOLEIAN, G. A. 2015. Life Cycle Assessment of Vehicle Lightweighting: Novel Mathematical Methods to Estimate Use-Phase Fuel Consumption. *Environmental science & technology,* 49**,** 10209-10216.

KIM, S. 2014. Engineering Sustainability of Mechanical Recycling on Carbon Fiber Composite Materials. University of Minnesota– Deluth.

KOFFLER, C. & ROHDE-BRANDENBURGER, K. 2010. On the calculation of fuel savings through lightweight design in automotive life cycle assessments. *The International Journal of Life Cycle Assessment,* 15**,** 128-135.

KRAUS, T. & KÜHNEL, M. 2014. Composites Market Report 2014 Market developments, trends, challenges and opportunities-The Global CRP Market.

KRISHNAN, S., BALASUBRAMANIAN, N., SUBRAHMANIAN, E., ARUN KUMAR, V., RAMAKRISHNA, G., MURALI RAMAKRISHNAN, A. & KRISHNAMURTHY, A. Machine level energy efficiency analysis in discrete manufacturing for a sustainable energy infrastructure. Infrastructure Systems and Services: Developing 21st Century Infrastructure Networks,(INFRA), 2009 Second International Conference on, 2009a. IEEE, 1-6.

KRISHNAN, S., BALASUBRAMANIAN, N., SUBRAHMANIAN, E., KUMAR, V. A., RAMAKRISHNA, G. & RAMAKRISHNAN, A. M. Sustainability Analysis and Energy footprint based Design in the Product Lifecycle. Indo-US Workshop on Designing Sustainable Products, Services and Manufacturing Systems, 2009b.

KUMAR, B. 2010. Energy dissipation and shear rate with geometry of baffled surface aerator. *Chemical Engineering Research Bulletin,* 14**,** 92-96.

LEE, S. M., JONAS, T. & DISALVO, G. 1991. The beneficial energy and environmental-impact of composite-materials - an unexpected bonus *SAMPE Journal,* 27**,** 19-25.

LI, F., PATTON, R. & MOGHAL, K. 2005. The relationship between weight reduction and force distribution for thin wall structures. *Thin-walled structures,* 43**,** 591-616.

LI, X., BAI, R. & MCKECHNIE, J. 2016. Environmental and financial performance of mechanical recycling of carbon fibre reinforced polymers and comparison with conventional disposal routes. *Journal of Cleaner Production,* 127**,** 451-460.

LIU, Z., WONG, K., THIMSUVAN, T., TURNER, T. & PICKERING, S. 2015. Effect of fibre length and suspension concentration on alignment quality of discontinuous recycled carbon fibre. *20th International Conference on Composite Materials.* Copenhagen.

LONGANA, M. L., YU, H. & POTTER, K. D. 2015. Aligned virgin and recycled short carbon fibre hybrid composites. *20th International Conference on Composite Materials.* Copenhagen, Denmark.

MADAN, J., MANI, M., LEE, J. H. & LYONS, K. W. 2014. Energy performance evaluation and improvement of unit-manufacturing processes: injection molding case study. *Journal of Cleaner Production,* 105**,** 157-170.

MALLICK, P. K. 1998. *Fiber Reinforced Composites: materials, manufacturing, and design*.

MATTIS, J., SHENG, P., DISCIPIO, W. & LEONG, K. A framework for analyzing energy efficient injection-molding die design. Electronics and the Environment, 1996. ISEE-1996., Proceedings of the 1996 IEEE International Symposium on, 1996. IEEE, 207-212.

MATWEB. 2016. *Technical Data Sheet-AISI 1017 Steel, cold drawn* [Online]. Available: http://www.matweb.com/ [Accessed July 2016].

MAZUMDAR, S. 2016. The road to success in carbon composites for the automotive market. *JEC composites magazine,* 107 August-September**,** 21-23.

MCCONNELL, V. P. 2010. Launching the carbon fibre recycling industry. *Reinforced Plastics,* 54**,** 33-37.

MENG, F., MCKECHNIE, J., TURNER, T. A. & PICKERING, S. J. 2017. Energy and environmental assessment and reuse of fluidised bed recycled carbon fibres. *Composites Part A: Applied Science and Manufacturing,* 100**,** 206-214.

MEPS (INTERNATIONAL) LTD. 2016. *MEPS - WORLD CARBON STEEL PRICES* [Online]. Available: http://www.meps.co.uk/World%20Carbon%20Price.htm [Accessed July 2016].

METAL SUPPLIERS ONLINE INC. 2015. *Material Property Data: Aluminum 3003* [Online]. Available: http://www.suppliersonline.com/propertypages/3003.asp [Accessed March 2015].

MICHAUD, V. 2014. *RE: Inventory Data of Carbon Fibre, Personal Communication with Prof. Véronique Michaud in Laboratoire de Technologie des Composites et Polymères(LTC), ÉcolePolytechnique FédéraledeLausanne (EPFL) in Switzerland.*

MITSUBISHI HEAVY INDUSTRIES PLASTIC TECHNOLOGY CO. LTD. 2016. *MMV series (large-sized injection molding machine)* [Online]. Available: http://www.mhi-pt.co.jp/injec_e/products/MMV/index.htm [Accessed October 2016].

MRC LTD. 2016. *Price report: polypropylene* [Online]. Available: http://www.mrcplast.com/reports/icis-mrc-price-report-polypropylene.html [Accessed July 2016].

NAGAI, H., TAKAHASHI, J., KEMMOCHI, K. & MATSUI, J.-I. 2001. Inventory analysis in production and recycling process of advanced composite materials. *Journal of Advanced Science,* 13**,** 125-128.

NAGAI, H., TAKAHASHI, J., KEMMOCHI, K., MATSUI, J.-I. & SAKAI, S. 2000. Inventory analysis of energy consumption on advanced polymer-based composite materials. *Journal of the National Institute of Materials and Chemical Research,* 8**,** 161-9.

NAKAGAWA, M., SHIBATA, K. & KURIYA, H. Characterization of CFRP using recovered carbon fibers from waste CFRP. Second International Symposium on Fiber Recycling, The Fiber Recycling, 2009.

NAM, E. K. & GIANNELLI, R. 2005. Fuel consumption modeling of conventional and advanced technology vehicles in the Physical Emission Rate Estimator (PERE). *US Environmental Protection Agency*.

O'NEILL, T. J. 2003. *Life Cycle Assessment and Environmental Impact of Polymeric Products*, iSmithers Rapra Publishing. 1859573649.

OAK RIDGE NATIONAL LABORATORY. 2016. *ORNL seeking U.S. manufacturers to license low-cost carbon fiber process* [Online]. Available: https://www.ornl.gov/ [Accessed August 2016].

OFFICE OF ENERGY EFFICIENCY AND RENEWABLE ENERGY, U. S. D. O. E. 2010. Vehicle Technologies Program: Multi-Year Program Plan (2011-2015).

OGI, K., NISHIKAWA, T., OKANO, Y. & TAKETA, I. 2007. Mechanical properties of ABS resin reinforced with recycled CFRP. *Advanced Composite Materials,* 16**,** 181-194.

OLIVEUX, G., DANDY, L. O. & LEEKE, G. A. 2015. Current status of recycling of fibre reinforced polymers: Review of technologies, reuse and resulting properties. *Progress in Materials Science,* 72**,** 61-99.

PALMER, J., SAVAGE, L., GHITA, O. R. & EVANS, K. E. 2010. Sheet moulding compound (SMC) from carbon fibre recyclate. *Composites Part A: Applied Science and Manufacturing,* 41**,** 1232-1237.

PATEL, M. 2003. Cumulative energy demand (CED) and cumulative CO2 emissions for products of the organic chemical industry. *Energy,* 28**,** 721-740.

PATTON, R., LI, F. & EDWARDS, M. 2004. Causes of weight reduction effects of material substitution on constant stiffness components. *Thin-Walled Structures,* 42**,** 613-637.

PÉREZ, J. S., PORCEL, E. R., LÓPEZ, J. C., SEVILLA, J. F. & CHISTI, Y. 2006. Shear rate in stirred tank and bubble column bioreactors. *Chemical Engineering Journal,* 124**,** 1-5.

PICKERING, S. 2010. *Management, recycling and reuse of waste composites-Chapter 6: Thermal methods for recycling waste composites,* Cambridge: Woodhead Publishing in Materials.

PICKERING, S. J. 2006. Recycling technologies for thermoset composite materials—current status. *Composites Part A: Applied Science and Manufacturing,* 37**,** 1206-1215.

PICKERING, S. J. 2012. Recycling Thermoset Composite Materials. *Wiley Encyclopedia of Composites.*

PICKERING, S. J., KELLY, R. M., KENNERLEY, J. R., RUDD, C. D. & FENWICK, N. J. 2000. A fluidised-bed process for the recovery of glass fibres from scrap thermoset composites. *Composites Science and Technology,* 60**,** 509-523.

PICKERING, S. J., LIU, Z., TURNER, T. A. & WONG, K. H. 2016. Applications for carbon fibre recovered from composites. *IOP Conference Series: Materials Science and Engineering,* 139**,** 012005.

PICKERING, S. J., TURNER, T. A., MENG, F., MORRIS, C. N., HEIL, J. P., WONG, K. H. & MELENDI, S. Developments in the fluidised bed process for fibre recovery from thermoset composites. CAMX 2015 - Composites and Advanced Materials Expo, 2015. 2384-2394.

PICKERING, S. J., TURNER, T. A., WONG, K. H. & WARRIOR, N. A. 2013. Low cost, high value reuse of recovered carbon fibres. *International SAMPE Technical Conference.*

PIMENTA, S. & PINHO, S. T. 2011. Recycling carbon fibre reinforced polymers for structural applications: Technology review and market outlook. *Waste Management,* 31**,** 378-392.

PLASTICOMP INC. 2016. *30% Long Carbon Fiber Reinforced PP – Complēt LCF30-PP* [Online]. Available: http://www.plasticomp.com/complet-lcf30-pp/ [Accessed June 2016].

PRINÇAUD, M., AYMONIER, C., LOPPINET-SERANI, A., PERRY, N. & SONNEMANN, G. 2014. Environmental Feasibility of the Recycling of Carbon Fibers from CFRPs by Solvolysis Using Supercritical Water. *ACS Sustainable Chemistry & Engineering*.

PRINCE ENGINEERING. 2016. *Carbon Fiber used in Fiber Reinforced Plastic (FRP)* [Online]. Available: http://www.build-on-prince.com/carbon-fiber.html#sthash.RRu9v5qB.DLTFmp6L.dpbs [Accessed October 2016].

QUINN, J. & RANDALL, J. 1990. Compliance of composite reinforcement materials. *Proceedings of the Fourth International Conference on Fibre Reinforced Composites.* Liverpool.

RAO, N. S. & SCHOTT, N. R. 2012. *Understanding Plastics Engineering Calculations: Hands-on Examples and Case Studies*, Carl Hanser Verlag GmbH Co KG. 3446431497.

RIBEIRO, I., PEÇAS, P. & HENRIQUES, E. 2012. Assessment of energy consumption in injection moulding process. *Leveraging Technology for a Sustainable World.* Springer.

RIDGE, L. 1998. EUCAR-automotive LCA guidelines-phase 2. SAE Technical Paper.

ROBERTS, A. 2011. The Carbon Fibre Industry Worldwide 2011-2020: An Evaluation of Current Markets and Future Supply and Demand. *Material Technology*.

ROGERS, G. F. C. & MAYHEW, Y. R. 1995. *Thermodynamic and Transport Properties of Fluids-SI Units*, Blackwell.

RUDD, C. D. 2000. *Composites for Automotive Applications*, Smithers Rapra Publishing.

SCELSI, L., BONNER, M., HODZIC, A., SOUTIS, C., WILSON, C., SCAIFE, R. & RIDGWAY, K. 2011. Potential emissions savings of lightweight composite aircraft components evaluated through life cycle assessment. *Express Polymer Letters,* 5**,** 209-217.

SCHILD, P. & MYSEN, M. 2009. Recommendations on Specific Fan Power and Fan System Efficiency. *Technical Note AIVC,* 65.

SCHMIDT, J. H. & WATSON, J. 2014. Eco Island Ferry: Comparative LCA of island ferry with carbon fibre composite based and steel based structures. *In:* CONSULTANTS, L. (ed.). Aalborg, Denmark.

SCHWAB CASTELLA, P., BLANC, I., GOMEZ FERRER, M., ECABERT, B., WAKEMAN, M., MANSON, J.-A., EMERY, D., HAN, S.-H., HONG, J. & JOLLIET, O. 2009. Integrating life cycle costs and environmental impacts of composite rail car-bodies for a Korean train. *The International Journal of Life Cycle Assessment,* 14**,** 429-442.

SHIBATA, K. & NAKAGAWA, M. 2014. Hitachi Chemical Technical Report: CFRP Recycling Technology Using Depolymerization under Ordinary Pressure. *Hitachi Chemical*.

SHUAIB, N. A. & MATIVENGA, P. T. Energy Intensity and Quality of Recyclate in Composite Recycling. ASME 2015 International Manufacturing Science and Engineering Conference, 2015. American Society of Mechanical Engineers, V002T05A005-V002T05A005.

SHUAIB, N. A. & MATIVENGA, P. T. 2016. Energy demand in mechanical recycling of glass fibre reinforced thermoset plastic composites. *Journal of Cleaner Production,* 120**,** 198-206.

SHUAIB, N. A., MATIVENGA, P. T., KAZIE, J. & JOB, S. 2015. Resource Efficiency and Composite Waste in UK Supply Chain. *Procedia CIRP,* 29**,** 662-667.

SLOAN, J. 2013. *Market Outlook: Surplus in carbon fiber's future?* [Online]. Available: http://www.compositesworld.com/articles/market-outlook-surplus-in-carbon-fibers-future [Accessed October 2014].

SOLOMON, S. IPCC (2007): Climate Change The Physical Science Basis. AGU Fall Meeting Abstracts, 2007. 01.

SONG, Y. S., YOUN, J. R. & GUTOWSKI, T. G. 2009. Life cycle energy analysis of fiber-reinforced composites. *Composites Part A: Applied Science and Manufacturing,* 40**,** 1257-1265.

SPIERING, T., KOHLITZ, S., SUNDMAEKER, H. & HERRMANN, C. 2015. Energy efficiency benchmarking for injection moulding processes. *Robotics and Computer-Integrated Manufacturing*.

STRONG, A. B. 2006. *Plastics: materials and processing*, Prentice Hall. 0131145584.

SULLIVAN, J., BURNHAM, A. & WANG, M. 2010. Energy-consumption and carbon-emission analysis of vehicle and component manufacturing. Argonne National Laboratory (ANL).

SUMITOMO (SHI) DEMAG PLASTICS MACHINERY NORTH AMERICA INC. 2016. *SYSTEC Hydraulic Series* [Online]. Available: http://www.sumitomopm.com/previousspecs.html [Accessed June 2016].

SUZUKI, T. & TAKAHASHI, J. Prediction of energy intensity of carbon fiber reinforced plastics for mass-produced passenger cars. The Ninth Japan International SAMPE symposium, 2005. 14-19.

SUZUKI, T., TESHIBA, F., ZU, S. H., TAKAHASHI, J., KAGEYAMA, K. & YOSHINARI, H. 2002. Life Cycle Assessment of Lightweight Automobiles using CFRP. *JSME annual meeting.* The Japan Society of Mechanical Engineers.

TAKAHASHI, J., MATSUTSUKA, N., OKAZUMI, T., UZAWA, K., OHSAWA, I., YAMAGUCHI, K. & KITANO, A. 2007. Mechanical properties of recycled CFRP by

injection molding method. *ICCM-16, Japan Society for Composite Materials, Kyoto, Japan.*

THE ENGINEERING TOOLBOX. 2015. *Fiberglass Insulation,Thermal conductivity - temperature and k-values* [Online]. Available: http://www.engineeringtoolbox.com/fiberglas-insulation-k-values-d_1172.html [Accessed March 2015].

THE JAPAN CARBON FIBER MANUFACTURERS ASSOCIATION 2006. Carbon fibre reinforced plastic report.

THE JAPAN CARBON FIBER MANUFACTURERS ASSOCIATION. 2016. Available: http://www.carbonfiber.gr.jp/english/index.html [Accessed July 2016].

THIRIEZ, A. 2006. An Environmental Analysis of Injection Molding. Master's Thesis. *Department of Mechanical Engineering*.

THIRIEZ, A. & GUTOWSKI, T. An environmental analysis of injection molding. Electronics and the Environment, 2006. Proceedings of the 2006 IEEE International Symposium on, 2006. IEEE, 195-200.

TOLL, S. & MÅNSON, J.-A. 1994. An analysis of the compressibility of fibre assemblies. *Proceedings of the Sixth International Conference on Fibre Reinforced Composites.* Newcastle-upon-Tyne.

TORAY PLASTICS. 2015. *Technical Information-Injection-molding-Estimating molding cycle time* [Online]. Available: http://www.toray.jp/ [Accessed December 2015].

TURNER, T., WARRIOR, N. & PICKERING, S. 2010. Development of high value moulding compounds from recycled carbon fibres. *Plastics, Rubber and Composites,* 39**,** 151-156.

TURNER, T. A., JIANG, G., WONG, K. H. & PICKERING, S. J. 2015. Measurement of short fibre length using a rheological method. *20th International Conference on Composite Materials.* Copenhagen.

TURNER, T. A., PICKERING, S. J. & WARRIOR, N. A. 2011. Development of recycled carbon fibre moulding compounds – Preparation of waste composites. *Composites Part B: Engineering,* 42**,** 517-525.

UK, C. 2016. THE UK COMPOSITES STRATEGY.

UK DEPARTMENT OF ENERGY & CLIMATE CHANGE 2015. Typical retail prices of petroleum products and a crude oil price index.

ULRICH, G. D. 1984. *A guide to chemical engineering process design and economics,* Wiley New York. 0471082767.

UNIVERSITY OF NOTTINGHAM 2005. UK DTI funded collaborative project: High Value Recycled Carbon Fibre in Automotive Applications (HIRECAR) (TP/2/MS/6/I/10359).

UNIVERSITY OF NOTTINGHAM 2009. UK TSB funded collaborative project: Affordabel Recycled Carbon Fibre (AFRECAR) (TP/8/MAT/I/Q1594G).

US EPA. 2016. *Dynamometer Drive Schedules* [Online]. Available: http://www.epa.gov/nvfel/testing/dynamometer.htm [Accessed June 2016].

WARREN, C. 2011. Low cost carbon fiber overview. *Oak Ridge National Laboratory, Oak Ridge, Tennessee*.

WEI, H., AKIYAMA, T., LEE, H., YAMANE, M., TAKAHASHI, J., OHSAWA, I., MURAKAMI, T. & KAWABE, K. 2013. Recycling of market CFRP/CFRTP waste for mass production application. *19th International Conference on Composite Materials.* Montreal, Canada.

WEI, H., LEE, H., NAGATSUKA, W., I. OHSAWA, K. K., MURAKAMI, T., SUMIMOTO, K. & TAKAHASHI, J. 2016. Two manufacturing processes to reinforce thermoplastics with discontinuous recycled carbon fibres. *Journal of Thermoplastic Composite Materials (Under review).*

WEI, H., NAGATSUKA, W., LEE, H., OHSAWA, I. & TAKAHASHI, J. 2014. Manufacturing Process and Mechanical Properties of Recycled Carbon Fiber Card Web Reinforced Thermoplastics. *9th Asian-Australasian Conference on Composite Materials.* Suzhou, China.

WEISSMAN, A., ANANTHANARAYANAN, A., GUPTA, S. K. & SRIRAM, R. D. A systematic methodology for accurate design-stage estimation of energy consumption for injection molded parts. Proceedings of the ASME 2010 International Design Engineering Technical Conference & Computers and Information Science in Engineering Conference, IDETC/CIE, 2010.

WERNET, G., BAUER, C., STEUBING, B., REINHARD, J., MORENO-RUIZ, E. & WEIDEMA, B. 2016. The ecoinvent database version 3 (part I): overview and methodology. *The International Journal of Life Cycle Assessment, [online],* 21**,** 1218–1230.

WHEATLEY, A., WARREN, D. & DAS, S. 2013. Low‐Cost Carbon Fibre: Applications, Performance and Cost Models. *Advanced Composite Materials for Automotive Applications: Structural Integrity and Crashworthiness***,** 405-434.

WITIK, R. A., GAILLE, F., TEUSCHER, R., RINGWALD, H., MICHAUD, V. & MÅNSON, J.-A. E. 2012. Economic and environmental assessment of alternative production methods for composite aircraft components. *Journal of Cleaner Production,* 29–30**,** 91-102.

WITIK, R. A., PAYET, J., MICHAUD, V., LUDWIG, C. & MÅNSON, J.-A. E. 2011. Assessing the life cycle costs and environmental performance of lightweight materials in automobile applications. *Composites Part A: Applied Science and Manufacturing,* 42**,** 1694-1709.

WITIK, R. A., TEUSCHER, R., MICHAUD, V., LUDWIG, C. & MANSON, J.-A. E. 2013. Carbon fibre reinforced composite waste: An environmental assessment of recycling, energy recovery and landfilling. *Composites Part a-Applied Science and Manufacturing,* 49**,** 89-99.

WONG, K., PICKERING, S., TURNER, T. & WARRIOR, N. 2007. Preliminary feasibility study of reinforcing potential of recycled carbon fibre for flame-retardant grade epoxy composite. *Composites Innovation 2007 – Improved Sustainability and Environmental Performance.* Barcelona, Spain: NetComposites.

WONG, K. H. 2006. *Use of recycled carbon fibre for electromagnetic interference shielding.* PhD, University of Nottingham.

WONG, K. H., PICKERING, S. J., TURNER, T. A. & WARRIOR, N. A. 2009a. Compression moulding of a recycled carbon fibre reinforced epoxy composite. *SAMPE 2009 Conference.* Baltimore, Maryland.

WONG, K. H., SYED MOHAMMED, D., PICKERING, S. J. & BROOKS, R. 2012. Effect of coupling agents on reinforcing potential of recycled carbon fibre for polypropylene composite. *Composites Science and Technology,* 72**,** 835-844.

WONG, K. H., TURNER, T. A. & PICKERING, S. J. 2014. Challenges in developing nylon composites commingled with discontinuous recycled carbon fibre. *16th European conference on composite materials.* Seville, Spain.

WONG, K. H., TURNER, T. A., PICKERING, S. J. & WARRIOR, N. A. 2009b. The potential for fibre alignment in the manufacture of polymer composites from recycled carbon fibre. *SAE International Journal of Aerospace,* 2**,** 225-231.

WOOD, K. 2010. Carbon fiber reclamation: Going commercial. *High Performance Composites,* 3**,** 1-2.

WRAP 2017. Gate Fees Report 2016.

YIP, H., PICKERING, S. & RUDD, C. 2002. Characterisation of carbon fibres recycled from scrap composites using fluidised bed process. *Plastics, Rubber and Composites,* 31**,** 278-282.

YU, H., LONGANA, M. L., JALALVAND, M., WISNOM, M. R. & POTTER, K. D. 2015. Pseudo-ductility in intermingled carbon/glass hybrid composites with highly aligned discontinuous fibres. *Composites Part A: Applied Science and Manufacturing,* 73**,** 35-44.

YU, H., POTTER, K. & WISNOM, M. 2014a. A novel manufacturing method for aligned discontinuous fibre composites (High Performance-Discontinuous Fibre method). *Composites Part A: Applied Science and Manufacturing,* 65**,** 175-185.

YU, H., POTTER, K. D. & WISNOM, M. R. 2014b. A novel manufacturing method for aligned discontinuous fibre composites (High Performance-Discontinuous Fibre method). *Composites Part A: Applied Science and Manufacturing,* 65**,** 175-185.

ZHANG, X., YAMAUCHI, M. & TAKAHASHI, J. 2011. Life cycle assessment of CFRP in application of automobile. *18 the International Conference on Composite Materials.*

ZOLTEK. 2017. *Carbon fibre: How is it made?* [Online]. Available: http://zoltek.com/carbonfiber/how-is-it-made/ [Accessed].